THEORETICAL MODELLING OF THE SULCATED SPRING

FAITH CARTER

Doctor of Philosophy

THE UNIVERSITY OF ASTON IN BIRMINGHAM

January 1994

THE UNIVERSITY OF ASTON IN BIRMINGHAM

THEORETICAL MODELLLING OF THE SULCATED SPRING

FAITH CARTER

Doctor of Philosophy
1994

Summary

Replacement of the traditional coil spring with one or more fibre-reinforced plastic sulcated springs is a future possibility. Spring designers of metallic coil springs have design formulae readily available, and software packages specific to coil spring design exist. However, the sulcated spring is at the prototype stage of development, so literature on these springs is very sparse. The thesis contains information on the market for sulcated springs, and their advantages and disadvantages. Literature on other types of fibre reinforced plastic springs has also been reviewed.

Design software has been developed for the sulcated spring along similar lines to coil spring design software. In order to develop the software, a theoretical model had to be developed which formed the mathematical basis for the software. The theoretical model is based on a choice of four methods for calculating the flexural rigidity; beam theory, plate theory, and lamination theory assuming isotropic and orthotropic material properties. Experimental results for strain and spring stiffness have been compared with the theoretical model, and were in good agreement.

Included in the design software are the results of experimental work on fatigue, and design limiting factors to prevent or warn against impractical designs. Finite element analysis has been used to verify the theoretical model developed, and to find the better approximation to the experimental results. Applications and types of assemblies for the sulcated spring were discussed. Sulcated spring designs for the automotive applications of a suspension, clutch and engine valve spring were found using the design computer software. These sulcated spring designs were within or close to the space of the existing coil spring and yield the same performance. Finally the commercial feasibility of manufacturing the sulcated spring was assessed and compared with the coil spring, to evaluate the plausibility of the sulcated spring replacing the coil spring eventually.

Key words:

COMPOSITE SPRINGS
SULCATED SPRING
DESIGN SOFTWARE
COMPOSITE SPRING LITERATURE REVIEW
FIBRE REINFORCED PLASTIC

Dedication

To My Parents

Acknowledgements

I would like to thank my supervisor Dr Sam Murphy for his help, guidance, support, and encouragement during the research and writing of this thesis. I would also like to thank Professor Tom Richards for his help and guidance as my adviser.

For the experimental work conducted I would like to thank Dr Zhidong Xiang at the University of Sheffield. Also to the Advanced Composites Group in Derby for the sulcated spring manufacture, and to the Spring Research and Manufacturers Association for the results on fatigue and coil spring designs.

For the payment of tuition fees I would like to thank the Science and Engineering Research Council, and Eltek Semiconductors Ltd. Finally I would like to thank Dr Ib Enevoldsen and Dr Said Taibi for their assistance, Mr Nasser Saadat and other friends at Aston University for their discussions and support.

List of Contents

Chapter 1

RATIONALE FOR THE PROJECT

Chapter 2

CRITICAL REVIEW OF COMPOSITE SPRING LITERATURE

Chapter 3

AN ANALYTICAL APPROACH TO COMPUTATIONAL SULCATED SPRING DESIGN

Chapter 4

ANALYTICAL MODEL FOR THE SULCATED SPRING DESIGN BASED ON LAMINATION THEORY

Chapter 5

FINITE ELEMENT MODEL FOR SULCATED SPRINGS

Chapter 6

DESCRIPTION OF THE DESIGN SOFTWARE

Chapter 7

SULCATED SPRINGS IN APPLICATIONS

Chapter 8

DISCUSSION

Chapter 9

CONCLUSIONS AND RECOMMENDATIONS FOR FUTURE WORK

REFERENCES

APPENDICES

APPENDIX 1

APPENDIX 2

APPENDIX 3

List of Figures

List of Tables

List of Notation

t = laminate thickness

n = number of sulcations

r = inner radius of sulcation

w = width

α = angle between straight limb and horizontal line

d = depth

M = Bending moment

V = Shear force

N= Normal force

p_1 = uniformly distributed load per unit length

p_2 = uniformly distributed load per unit length

L_1 = Length as defined in Figure 3.9

L_2 = Length as defined in Figure 3.9

x_1 = Length at which bending moment is applied

x_2 = Length at which bending moment is applied

θ = Angle at which bending moment is applied

β = Angle as defined in Figure 3.9, $\pi-\alpha$

β_1= Angle as defined in Figure 3.9, $\pi-2\alpha$

ρ = Radius to the centroidal axis

P = Load

I = Second moment of area

A = cross-sectional area

r_n = radius of curvature to the neutral axis

y = distance of any fibre from the neutral axis

$\bar{y}$ = distance of the neutral axis from the centroidal axis

σ_{x_1} = normal stress in material 1 as defined in Figure 3.11

σ_{x_2} = normal stress in material 2 as defined in Figure 3.11

E_1 = elastic modulus in material 1

E_2 = elastic modulus in material 2

κ = curvature

L = straight length at start of curved section for variable rate springs

Chapter 1

RATIONALE FOR THE PROJECT

1.1 Introduction

This chapter is divided into two main sections. The first section provides a general introduction to the thesis, and the second shows the potential of sulcated springs. In the first section the purpose and scope of the study is outlined, discussing the reasons for the study, and what is to be covered by the thesis. A statement of objectives then follows to give a clear idea what the thesis is aiming to achieve. Background information is then provided so that the reader is informed of the circumstances surrounding the project. Also of concern are the political and practical limitations of the project which may have affected the content or direction.

In the second half of this chapter the market for sulcated springs is discussed to show that there is a place in the market for the sulcated spring. In the series of sub-sections which follow, a description of how the spring market is segmented is given. The product's strengths and weaknesses are also assessed. This section also serves the purpose of publicising the weaknesses which are sometimes overlooked when promoting a product. Outlining the weaknesses also highlights the areas in which future research could be directed. Finally the technological trend and demand for springs is outlined to demonstrate the feasibility of the sulcated spring market. This sub-section also shows how technical changes in applications affect, the demand for different spring types and, hence, spring supplies and sales.

1.2 Introduction to the Research Project

1.2.1 Purpose and scope of study

The purpose of this study was to assess the design of the sulcated spring as a viable replacement for the conventional helical compression steel spring. This study was prompted by a previous one conducted by the National Engineering Laboratory which showed the sulcated spring to have many advantages over the conventional steel spring. The main aim of the research in this thesis was to create and develop a theoretical model which may be used to make predictions of the likely behaviour of a sulcated spring. The theoretical model then forms the basis of a design computer software package that may be used by spring designers to design sulcated springs to replace conventional helical springs.

The scope of the study covers a variety of topics to assess the sulcated spring design. First, a critical review of the literature about other types of composite springs, of various designs and for a variety of applications. Secondly an analytical approach to sulcated spring design is investigated and the developments shown towards an analytical solution. This approach includes design, formulae and methodologies specific to the sulcated spring design, and applications. Also covered within the study is a closer examination of the effect of the orthotropic material properties on the sulcated spring design, and the progress towards a more refined analytical model. Finite element analysis is used to compare its predictions with those of the developed analytical model. Experimental results are used at all stages to verify the accuracy of both the results from the finite element and the analytical model. The scope of the study finally extends to replacement sulcated spring designs for selected applications, and ways of assembling a sulcated spring in an application.

1.2.2 Statement of Objectives

The objectives of this research work are:-

(i) To publicise the findings of the research and promote the development of the sulcated spring.

(ii) To review literature on sulcated springs and other types of composite springs, so that the problems encountered in composite spring design are appreciated, and to generate ideas which may assist in the development of the theoretical model.

(iii) To describe the development of mathematical models for sulcated spring design.

(iv) To validate the model by comparing the results with those from finite element analysis and experimental work.

(v) To produce design computer software for a theoretical model for the sulcated spring.

(vi) To show how a sulcated spring can be housed in an application, and to demonstrate how the design computer program can be used to find replacement sulcated spring designs for selected applications.

1.2.3 Background Information

A programme of research was started in 1981 to develop design and manufacturing technology for making selected structural components for vehicles from composite materials. Initially the work was carried out on a road wheel, suspension arm, and a coil spring. [1] When finding a replacement for coil springs, it was realised that the unique properties of fibre-reinforced plastic could be more fully exploited by forming it into grooves or furrows. The replacement spring was named the sulcated spring which comes from the latin word "sulcus" which means a "furrow". The grooves or furrows of the spring are similar to a wave-like form. Figure 1.1 shows a photograph of a coil spring and three sulcated springs of different sizes.

Figure 1.1 Photograph of steel coil spring and three different-sized sulcated springs.

The sulcated spring has advantageous properties over conventional steel springs; it is lighter, non-corrodible, silent and the stiffness and damping can be tailored to meet a wide range of requirements. Fracture toughness and fatigue endurance characteristics allow the spring to continue carrying a load after initial failure of a 5% reduction in the load-carrying capacity has occurred.

In 1983, the National Engineering Laboratory (NEL) won the British Innovation award at the Design Engineering show for the sulcated spring. Another award, the 'Quality by Design Award' sponsored by the British Plastics Federation was also won by NEL for the sulcated spring. A patent for the sulcated spring [2] is held by the Secretary of State for Trade and Industry. Two patents for sulcated spring assembly are held by GKN Technology Limited, as described in Chapter Seven.

In 1985 NEL invited five companies to take out licences to manufacture, test and develop sulcated springs. NEL provided the knowledge required to manufacture and design prototypes. It was through this invitation that West Bromwich Springs Ltd began a two year programme to manufacture and test sulcated springs. The potential of these springs and the need for further development was realised. Funding to continue research was applied for and received for two years from the Commission of the European Communities under the BRITE/EURAM (Basic Reseach in Technologies for Europe /European Research in Advanced Materials) programme. The BRITE/EURAM scheme involved cooperation with four partners which were the Spring Research and Manufacturers Association (SRAMA) based in Sheffield, UK., Ressort Martin Prunier based in France, and Mica and Micanite based in Southern Ireland. Prior to this a subsidiary company called Disc Computer Services had been formed from West Bromwich Springs Ltd and this company became the fourth partner.

It was at the start of the BRITE/EURAM project in January 1989 that the author joined Disc Computer Services Ltd as a Support Analyst, responsible for the development of computer based facilities for sulcated springs. It was agreed by Aston University and Disc Computer Services Ltd that the work could form the basis of a programme of research for a PhD. Regular meetings have taken place to ensure progress has been made, and the requirements of DISC and Aston University were being satisfied. Towards the end of the BRITE/EURAM contract, it was realised that further research was necessary. The Department of Trade and Industry (DTI) was approached for further assistance. Funding was agreed, and the next phase of the project commenced on the 14th January 1992 with two new partners: The Advanced Composites Group in Derby, and The University of Sheffield. They were not able to begin work on the project until funding was provided, so they were unable to start until much later on in the year.

1.2.4 Limitations

Practical and political limitations can affect the scope, direction and content of a project. The research for this thesis was affected to some degree by limitations. One limitation has been the lack of published material on the sulcated spring. There was only one paper published on the sulcated spring, which did not include much theoretical detail. It has therefore been necessary to start from the beginning without reference to existing work published on the sulcated spring and develop the model from first principles. Therefore the majority of this thesis has been original work.

Another limitation is the timing and availability of experimental work. The initial experimental results were obtained from the Spring Research and Manufacturers Association (SRAMA). If a particular experiment or result was required for this thesis it had to be fully justified and approved by the technical

staff conducting the experiments. At all times the contractual objectives were foremost. This has been a minor limitation, in that the direction of the project has not been fully under the present author's control, but in the control of the contractual objectives.

New experimental results were not available from January 1991 to November 1992, due to the end of the BRITE/EURAM contract, and further delays due to the project being transferred to another company following the commercial collapse and liquidation of Disc Computer Services Ltd. During this period meetings were held to determine how the next phase of the project would continue. Delays in commencing the experimental work were experienced due to administration problems and negotiations with the DTI during this time. Experimental work for the DTI contract was restarted in November 1992. Therefore the research was limited during this time to model development and refinement using experimental results found during the BRITE/EURAM contract. The model was further refined when the experimental results under the DTI contract were available.

1.3 The Market for Sulcated Springs

1.3.1 Segmentation of the spring market

The spring market can be segmented in several ways, e.g. by hot and cold formed springs, end use, or type of spring. The major end use market for hot formed springs is in the transport industry where most hot formed springs find a market in the suspension systems of vehicles. Cold formed springs are used in more diverse applications, the major application being the automotive industry for clutches, engine valves, and door, boot or, bonnet springs. They usually need a greater degree of accuracy and are smaller and more complex in design.

Information obtained by personal communication has revealed that a market study on sulcated springs conducted by the NEL had a market emphasis towards large hot formed coil springs. This market can be subdivided into three major markets, coil springs for automotive suspension, railway suspension and industrial use. The market for automotive suspension coil springs is typified by springs made from 12 mm to 20 mm diameter rod. The world market for car suspension springs is estimated to be £100 million per annum. Coil springs for industrial use are made from 15 mm up to 75 mm rod, with an estimated world market of £50 million per annum. This market appears to be the most attractive of the industrial springs market where the production is labour intensive. Examples of major consumers are the pipe support industry for power stations, earthmoving equipment, military applications, and industrial valves.

1.3.2 Commercial strengths and weaknesses of sulcated springs

As with any new product, the sulcated spring must display positive strengths if the market effort is to be successful. It is therefore necessary to understand what benefits can be expected. Personal communiction from NEL has revealed several advantages, these are as follows. The sulcated spring compared with its steel equivalent offers a weight saving of 65% to 96% whilst retaining the equivalent load carrying capacity, size and performance, fuel savings are thus obtained. As a result of the new design, the weight of support and housing may also be reduced, thereby reducing the overall weight. The cost of handling and transporting a fraction of the previous weight is another weight saving advantage.

The benefits of sulcated springs are evident in other areas too. Steel springs often need a protective coating to reduce corrosion. Sulcated springs

manufactured from fibre-reinforced plastic are subject to virtually zero corrosion, thereby eradicating the need for non-decorative paint, electro plating or plastic coating, and the costs associated with applying these protective coatings. Steel springs generate noise where the ends interact with the securing fitting and when the coils touch. Noise is also transmitted through the resonance of sound created by other components. Another benefit therefore is that there is no inherent noise generation characteristic and, in fact, the sulcated spring operates as a sound deadening device.

In the area of transportation and storage, sulcated springs have a major advantage. Coil springs, when packed for storage or transportation, occupy 30% of the bulk storage space. Sulcated springs can be interlaced for storage, consequently 2.5 times as many identical components can be housed in the same volume of space.

In terms of load/ deflection characteristics, the sulcated spring is capable of producing a linear or non-linear effect. The non-linearity is achieved by the changes in section form. This is one of the main advantages of this type of spring, since it is possible to obtain almost any desired variation in spring rate.

The material properties of a fibre-reinforced plastic can be manipulated such that the maximum elastic, flexural stiffness, strength, and fatigue endurance properties can be fully exploited. Incorporating elastomers, as conducted in the research programme conducted by NEL, and using fibre-reinforced plastic such as epoxy or polyester resin for the matrix, gives improved fracture toughness and fatigue endurance characteristics. In multi-cycle fatigue testing to destruction, NEL found the fatigue life of a sulcated spring to be approximately 80% longer than the equivalent coil spring.

The weaknesses of the sulcated spring were not reported by NEL. This information has only been found through the manufacture and testing of these springs during the BRITE programme of research. One of the main weaknesses was found from relaxation tests. It became evident that the performance of sulcated springs at temperatures above 60°C rapidly deteriorated[3]. Another weakness found from load tests conducted showed that sulcated springs with an even number of sulcations and horizontal end portions produced an excessive sideways movement. The laminate thickness was also found to be a very sensitive parameter. In sulcated spring manufacture it was difficult to maintain a uniform thickness throughout the spring design, and the design was thus susceptible to slight variations in stiffness for each spring manufactured[3].

1.3.3 Technological trend and demands for springs

Within the vehicle industry, there are some technical changes which could affect the market for springs in the medium to long term. In piston engines, there is a move to four valves per cylinder, instead of the two valves which is the norm at present, in order to meet more stringent emissions legislation as well as increasing the power. The springs will be lighter in weight and of superior performance.

However, in the much longer term, in the next decade or so, the consumption of springs in the vehicle industry could be threatened by radically different engine designs. A spring wire supplier in Sweden has stated its concern at the possible development of Wankel or two-stroke engines, which do not require valve springs, as alternatives to the conventional four-stroke petrol engine[4]. Consumption of valve springs will therefore increase in the more immediate future, say 10 years, but the long term trend of valve springs consumption is uncertain.

The most significant technological changes will occur in the automotive sector where the aim is always to reduce weight, space and costs, preferably with increased levels of performance at the same time. GKN in the UK were developing a prototype parabolic suspension spring in composite carbon - fibre for IVECO. This aimed to displace the conventional steel suspension spring and was to be introduced on lighter commercial vehicles by 1992. Its main advantages are less weight, less material, more efficient use of material, less maintenance and lower ultimate costs[4]. The actual cost of the composite spring is likely to be higher than its conventional counterpart but will require less maintenance and may reduce tyre wear. For large lorry fleets, the composite spring will be cheaper than the conventional spring. The exact date for introduction into production is said to depend more on lorry manufacturer's tactical selling policies than on development of the product itself.

Another alternative to the conventional spring has been proposed to IVECO by Tinsley Bridge of the UK. This involves a dual-material parabolic spring in which one part of the unit is made of steel and one part of composite. Fiat are looking at the possibility of using pneumatic suspensions on some of the larger, top of the range, cars[4]. This is still a future plan due to the considerable modifications to other parts of the vehicle, such as the incorporation of air compressors.

There has been a move away from leaf suspension springs in cars, primarily for reasons of cost and space. Virtually all modern cars use coil springs in the suspension system. Elsewhere in vehicles, many small springs have been replaced by plastics or rubber-to-metal bonding. This trend is likely to continue.

Chapter 2

CRITICAL REVIEW OF COMPOSITE SPRING LITERATURE

2.1 Introduction

Six different types of composite springs have been selected for a critical review of the literature on composite springs. The aim is to show the diversity of composite spring design and how the material properties of composites affect the design. Each type of composite spring illustrates an important point. The composite leaf spring shows the commercial implementation and success of a composite spring. Carbon fibre coil springs demonstrate some of the problems that can occur when a direct replacement design with a dissimilar material is attempted. Composite elliptic springs are compared with sulcated springs to show the similar way in which the composite is utilised in tension and bending. Composite cylindrical springs show the theoretical analysis of model development involved in a composite spring. Finally, the sulcated spring literature shows what work had been done before the start of this project.

2.2 Composite Leaf springs

Composite leaf springs constructed of glass fibre reinforced polymeric materials have been recognised and used as viable replacements for steel springs in truck and automotive applications. Experience gained in the use of composite leaf springs in vehicles is encouraging and clearly demonstrates the feasibility of composite leaf springs. Various papers have been published; of which the most recent papers have been selected for critical review and discussion.

The scope for using composite materials for making leaf springs for car suspensions was studied in the U.S.A between 1963 and 1967. Therén and Lundin [5] reported that 150 springs were produced which served to demonstrate the potential for substantial weight savings. Unfortunately the absence of cost effective production methods delayed the project by 10 years. Development was resumed in 1977, and the first transversely mounted leaf springs of wound glass fibre composite material were produced in 1981 as a rear suspension spring for the GM Corvette. The new leaf spring improved the standard of comfort by providing a quieter and smoother ride, and the useful life of the springs was substantially extended.

A vehicle leaf spring is interposed between the road wheels and the vehicle chassis. The leaf spring should buffer the vertical vibrations or impacts due to road irregularities. It does this by means of variations in the spring deflection. In this process, the leaf spring absorbs and / or releases the potential energy of the fluctuating vertical forces. Absorbed energy is stored in the leaf spring as strain energy. The aim in leaf spring design is to maximise the energy storage capability. In general there are two factors which decisively influence the quantity of storable energy in the leaf spring. The first is the spring material and the other is the shape or design.

To assess the potential use of a material for a leaf spring, it is expedient to investigate the specific strain energy

$$U = \frac{\sigma_t^2}{2\rho E} \qquad \textbf{-(2.1)}$$

where E is Young's modulus

ρ is the density

σ_t is the maximum allowable stress

Yu and Kim [6] compare the specific strain energy of spring steel and several Fibre-Reinforced Plastic (FRP) materials, as shown in Figure 2.1.

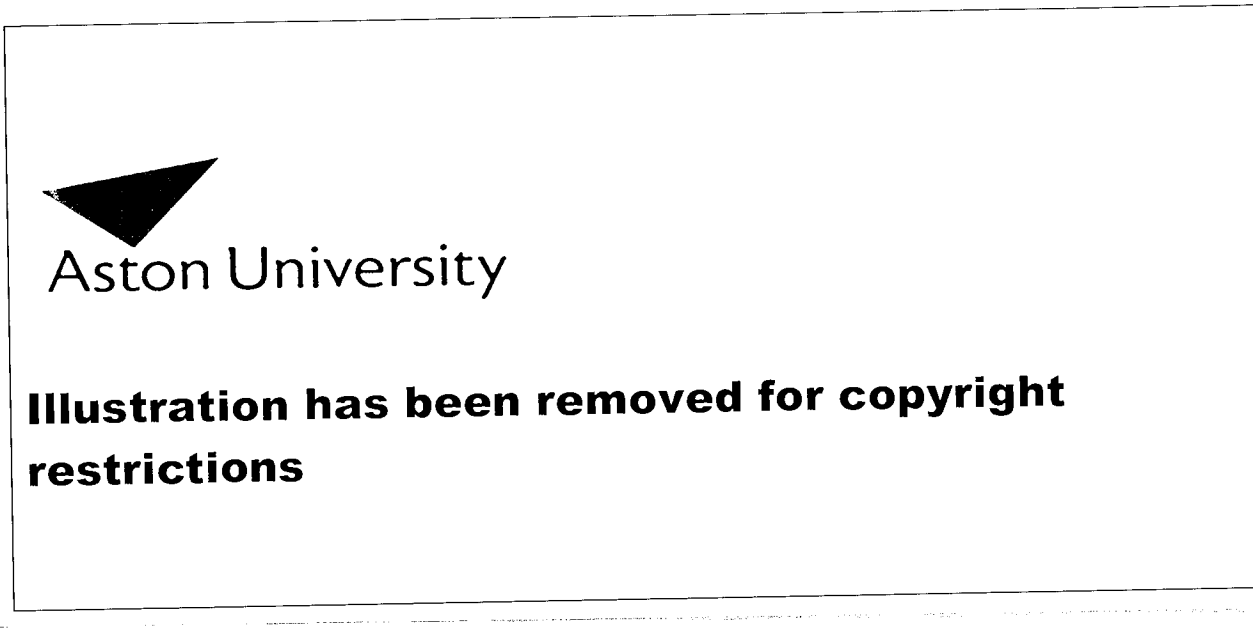

Figure 2.1 Specific strain energies of the spring materials (unidirectional properties)

The values are expressed in relation to the S2 - glass / epoxy value which is set to unity. Static ultimate strength and dynamic fatigue strength for σ_t are used since the leaf spring is subjected continuously to a dynamic load as well as a static load. From Figure 2.1, for static loads, the S2 - Glass/ Epoxy material shows the highest specific strain energy. However in the case of dynamic loading the high strength (HT) carbon/epoxy material is found to be superior to the other materials. This material therefore has a great potential for the light weight construction of the leaf spring. However its excessively high cost is an obstacle for practical use. Favourable relationships between the cost and material properties are found with glass/epoxy FRP. Gotte *et al.* [7] also use equation 2.1 to compare spring materials as a function of the permissible bending stress under dynamic load. GRP (Glass Reinforced Plastic) and CRP

(Carbon Reinforced Plastic) possess good dynamic fatigue strength values. For the range of permissible bending stresses shown in the hatched areas of Figure 2.2 the weight is reduced considerably in comparison with spring steel.

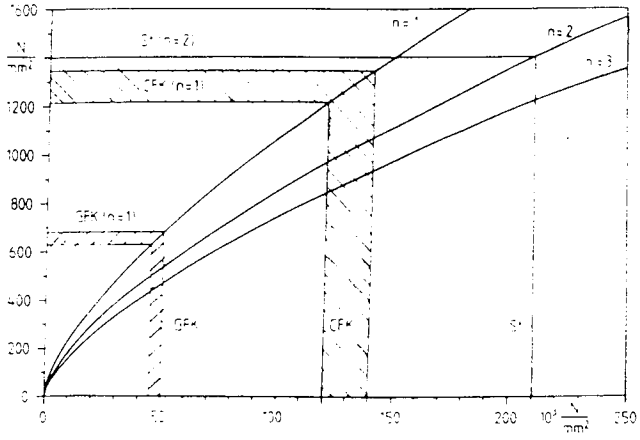

Figure 2.2 Bending stress occurring as a function of Young's modulus and number of leaves.

The x-axis represents the elastic modulus (E) and the y-axis represents the bending stress occurring (σ). Although materials such as aluminium are usually used advantageously in many light-weight constructions, it is unsuitable as a leaf spring material due to its low permissible stress values resulting from poor fatigue strength.

The second factor which influences the quantity of storable energy is the shape. High efficiency with low levels of shear stress can be attained by designing the leaf spring so that a constant bending stress state occurs along the length of the leaf spring under the main vertical force. This can be achieved by applying a taper across the depth and thickness simultaneously to maintain a constant cross-sectional area, as shown in Figure 2.3. The constant cross-section ensures the fibres pass continuously without interruption along the length direction, which is advantageous to FRP structures.

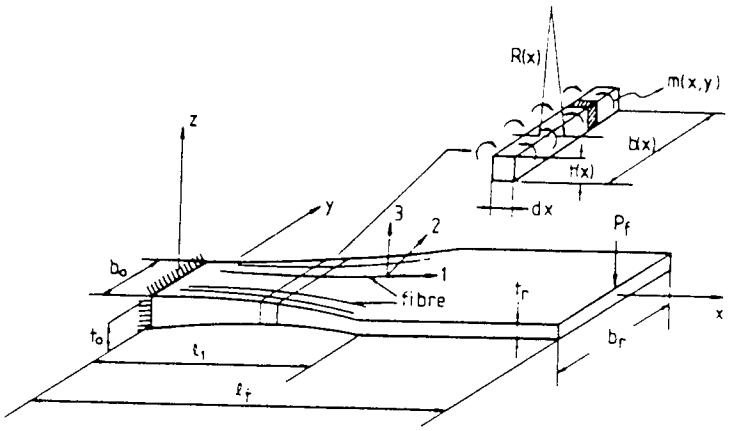

Figure 2.3 Front half of the leaf spring with the coordinate systems x, y, z and global coordinate system 1, 2, 3.

Design formulae for the composite leaf spring were derived in papers by Lo *et al.* [8] and Gottenberg and Lo [9] which are based on the fundamental equations of elementary beam theory. These design formulae are also applicable to anisotropic beams. Yu and Kim [6] found that the geometry of the beam could be optimised by minimising the level of bending stress using maximum values of length and width at the rectangular region, and an optimal value of taper ratio.

For composite leaf spring manufacture, the filament winding technique followed by compression moulding appears to be the most popular methods, offering moderate production volume. For high - volume production, of the order of several hundred thousand per year, a completely automated continuous process such as curved pulforming is essential. Gottenberg and Lo [9] describe some of the limitations of their present filament winding method of manufacture which only provided for production springs with the same cross-sectional area

from end-to-end. A post - moulding machining operation was required to produce variable thickness / constant width springs. In both instances, end-to-end continuity of the fibres was lost by trimming the width. This was of particular significance near the upper and lower faces of the spring which were subject to the highest levels of tensile and compressive normal stresses. A practical solution was found which involved forcing excess material out of the mid-thickness region during moulding. This ensured continuity of fibres in the highly stressed upper and lower face regions, thereby producing a natural cut off edge. Fabrication production methods suitable for composite leaf spring manufacture have been tabulated by de Goncourt and Sayers [10] as shown in Table 2.1. The table shows the respective production volumes, and advantages or disadvantages for each method.

Method type	Comments	Production volume
Manual layup + Autoclave	-Labour intensive -Enables rapid prototype fabrication -Low tooling costs	Low (<100)
Prepreg layup + pressing	-Prototype fabrication and/or production use	Moderate
Winding processes + pressing	-Production use -Fibre positioning problems	Moderate
Curved pulforming	-Material cost intensive -Special purpose machine Continuous process	High

Table 2.1 Spring fabrication methods.

Other design and manufacturing considerations depend on how the composite leaf spring is attached to the vehicle. Attachments involving holes, cutting,

damaging the reinforcing fibres or poorly distributed clamping loads may be detrimental, since the permissible shear stress in a unidirectional composite is relatively small. The tensile strength of a fibre reinforced plastic is approximately 20 to 100 times the shear strength which is a resin-dominated property. The ratio of tensile strength to shear strength depends on the fibre type. Gotte *et al.* [7] suggest integrally moulding a 100% GRP eye as part of the spring at the production stage. Another method of attachment was described in an internal document on composite and hybrid leaf springs produced by Tinsley Bridge Ltd., Sheffield, U.K. The method involved using a conventional steel backplate with a conventional forged eye fitted, as shown in Figure 2.4.

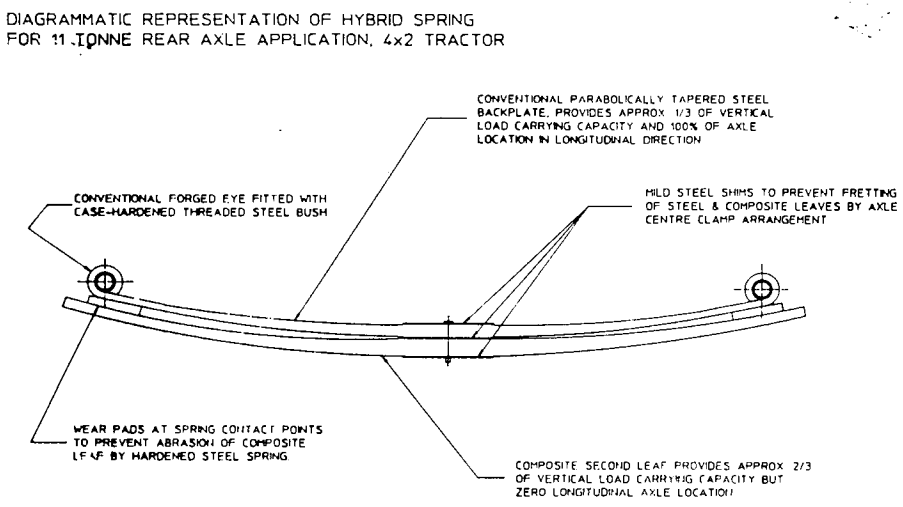

Figure 2.4 Diagrammatic representation of a hybrid spring for the rear axle of a tractor.

The steel backplate provides approximately one third of the vertical load-carrying capacity as well as providing a means of attachment. A composite second leaf supplies the majority of the vertical load-carrying capacity. Yu and Kim [6] designed their GRP leaf spring with a concave width profile at the load introduction regions, at the axle seat, and at each of the two eyes. This enabled a steel fitting with the same concave profile to be mounted easily and reliably together with rubber pads. Starkey and Wood [11] describe how the eye ends will react to all of the complex forces shown in Figure 2.5.

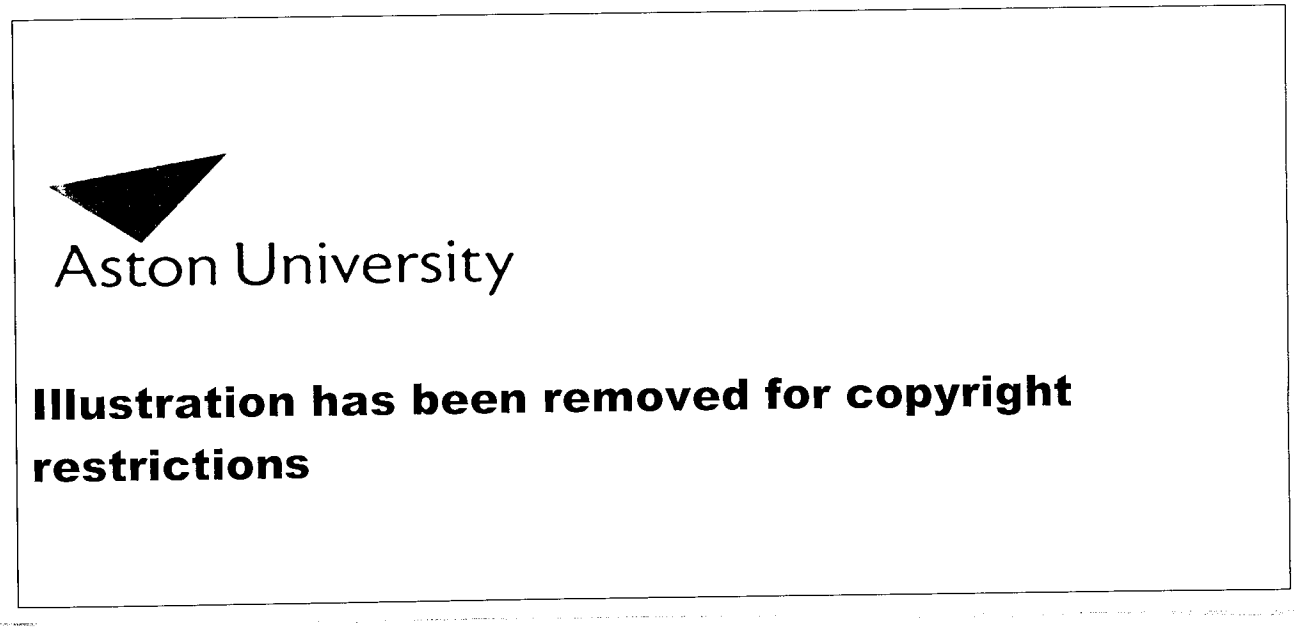

Figure 2.5 Force system acting on a composite leaf spring.

In order for the leaf spring to remain interchangeable with a steel spring, the eye end has to contain a rubber bush which must remain in place throughout these loadings.

Premature failure of composite leaf springs was found by Chang and Lo [12] to result from improper material selection, poor fabrication processes, inaccurate mould construction, severe service conditions or incorrect installation procedures. Chang and Lo [12] used various procedures for failure analysis of the FRP leaf springs. After visual examination of the failed spring, photographs were taken of the spring and the resulting surface damage. Various modes of failure such as fibre cracking, fibre waviness, fibre mis-orientation, resin cracking, delamination, interface debonding, and abrasive damage were easily observed under the microscope. Attempts were made to correlate the type of damage to the information gathered about the failed spring. For example the type of resin system and glass fibres used, fabrication method, curing cycle, service environment, and the loading history of the spring. If the causes of failure were not identified, material characterization of the failed spring was performed to obtain more information by sectioning the spring into test samples to determine its microstructure, chemical structure and mechanical properties.

Therén and Lundin [5] found that braking loads gave rise to a different and decisive potential failure mode compared to the failure due to bending stresses which occurred in steel leaf springs. The failure mode of the FRP leaf springs was composite delamination caused by the shear stresses. The reason for this is that the shear strength is about 5% of the bending strength, whereas the corresponding value for steel is about 60%. As a result, the composite spring splits into two halves when subjected to high transverse loads. A beneficial secondary effect of this phenomenon is that the spring cannot break. When delamination occurs, the spring splits horizontally into two thinner elements and its stiffness is substantially reduced. However, the spring retains its grip on the axle mountings. Yu and Kim [6] state that failure in their preliminary work

always occurred at the upper surface subject to tensile bending stress, the main consideration was given to the stresses on that surface.

Weight savings of 50-60% compared to the steel spring have been noted in several papers. In terms of cost, de Goncourt and Sayers [10] estimated the cost to be 10% cheaper than the current design for the whole passenger car suspension front and rear. Yu and Kim [6] concluded higher durability and fail safe characteristics of prototype GRP leaf springs has yet to be road tested. Lo *et al.* [8] concluded that composite tank trailer leaf springs were well received by the tank trailer operators with no significant changes in the ride and handling characteristics of the trailer.

The literature on composite leaf springs provides a significant contribution to composite spring literature in general. Of all the different types of composite springs, the leaf spring has been the most popular and successful. Its success and implementation in automotive suspensions has several advantages:-

(i) Significantly lighter in weight than equivalent steel spring.

(ii) Not affected by corrosive environment.

(iii) A moulded component can be very accurately and consistently manufactured, presenting vehicle manufacturers with very few assembly problems.

(iv) Fatigue failure is by progressive delamination of the spring which gives ample visible warning to the vehicle operator.

(v) Glass fibre composites have better natural damping properties than steel. They are therefore better able to reduce transmission of road noise.

From the papers reviewed on composite leaf springs, there was common agreement that the composite leaf spring has the potential for use in automotive

suspensions. There were several limitations that were apparent when comparing papers on composite leaf springs. One of the limitations was the lack of clarity as to how each leaf spring design varied and its dimensions, for example the difference in design for a tank trailer or a passenger car. Another limitation was that each paper had a different emphasis. For example some stated the experimental work which had been carried out, while other papers had more emphasis on design considerations, or failure. All the papers described the development of the leaf spring in Sweden, USA, UK, France, Germany and Korea where each author appears to have their own version of the composite leaf spring. The authors also had the common difficulty of retaining the important installation dimension so that the FRP leaf spring could be dimensioned under the restriction of length and width, since modification of the vehicle body was not allowed. This was a restriction imposed on many authors' work although it was not always evident from the papers examined. Another limitation was that suspension springs are a safety component and therefore strict demands on testing make it necessary to allow a long experimental programme for complete testing. From the papers reviewed, it was often difficult to visualize the leaf spring design without the aid of a diagram, which was not always clearly provided.

The composite leaf spring literature surveyed has provided a useful contribution showing how spring design is affected when fibre reinforced plastics replace metal components. In the paper by Therén and Lundin [5] the most difficult problem was tacked first, which was to replace a three-leaf steel spring with a single composite leaf. One reason was that the potential gain was higher if the load was carried by a single spring. Another reason was that with only one leaf there is no friction between individual leaves therefore making the spring silent. It was also difficult for two leaves to operate together. If a stone or hard metal became trapped between the leaves, the results would be disastrous for

relatively soft composite material. This shows the difficulties of applying exactly the same design for the two-three-or four-leaf configuration. Figure 2.6 shows the design of the multileaf steel spring, and Figure 2.7 shows the design of the composite single leaf replacement spring.

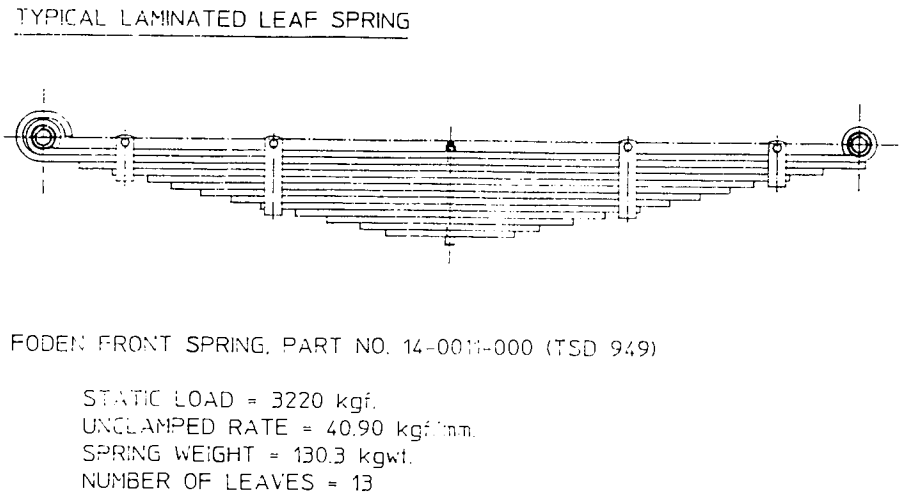

Figure 2.6 Conventional multileaf spring.

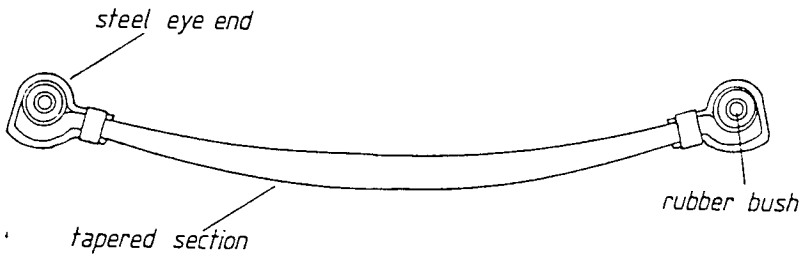

Figure 2.7 GKN FRP leaf spring.

The difficulties of finding exact replacement spring designs is a recurring theme in the complete review of composite spring literature. From the literature reviewed, it is often the conventional design that has to be changed to accommodate and utilise the composite material. A good contribution was also given by the authors by highlighting one of the weaknesses of composites in leaf spring design in that procedures used in developing steel leaf springs need to be adapted to cater for the differences in material properties. A good contribution was given by Therén and Lundin [5] where they gave an example of how the fatigue rig had to be modified for combined vertical and braking loads to satisfactorily test the composite spring. This was not necessary for testing steel springs, since both load conditions cause failure due to bending stresses. The analysis of the comparable strain energy by Yu and Kim [6] is also a useful contribution which may be applied to other spring designs.

2.3 Carbon Fibre Coil springs

Hendry and Probert [13] described an investigation conducted at the National Engineering Laboratory to assess the feasibility of replacing metallic coil springs with fibre-reinforced plastic coil springs. The feasibility was assessed by designing and manufacturing a replacement spring for an existing car rear suspension spring.

Conventional spring manufacture utilises the ability of metals to deform plastically to create the helical coils of the spring. This type of deformation is not possible with fibre-reinforced thermosetting plastics. Therefore coiling of the FRP would have to be complete before the resin was cured to solid. A new method of spring manufacture had to be used for carbon fibre coil springs. The method of manufacture selected was braiding as shown in Figure 2.8.

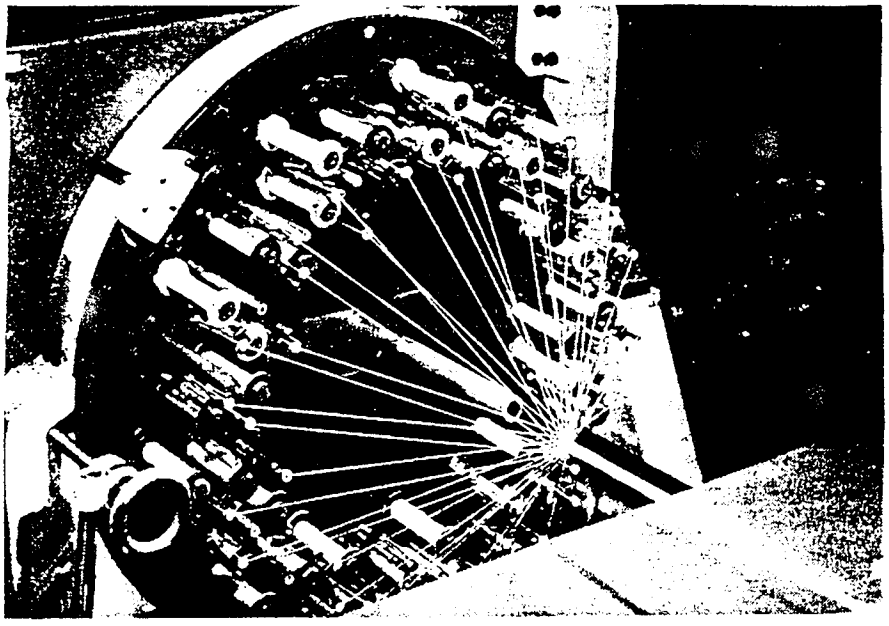

Figure 2.8 Forty carrier braiding machine.

The method involved producing long or continuous lengths of FRP stock material in a 'wet' or partially cured condition and post-forming the material into helical coils without losing the form or integrity. This process offered proven existing technology and the necessary fibre orientation. A centrally non-braided core was used in the stock for efficient use of the material.

After the manufacturing method was implemented, it became apparent from the results that, firstly, the helical geometry needed to be more closely defined and controlled. Secondly, the circularity of the cross-section of the stock needed to be retained. These limitations were overcome by using a helical-grooved former in which the segments could be collapsed inwards from the coils after the spring had cured. Considerable improvements in performance, reproducibility, consistency and a more accurate determination of the shear modulus of the coiled stock were achieved. The major disadvantage of using this technique was that there was no longer the same opportunity to easily modify a spring design to accommodate improvements in material properties.

Although the major part of the investigation concentrated on linear rate springs, due to the simpler design formulae and procedures involved, variable rate springs were also investigated. Traditionally, a variable rate spring design is achieved through geometric changes. With FRP's a variable rate spring may be achieved by varying the material modulus along the stock by varying the angle of the fibres. Verification of this concept was sought through the manufacture of carbon fibre reinforced plastic (CFRP) springs in which the fibre angle changed halfway along its length. This method successfully produced a progressive increase in spring rate with displacement.

Direct replacement of the automotive spring proved too extreme a test due to the allowable stresses of surface-treated high quality steels to enhance their fatigue performance. It would have been possible to manufacture a CFRP spring offering 50-60% saving in weight given a slightly larger space envelope. However the overriding case against the acceptance of automotive coil springs in CFRP was cost. An analysis predicted that the cost of the final CFRP replacement spring design would be approximately three times greater than that of steel, the greater part being material costs.

The study had several limiting factors. Firstly the method of spring manufacture as used for steel coil spring manufacture had to be revised. Secondly the major differences in material properties between metals and FRP's makes it difficult to implement the same design. If the same design is used, new design formulae have to be derived. However, the main limitations of their research was that the same manufacturing method for conventional spring manufacture could not be used for conventional springs.

In a coil spring design torsional and direct shear stresses are created on the application of a load. If FRP is used in a coil spring design, an increase in coil diameter is therefore required to compensate for the weakness of the material, hence reducing the weight advantage. An additional disadvantage is that it is also difficult to maintain the desired fibre orientation in the coil while it is being wound into a helical shape.

The paper provides a good contribution to the idea of replacing a metal component with an equivalent FRP component and highlights the difficulties of developing a method of manufacture with FRP. The idea of changing the material properties by changing the fibre angle to create a variable rate design has also been verified, thus showing the versatility of FRP. Information on the shear properties of braided filament-wound, and wave-wound materials has been provided by the study. Useful information has also been generated on the working range of these springs and of composite structures in torsion. This was the only paper on carbon fibre coil springs, nevertheless valuable information has been provided and by making mistakes, lessons have been learnt. The problems of direct replacement are evident from the study. It was perhaps the results of this investigation which prompted the invention and development of the sulcated spring. The authors in their conclusion state "that it is better to start from a close identification of the part's design specification. Then to progress to tailor the design to utilise the particular and unique features of the new material". So, for the ideal replacement design, the material properties need to be optimised to their most suitable configuration.

2.4 Composite Elliptic springs

A new composite elliptic spring design as shown in Figure 2.9 is described by Mallick [14], for automotive suspensions.

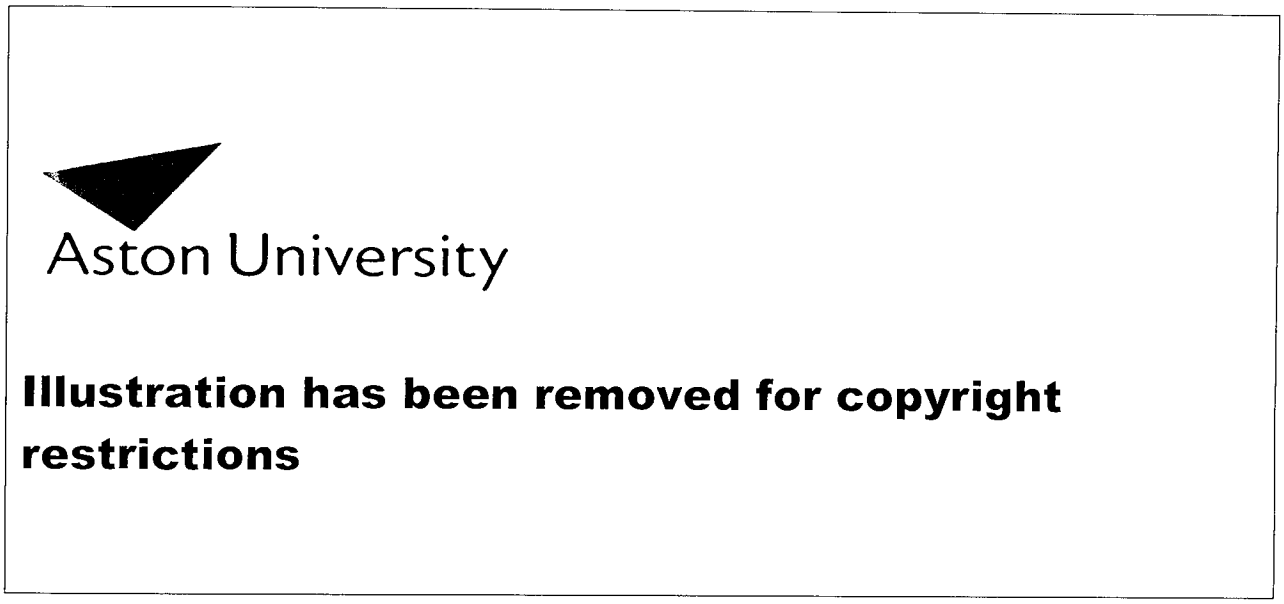

Figure 2.9 Composite elliptic spring.

Several elliptic spring elements can be mounted in series to obtain the desired spring rate, and to function in the same vertical deflection mode and space as a coil spring. The composite elliptic spring has the potential of saving up to 50% by weight due to the high flexural strength-to-weight ratios of unidirectional FRP's. A composite elliptic spring consists of several elliptic spring elements which are joined together by bolts and flat washers. Elliptic spring elements are constructed from unidirectional E - glass fibre reinforced epoxy tapes.

The paper is one of only two papers on the composite elliptic spring published by Mallick. The paper aimed to present the mechanical performance and failure of the composite elliptic spring under static loads, which is of considerable interest and relevance to the sulcated spring. There are several similarities between the composite elliptic spring and the sulcated spring. Both springs were designed primarily to replace the helical coil spring in automotive suspensions. Another similarity was that the fibres of the composite material are utilised in tension instead of shear, to avoid the poor resistance to shear stresses inherent in fibre-reinforced plastics.

Composite elliptic springs were manufactured by dry winding unidirectional E - glass fibre-reinforced epoxy preimpregnated (prepreg) tape around a segmented elliptic mandrel. The top and bottom of the minor diameter of the elliptic mandrel were machined to form a flat surface. Figure 2.10 shows an elliptic spring element.

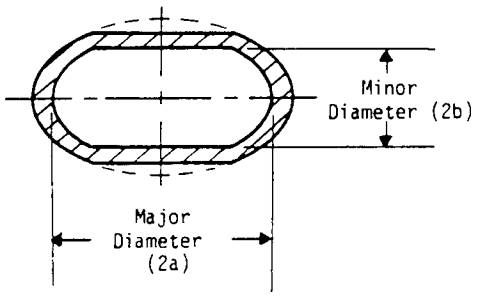

Figure 2.10 Elliptic spring element.

After winding the tape to the desired thickness, spring elements were cured on the mandrel at 149^{o} C for at least 14 hours, then cooled down slowly to room temperature. Except for a nominal clamping pressure at the flat ends, no external pressure was used during the curing process.

Tests on the composite elliptic spring were conducted for spring rate and failure. In load tests, friction at the platen surfaces caused the flat ends at the minor diameter to bow inwards as shown in Figure 2.12.

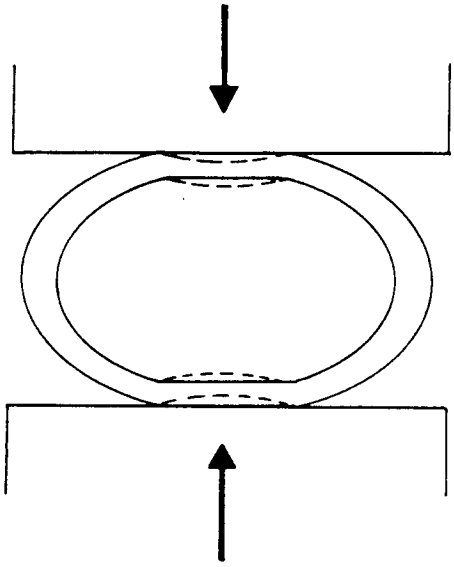

Figure 2.12 Deformation at the ends of minor diameter in spring elements.

A few minor audible noises were heard during the initial stages of loading. Close examination of the spring elements revealed interlaminar shear cracks at the curved wall near the minor diameter, at the position of maximum bending moment as the deflection is increased. Eventually tensile splitting of fibres occurred at or near the outside surface of the major diameter. Concurrently, compressive damage appeared on the inside surface of the major diameter. The normal stresses at which tensile and compressive cracks first appeared were estimated to be very close to the tensile or compressive strength of the material. At the ends of the major diameter the shear force was zero. Near the minor diameter the shear force increased where interlaminar shear failure was observed.

Mallick concluded that the primary failure mode in composite elliptic spring elements was interlaminar shear which occurred at or near the minor diameter. The spring elements were capable of absorbing large deformations, and exhibited a linear behaviour until the first interlaminar shear failure occurred. Both spring rate and failure load increased with increasing wall thickness. Mallick finally concluded that, with better consolidation between the layers, the failure load for the springs can be improved.

This paper has some interesting test results, particularly for FRP in bending under static load. The author fails to mention any results from fatigue tests, which are of considerable importance for the stated application of automotive suspensions, and fails to account for what remains to be done, and what problems need to be overcome. There is no mention of its feasibility in the proposed application or how near the research has brought the concept of the composite elliptic spring to being assembled in an automotive suspension. The literature has been particularly useful in outlining the idea of exploiting the material properties for novel designs rather than using the same traditional design concepts inappropriately.

2.5 Composite Cylindrical springs

So *et al.* [15] suggest a theoretical analysis of composite cylindrical springs using a strain energy approach. The paper shows how theoretical analysis can be applied to the prediction of the loading response to mid-plane symmetric laminated circular rings as shown in Figure 2.13. In the composite cylindrical spring design, the fibres are utilised in tension or bending instead of shear.

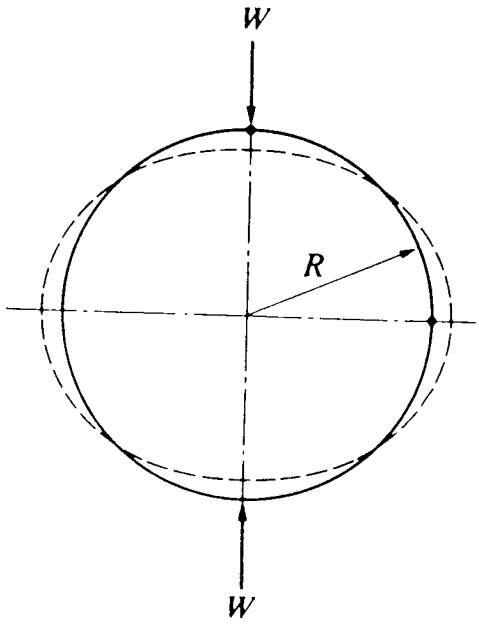

Figure 2.13 Uniaxial loading of a circular ring.

Composite cylindrical springs were manufactured by circumferential winding of E-glass bidirectional woven cloth impregnated with Ciba - Geigy epoxy resin on a PVC mandrel of 114 mm nominal diameter. After gelation at ambient temperature, the GRP tube was post-cured at 80°C for 24 hours and cut into spring elements for compression tests. To determine the glass content, burn-off-tests were conducted from the cut spring elements. In other tests, electrical resistance foil strain gauges were mounted on the inside and outside surfaces of a cylindrical spring to measure the strain distributions in the circumferential direction at various locations under compression.

The authors concluded that strain distributions indicated the existence of points at which the strain was zero on both the inner and outer surfaces of the shell when the fibre orientation was +/- 50.5° or 180°+/-50.5° or at the mid-plane.

These points free of stress and strain are of great interest for the development of the composite spring since its performance is not affected by fixing attachments made from, say, high-damping elastomer at these locations. It is at this stage that the authors make reference to the sulcated spring paper described in section 2.6. In the study, elastomers were inserted into the composite to enhance the fatigue performance. Their theoretical analysis for the calculation of spring stiffness and stress - strain distribution was based on the principle of minimum potential energy. Experimental data were used to validate the analysis. Since the elastic properties of the circular rings were estimated based on the modified rule of mixtures, the theoretical spring rates were generally higher than the experimental values. This discrepancy can be attributed to the fact that the engineering properties estimated by the modified rule of mixtures also tended to be higher than the actual values.

This paper has proved to be very useful and relevant. There is a considerable amount of theory relating to spring stiffness, stress and strain in the development of the orthotropic theoretical model for the sulcated spring. This has proved valuable for the work of this thesis. The strain energy approach adopted in this paper is used as a basis for the orthotropic model for sulcated springs discussed in Chapter Four. The paper has also been useful in identifying the stress/strain-free areas of a composite cylindrical spring, and to show that the existence of these areas is dependent on fibre orientation. An interesting point the authors mention is that, in order to compare the stiffness of each spring, the ratio of stiffness to elastic modulus was used. The reason was that it was difficult to compare the stiffness when the Young's Modulus varied with each spring manufactured which highlights one of the problems with composites. It has particular significance for composites where the fibres and resin are mixed and then cured immediately, as opposed to prepreg fibres and resin. Although pre-pregs are more expensive, they have the advantage of

being easy to lay-up and there is less variation from specimen to specimen due to the controlled manufacturing environment.

The paper develops the theory in a clear fashion and, as far as the present author is aware, it is the only one which embodies the orthotropic properties of the material. The authors point out many of the advantages of composites discussed in previous sections on other types of composite springs. However, there is no mention of the practical purpose or application where these spring can be used. There is also no reason given for manufacturing or analysing these springs, or why this particular design was used, or what metallic spring the composite spring replaces. If the composite cylindrical spring is intended to replace the steel cylindrical spring, it is not mentioned. The experimental results were given to validate the theory derived, and not to show the performance of the cylindrical spring. It would be useful to have another article or paper written which approaches the composite cylindrical spring from a replacement or performance point of view. Although the approach given by the authors has been unusual in terms of composite spring literature, it has been greatly valued.

2.6 The Sulcated spring

The sulcated spring was the result of part of the research to find a replacement for the coil spring in an automotive suspension system. Scowen and Hughes [16] describe, in their paper, the concept of the sulcated spring, including the basic theory and details of the experimental validation.

The sulcated spring concept was formulated out of the practical necessity to make a spring element with a high specific energy storage potential. There was also a need to minimise the component size to fit within a confined working space. By judicious choice of geometrical parameters and composite material

properties such as the Young's Modulus (E_{11}), a spring with a high specific energy storage is possible.

Theoretical considerations affect the geometry and design of the sulcated spring. Figure 2.14 shows the basic geometry for a sulcated spring. The diagram shows circular arc sections (B-C), joined to the straight limb sections (C-D). One sulcation is defined as the length from point A to bc, and the total deflection is a function of the number of sulcations as well as the applied load P, radius r, spring thickness t_c, width w. Also y* is the limb length to tangent point and y is the limb length along the centre line, as shown in Figure 2.14.

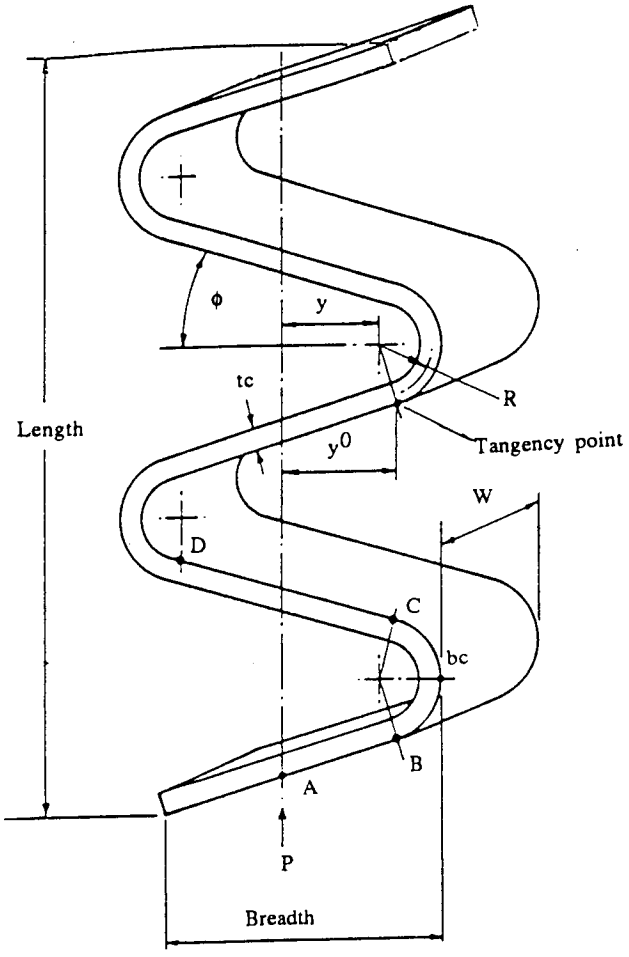

Figure 2.14 Basic geometry for sulcated spring.

The parameter Z is proportional to a complex relationship, the expression of which is not stated by the authors between $(\frac{y^*}{R})$ and ϕ. This parameter Z is an important feature of the sulcated spring concept which allows virtually any combination of (y+R) and $(\frac{y^*}{R})$ to come within a specific space envelope, and desired spring stiffness. To increase or decrease the spring stiffness, the number of sulcations (N), thickness, and width are varied. By taking advantage of the anisotropic behaviour of composites, the fibre lay-up and the fibre angle θ_{1c} can be changed so that the spring rate may be adjusted to any desired value. Figure 2.15 shows how the fibres can by laid up, and how the fibre angle is measured. Bending stresses can also be reduced by precise manipulation of the fibre angle and lay up scheme.

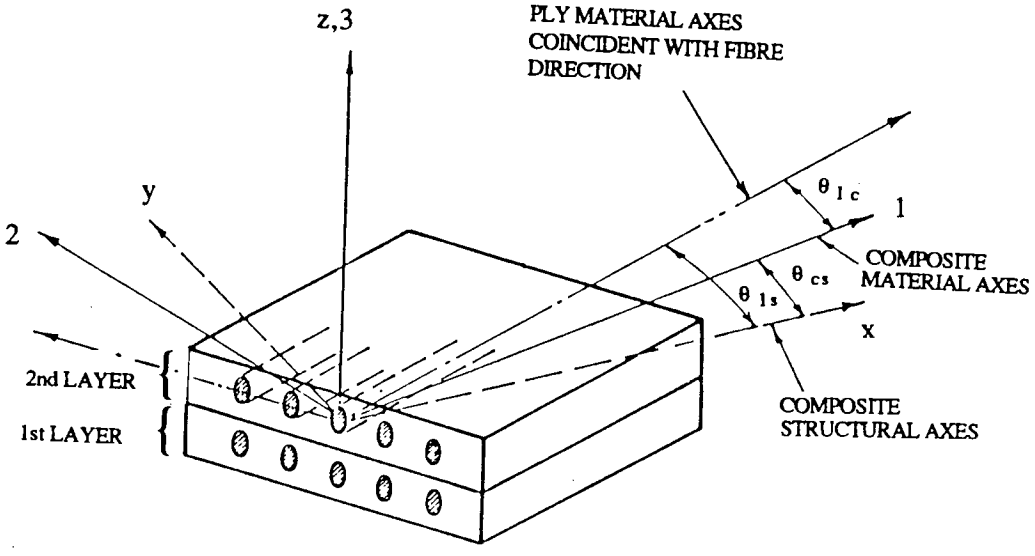

Figure 2.15 Lay up and fibre angle of a composite.

Thompson *et al*. [17] state that "the sulcated spring is an extremely flexible concept in that its construction offers scope for a large degree of geometrical and material permutatations to be considered for any application." The initial

spring design according to Thompson *et al.* must be based on the following two design requirements;

1) a specific axial stiffness or spring constant.

2) a maximum operating load or a maximum deflection.

The initial models which they developed for predicting these two design requirements considered the spring as a two-dimensional structure. This assumption allows classical beam theories to be employed. Castigliano's strain energy method was used for calculating the spring stiffness, and for circumferential, radial and interlaminar shear stress distributions, continuum models for a curved beam from Lekhitskii [18] were used. A computer-based theoretical design procedure was developed which could produce feasible designs. Finite element modelling was used to assess the theoretical methods and to predict some of the other behavioural characteristics. All the results for stiffness and stress were in good agreement, with the exception of the free edge on the inside surface where the theoretical model over-estimated the stress compared to the prediction of the finite element model. Their finite element study found that for 2,6,10 etc. sulcations the sulcated spring deformed eccentrically under axial load, the definition used by NEL (as in Figure 2.14, page 52) is different to the definition used by the Spring Research and Manufacturer's Association (SRAMA) as shown in Figure 3.1, page 61.; two sulcations as defined by NEL make one sulcation as defined by SRAMA.

In the work carried out by Scowen and Hughes [16] , elastomeric inserts of different forms were moulded into the curved portions of the spring structure to achieve a non-linear load/deflection characteristic. Varying the geometrical parameters of the spring such as tapering the width, breadth, and thickness or varying the fibre ply angle in different regions of the spring was another way of producing non-linear behaviour. This is one of the main advantages of using

composites, since it is possible to obtain almost any desired variation in spring rate. Figure 2.16 shows examples of the variety of load/deflection spring characteristics which they achieved.

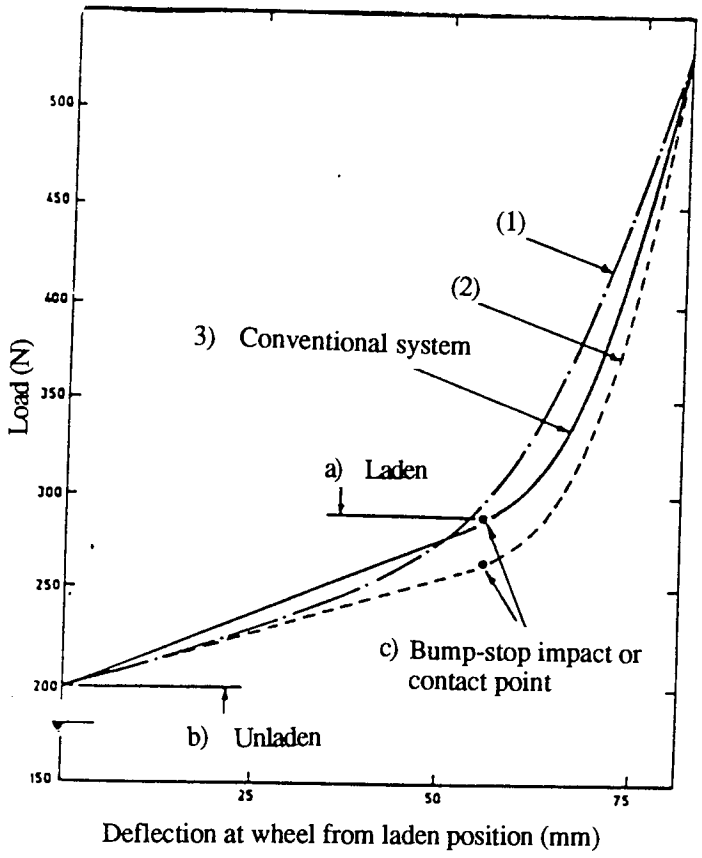

Figure 2.16 Load characteristics for various suspension systems.

The curve numbered (1) is the characteristic of a sulcated spring with elastomeric inserts. The second curve (2) represents the characteristic of a sulcated spring without inserts, and the solid line curve (3), represents a conventional suspension system with spring and separate bump stop. Suspension systems represented in curves (2) and (3) show an abrupt transition in the load/deflection characteristic at point (c). This is where the separate bump stop starts to react or sulcation contact occurs. In contrast, the variable rate sulcated spring curve (1) has a smooth transition.

A multi-limbed design in an automotive suspension application, as shown in Figure 2.17, was stated to improve the fail-safe characteristics.

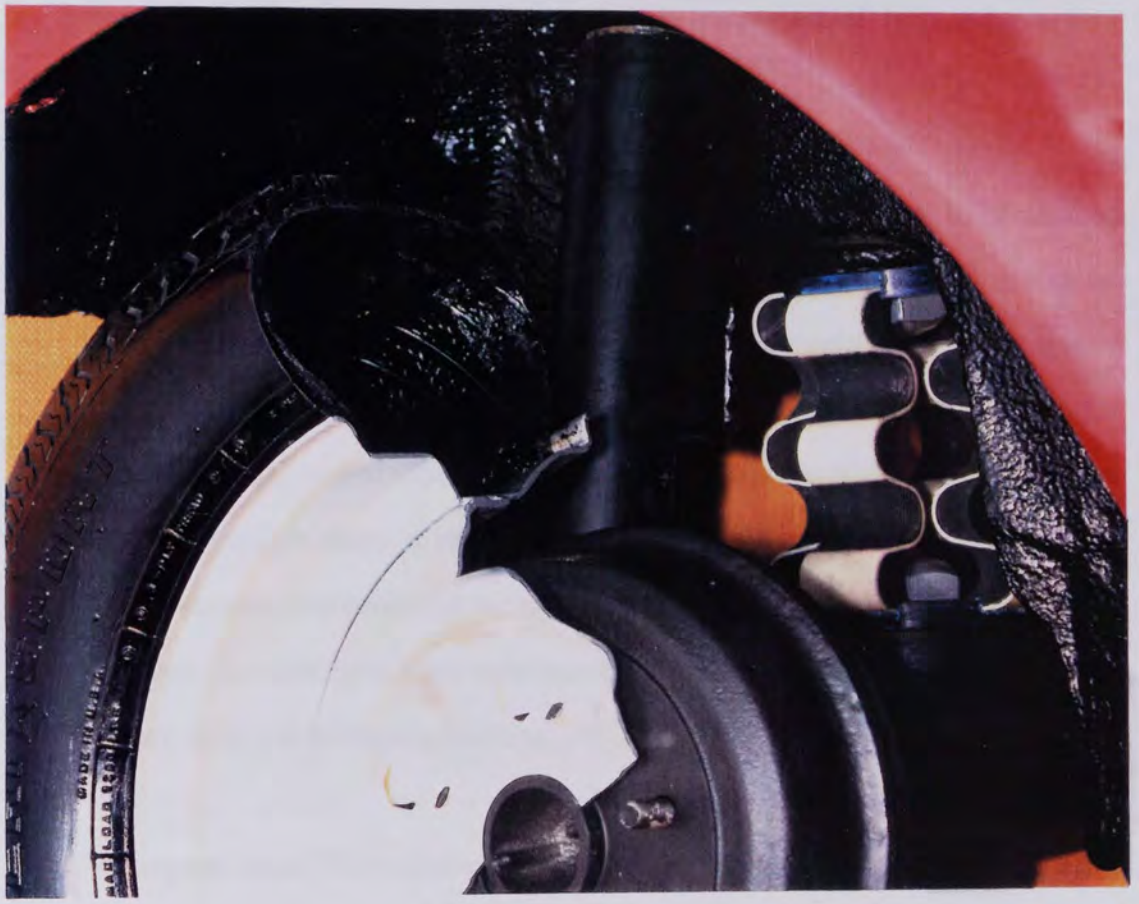

Figure 2.17 Multi-limbed sulcated spring in an automotive suspension application.

For example, when tested in compression, a four-limbed sulcated spring failed at a measured load. When the spring was re-tested, 75% of the original load at which the spring failed previously could still be supported. It was concluded that sulcated springs are feasible for high stress applications, such as suspension springs for commercial and automotive vehicles, and high temperature applications such as automotive engine valve springs could also benefit with regard to operational performance. They considered that another major advantage over other forms of springs in bending is that the curved elements of the sulcated spring enable bending stresses to be reduced to safe

working levels (<600 MN/m^2 for glass reinforced plastic (GRP)) by increasing the number of sulcations. Furthermore, when elastomers are used in the curved sections, further 'stress smoothing' occurs, accompanied by a progressive damping characteristic.

Scowen and Hughes [16] concluded that although more work needs to be done to optimise the process route and design procedures, the sulcated spring was an extremely promising concept. Sulcated springs offered many advantages compared with more traditional springs; examples are light-weight, high specific energy storage capacity and corrosion resistance of the springs, and the ability to produce them by conventional FRP fabrication routes. Good damping characteristics, and scope for incorporating a smooth bump stop are also useful features, and low cost glass reinforcement can be used in designs to match current steel coil spring applications.

Thompson *et al.* [17] concluded that finite element modelling had highlighted some interesting behavioural characteristics of the spring under clamped end conditions. Either asymmetric or eccentric behaviour will occur under uniaxial load depending on the number of sulcations chosen. The final design would have to account for numerous other requirements such as fatigue loading dynamic response, manufacturability and environmental conditions.

The paper by Scowen and Hughes [16] was the first paper to be published on sulcated springs, it is an extremely relevant paper, as it describes the initial results of tests on sulcated springs. This paper has not contributed to the work described in this thesis, but it served to show that there is a potential market for sulcated springs. Detailed technical information given in the paper is minimal, but a good point about the paper was that the sulcated spring was not examined in isolation, but was often referred to in terms of the advantages which were

suitable to particular applications. The paper appears to have adopted a practical approach concentrating on the end use of the product, with not much disclosure of the theory involved, in contrast to the present work which has concentrated on providing a theoretical basis for the design of the sulcated spring.

The paper by Thompson *et al.* [17], although relevant, has not been referred to due to the fact it was not discovered until three months before the submission of this thesis. At that stage, the majority of the research work had been completed. One of the main differences is that the work in their paper has been oriented towards a sulcated spring with straight end sections which are inclined at an angle. In this thesis only sulcated springs with horizontal straight end sections have been considered. The theoretical approach for the calculation of spring stiffness appears to be similar to that used in Chapter Three of this thesis. Although beam theory was used for the stress calculation in their paper and in this thesis, a different approach was used. Since there was no comparison with experimental results, there is no evidence that one method is better than another.

The theoretical design program of Thompson *et al.* appears to comprise of an iterative process for selecting possible geometrical permutations within the acceptable tolerances for stiffness and stress. Although a flow diagram is given, the process is not clearly defined. The authors use words like 'geometry of a representative section' when there is no definition of what a representative section is or what parameters are required to generate such a section. What is clear is that, at the end of the process, suitable designs may be found, but the parameters of the design are not listed, they are simply referred to as design 1, design 10 or design 18.

The finite element study by Thompson *et al.* showed that even sulcations produced asymmetric behaviour and odd sulcations produced "eccentric

behaviour". This is contrary to the results produced by SRAMA [4, 19]. The difference could be attributed to the fact that SRAMA used sulcated springs with horizontal straight end sections and their conclusions were based on experimental observation. On the other hand, Thompson *et al.* used angled straight end portions and their results were determined from finite element analysis. There may have also been a difference in the end constraints to allow clamping, which was not present in the experiments conducted by SRAMA.

Overall, the paper does not compare the theoretical and finite element results with experimental results. There is no way of knowing how these predictions compare with the tested spring. There is no mention of hybrid sulcated springs (see section 3.3.2) or sulcated springs of different fibre orientations. The weakness in their theoretical model is that different fibre orientation stacking sequences cannot be accommodated in the stiffness and stress calculation, and orthotropic material properties are not considered in the model to compute the stiffness. Their finite element model is in three dimensions and uses orthotropic elements, therefore the model is capable of considering different fibre orientations. However no predictions for different fibre orientations are shown.

Chapter 3

AN ANALYTICAL APPROACH TO COMPUTATIONAL SULCATED SPRING DESIGN

3.1 Introduction

There has been a need for specialized knowledge of spring materials and spring design since the spring industry began in the 1850's. The basic principles of spring calculation and material selection (see Appendix 1.3 and 1.4) are the same for a composite spring. Whatever the proposed composite replacement design, the requirements of spring design as described in Appendix One must be adhered to. This chapter shows the initial research carried out to obtain theoretical predictions of the mechanical behaviour for the sulcated spring.

3.2 Sulcated spring Geometry and Parameters defined

The geometry of a sulcated spring is shown in Figure 3.1. A curved section B-C is thus defined as the circular section between the two points of the radial tangents. A straight limb is defined as the section between the tangent points C and D at their respective radial sections. Other notations are the radius, r, spring thickness t, and depth d. The limb angle α is defined as the angle between the straight limb and the horizontal.

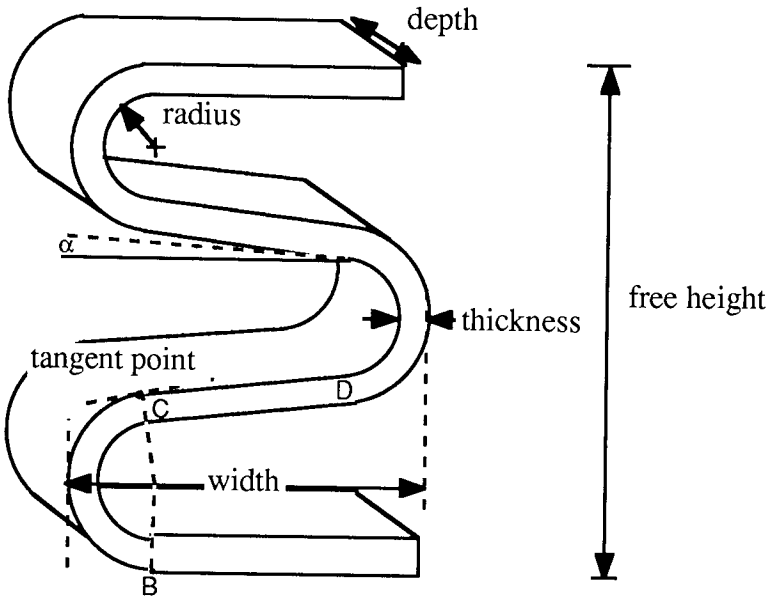

Figure 3.1 Sulcated spring geometry and parameters defined.

The spring width w, is the shortest horizontal distance between the two vertical tangents of the curved section. The number of sulcations n, is defined as the number of curved sections. The free height is defined as the vertical height of the spring with no load applied. Finally the solid height is defined as the vertical height of the spring when the tangent point of the sulcation above and below make contact on one side of the spring.

3.3 Types of Sulcated springs

3.3.1 Sulcated springs of one fibre type

Linear rate sulcated springs are designed to produce a linear load-deflection characteristic, they are simpler to understand, predict and are used more often. Hence more basic research was conducted in this area. The majority of sulcated springs have been manufactured from glass fibre epoxy resin. A few springs were manufactured from carbon fibre epoxy resin. In both cases the springs are manufactured from one type of fibre and one resin system, thus producing one material.

3.3.2 Sulcated springs of two fibre types

In order to produce different material properties, some linear rate sulcated springs were manufactured using two fibres and one resin system. These springs are otherwise known as hybrid sulcated springs which are fabricated by placing layers of different fibres in a symmetrical and balanced (see 4.3.2 for explanation) layer scheme. If the layup scheme is non-symmetrical, changes in temperature would lead to bending, stretching, coupling and warping. A hybrid composite material may be used in preference to a composite of one-fibre type for reasons of cost, weight, strength or to reduce stresses.

In sulcated spring designs, of one-fibre type there are sections of the design which are least utilised, for example the core of the laminate. This portion has the least bending stress, due to its location near the neutral axis, and the contribution to spring stiffness in this portion is minimal. It is therefore possible to replace these under-utilised fibres with fibres of less cost, strength or stiffness. Another reason for chosing a hybrid combination may be to obtain a wider range of physical and mechanical properties. At the interface of each dissimilar lamina, the normal stress and shear stress distributions are non-uniform and discontinuous. It is possible to create a stress distribution with maximum normal stresses and shear stresses at desired places by altering the lamination configuration.

3.4 Design Procedure for Sulcated springs

3.4.1 Overview of Design Requirements

Theoretical conventional spring design can be divided into two forms for obtaining information, as shown on the following page in Figure 3.2. The first is often termed a parametric checking routine which allows a spring designer the opportunity to obtain theoretical estimates of the spring's likely behaviour.

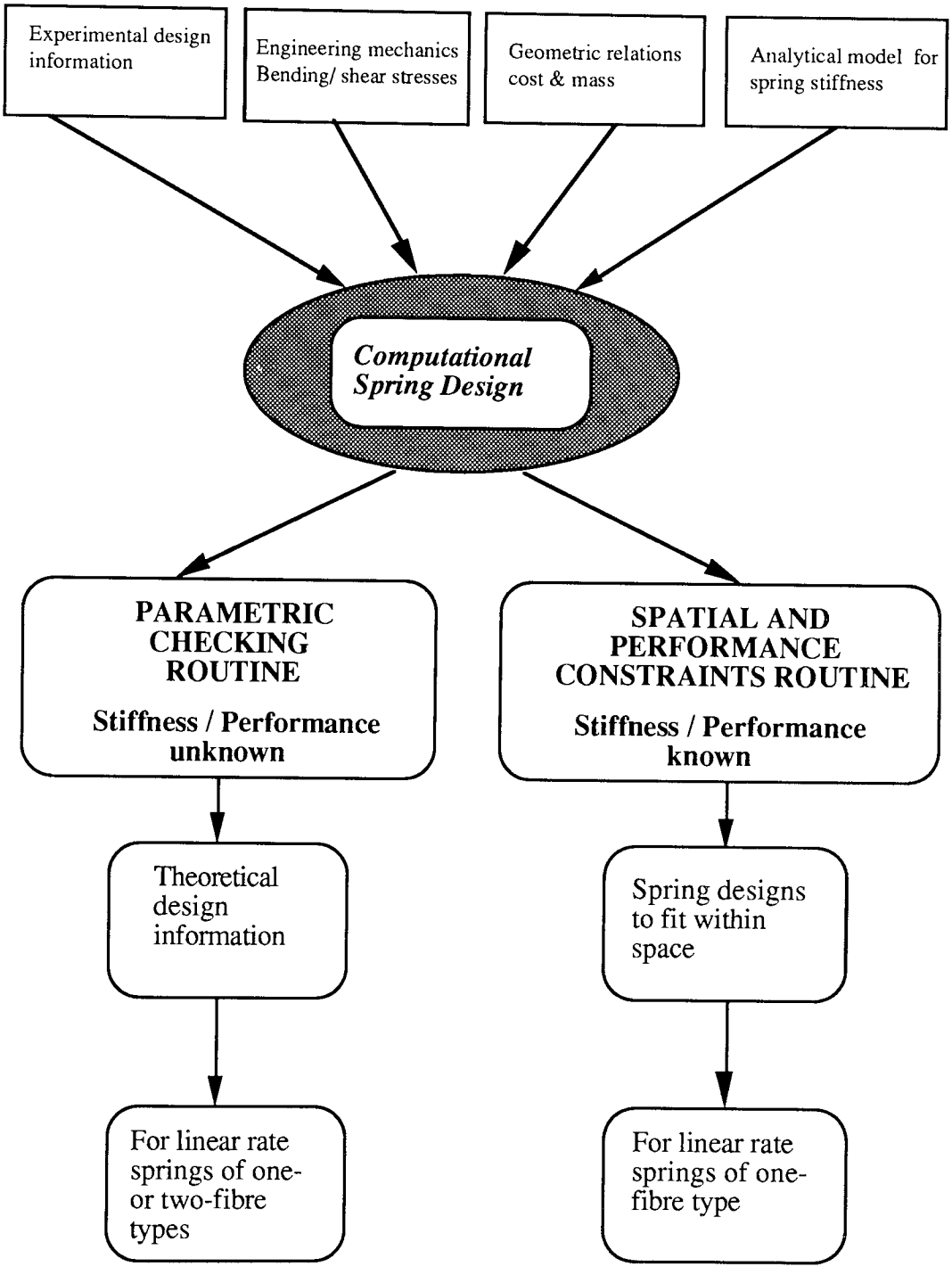

Figure 3.2 Format for computational sulcated spring design.

In conventional coil spring design, parameters such as the number of coils, the helix angle, inside and outside diameter (see Appendix 1) are entered into spring design formulae or spring design software. Estimates for the load/ deflection characteristics, solid height, solid load, and maximum stresses can then be obtained. The second type is when the spring design is unknown, and a design is required to fit within a given space whilst satisfying specific performance requirements. The same principle has been applied to the sulcated spring design software.

The parametric checking routine has been developed for sulcated springs of one and two (hybrid) fibre types. The spatial and performance constraints routine has been developed for springs of one-fibre type. In order to provide computational design information various sources were used. These were,

1. Design information from literature and experiments.
2. Geometric relations of spring parameters.
3. Engineering mechanics, bending and shear stresses.
4. An analytical model for spring stiffness.

Experimental design information established what the design limitations were. Literature and discussions on design recommendations can also help. This information can be used directly in the design software to advise the user, or reject impractical spring designs. Geometric relations have been derived to relate the parameters to the free and closed height, so that these equations can be used to provide information directly or indirectly by algebraic manipulation to produce spring designs. Engineering mechanics has been used to derive equations for the bending and shear stresses of a sulcated spring of one and two materials and an analytical model was developed to predict the spring stiffness. The spring stiffness is an important parameter which is used to

calculate the theoretical estimate of deflection and solid load. It was also used to calculate the spring stiffness for spring designs within the designer's spatial and performance requirements.

3.4.2 Parametric checking spring design routine

The parameter checking routine consists of the user specifying the sulcated spring parameters of: sulcation radius, laminate thickness, width, depth, number of sulcations and elastic modulus of the material. Parameters were then checked for impractical designs. From experimental work conducted the design limiting factors shown in Table 3.1 have been found.

PARAMETER	Value	COMMENTS
Number of Sulcations	> 1	Spring must have an odd number of sulcations otherwise excessive lateral deflections will occur.
Laminate Thickness (mm)	> 0.125 mm	
Sulcation Radius	> 3 mm	
Ratio radius to thickness	>3	
Maximum Bending stress	< 750 MPa < 1200 MPa	(for glass fibre) (for carbon fibre)

Table 3.1 Design limiting factors for parameter checking routine.

After the spring parameters have been verified to be practically feasible, theoretical calculations can be obtained to predict the mechanical behaviour of the sulcated spring. Theoretical predictions such as the spring rate, free height, solid height, solid load (load supported at solid height), solid stress (maximum bending stress value at solid height), and weight can be made. More specific

calculations are possible such as the deflection under a specified load, maximum shear stress under a specified load, or material cost. The format is shown in Figure 3.3. For hybrid sulcated springs, the parameter checking routine remains the same, the format is more or less the same for hybrid sulcated springs as shown in Figure 3.4.

3.4.3 Spatial and performance constraints routine

The spatial and performance constraint routine produces sulcated spring designs which conform to the user's requirements. The spatial constraints form a "space envelope" of the dimensions: width, height and depth. Performance criteria include the range of maximum load to be supported, spring rate required, and the elastic modulus of the material.

PARAMETER	Value	COMMENTS
Number of Sulcations	$3 \leq n \leq 19$	Spring must have an odd number of sulcations .
Laminate Thickness	$t > 0.125$ mm	
Sulcation Radius	$r > 3$ mm	
Angle alpha	$-20 \leq \alpha \leq 20$	
Maximum Bending stress for glass fibre for carbon fibre	 < 750 MPa < 1200 MPa	

Table 3.2 Design limiting factors to allow only practically feasible spring designs.

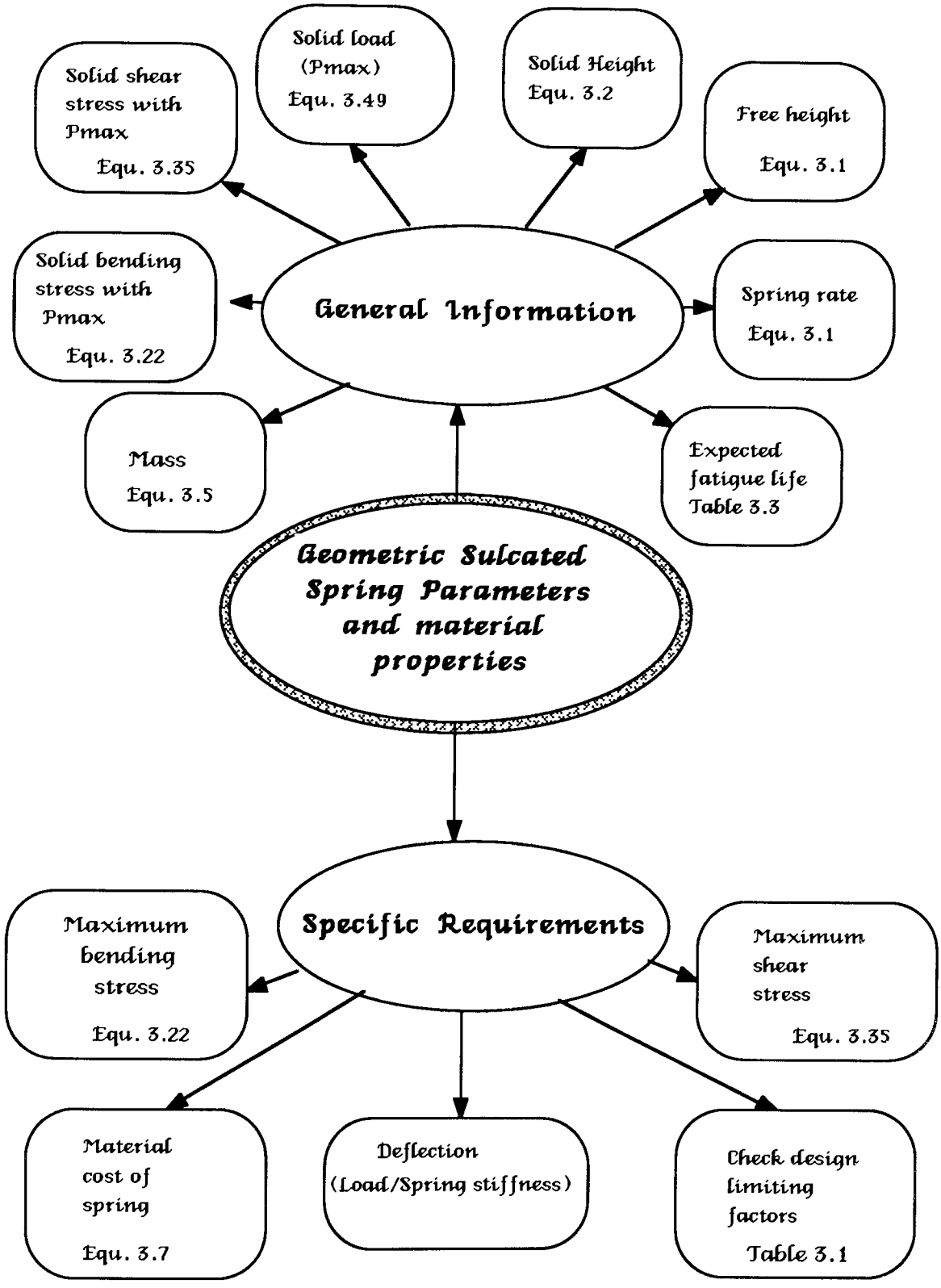

Figure 3.3 Format of parameter checking routine.

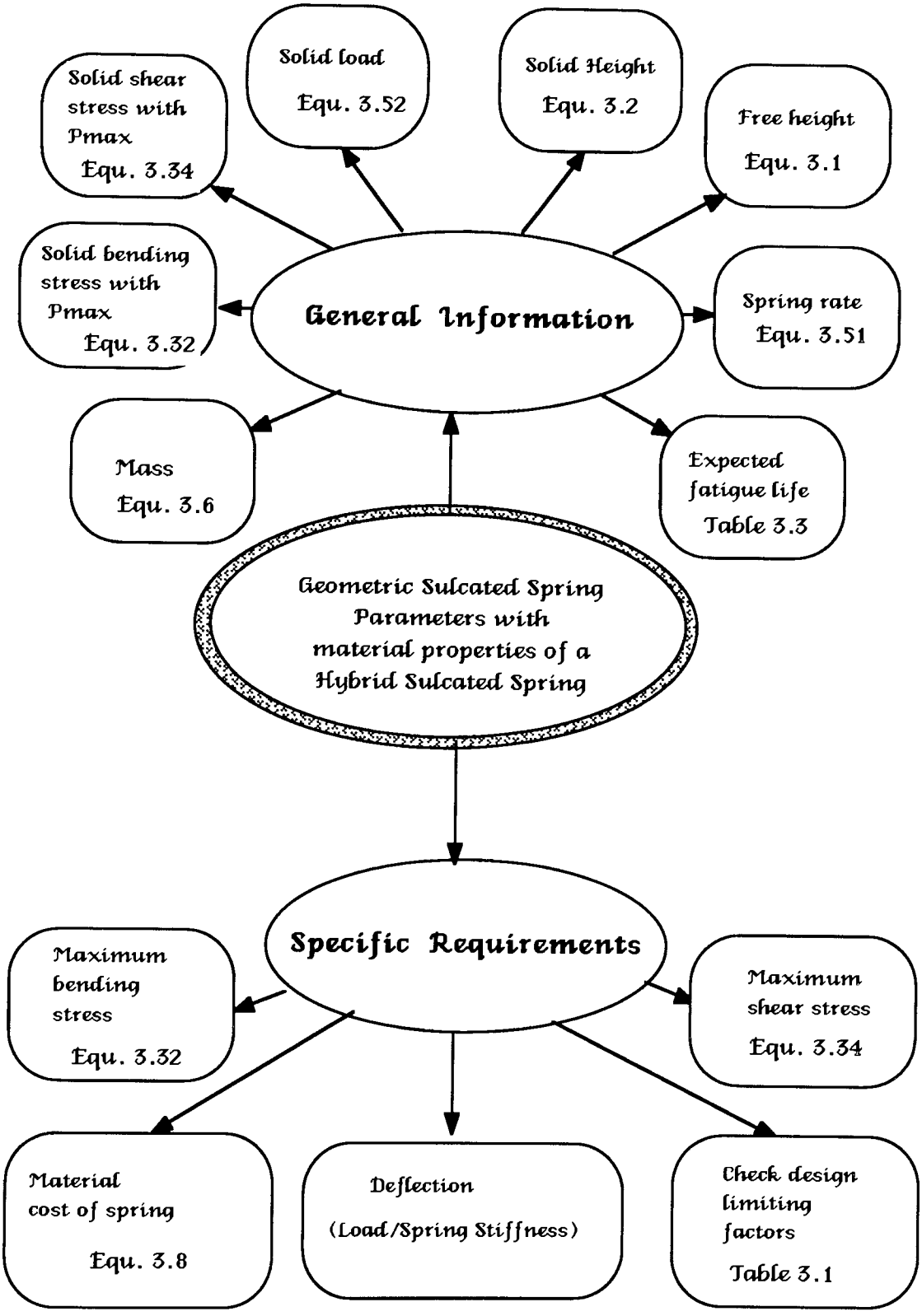

Figure 3.4 Format of the parameter checking routine for hybrid sulcated springs.

There are six known variables in the spatial and performance requirements routine, the width, height and depth of the space envelope, and the range of maximum load support, spring rate, and elastic modulus of the material. The method assumes the dimensions of the free height, depth, and width of the sulcated spring to be equal to the height, depth, and width of the space envelope. Initial values are set at the start of the routine for the number of sulcations, angle α, and thickness. The radius is calculated from the geometric relation for free height (see equation 3.1). There are three design requirements for the radius, one is that the width must be greater or equal to two times the radius plus two times the thickness. The other is the radius must be greater than the thickness, to make fabrication easier. Finally the radius must be greater or equal to the minimum radius specified by the user. The absolute minimum is 3 mm however, depending on mould tool production and fabrication facilities, designs with a small radius may not be possible, so including this option allows flexibility.

After the requirement for the radius has been satisfied, the spring stiffness using the initial and calculated values is found using equation 3.47 (page 94). The maximum deflection (equation 3.50) and maximum load supported (equation 3.49) are calculated. Using the maximum load supported and the current geometric parameters, the maximum bending stress is calculated using equation 3.22. If this value is below the user's recommended specified design stress, then the geometric parameters form one of the suggested sulcated spring designs. The routine continues by increasing the number of sulcations, angle α, and thickness until the range is exceeded. After a suitable design has been found using this design routine, the weight of the sulcated spring design is calculated.

The values for the maximum bending stress are obtained from the manufacturer's published compressive strength values for the respective materials. A sulcated spring should be capable of withstanding a bending stress up to a value equal to the compressive material strength. For glass fibre/ epoxy resin material, the value is 750 MPa, for carbon fibre /epoxy resin the compressive strength is 1200 MPa. These are the recommended design stresses, however it is also important to consider Table 3.3 which shows the results from fatigue tests, so that the user is aware of the set down (softening effect) which may occur if the maximum bending stress becomes close to the compressive strength.

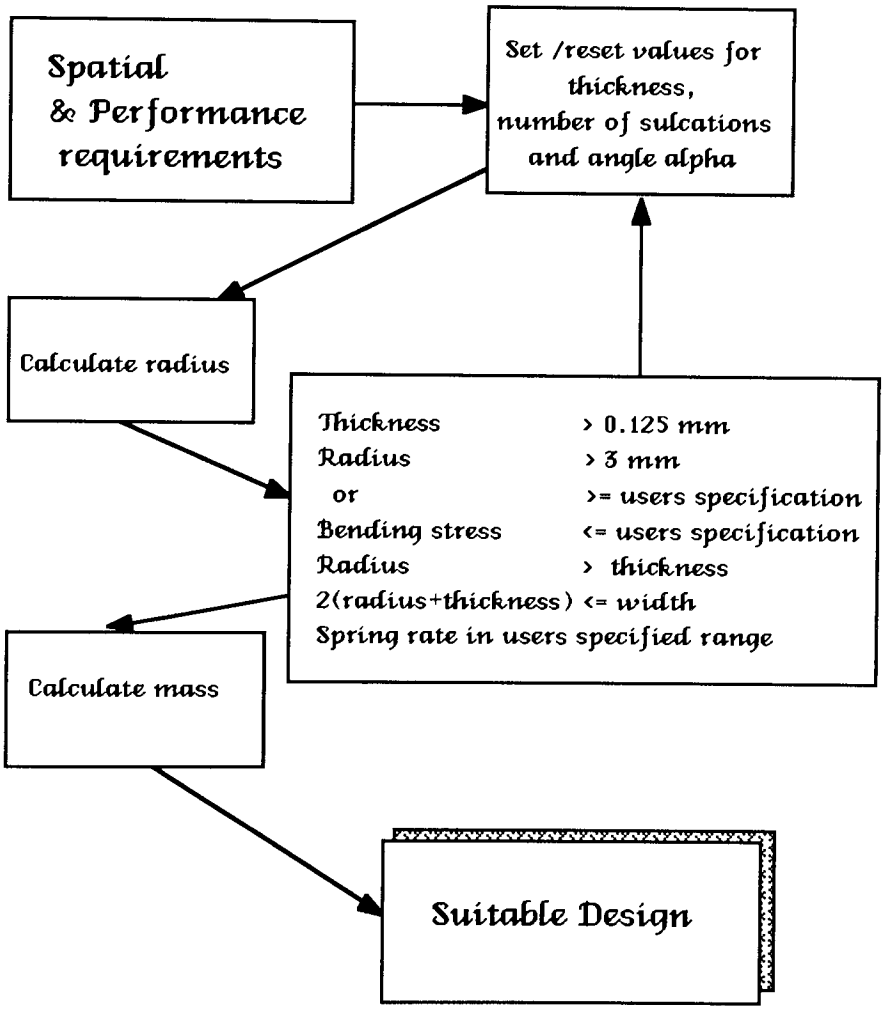

Figure 3.5 Method for finding suitable spring designs.

3.5 Experimental Design Information

Of the experimental results available, information on the fatigue life is the most important to computational design. The inclusion of fatigue results allows the user to obtain advice on a particular sulcated spring design, and to warn or reject impractical spring designs. Figure 3.6 shows the S-N curve of a glass fibre epoxy resin sulcated spring showing a design life of 10^6 cycles when up to 5% loss of load carrying capacity can be accommodated, a maximum applied stress of up to 590 N/mm^2 is possible. A design for infinite life would have to survive 10^7 load cycles.[4] Figure 3.7 shows a graph of the percentage load loss against number of cycles for a sulcated spring design.

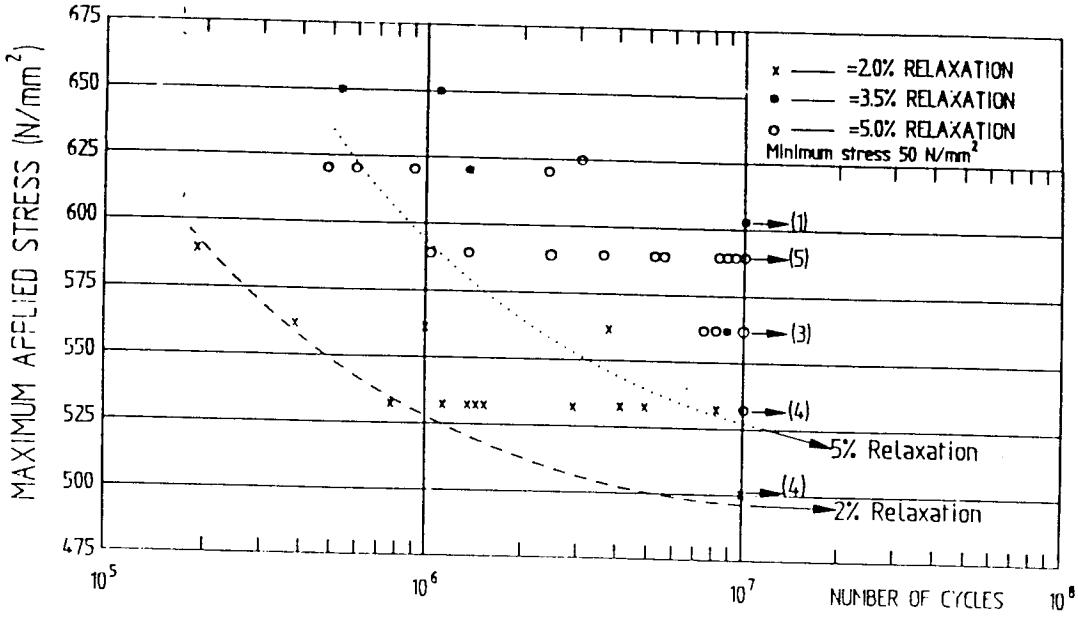

Figure 3.6 S-N curve for a sulcated spring.[19]

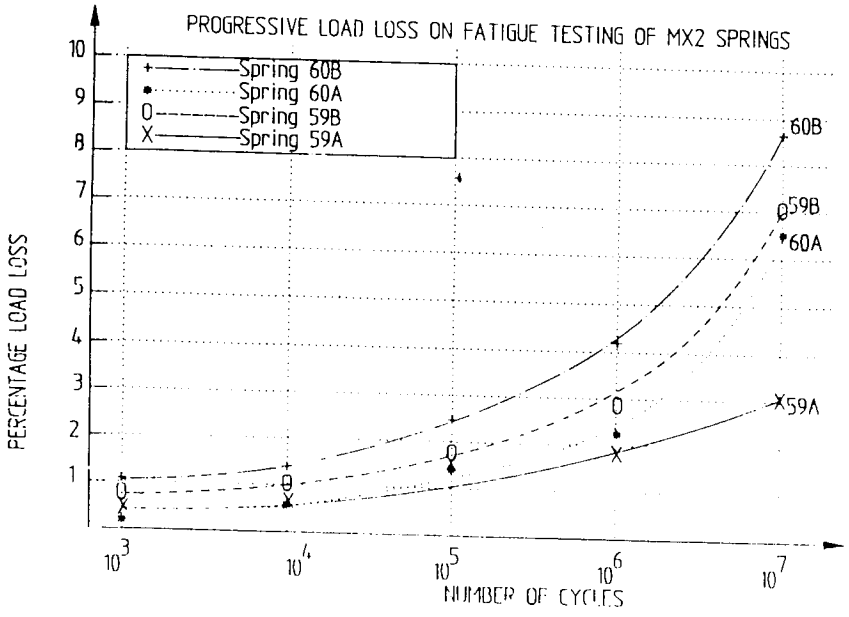

Figure 3.7 Percentage load loss in a sulcated spring in fatigue. [4]

From these fatigue graphs it has been possible to summarise this information as shown in Table 3.3. This information has been included in the design computer software.

Material	**No. of load cycles**	**% loss in load**	**Applied stress (N/mm^2)**
Glass fibre /epoxy resin	10^6	2	530
"	10^7	2	490
"	10^6	5	590
"	10^7	5	530
Hybrid carbon(4)/glass(12)/carbon(4) fibre epoxy resin	10^7	2	1000

Table 3.3 Design Table for fatigue life estimation of sulcated springs.

3.6 Geometric relations, Cost and Mass

Geometric relations are equations which relate the geometric parameters of thickness (t), radius (r), width (w), depth (d), number of sulcations (n) and angle α. Thus the equations for free height (F) and solid height (S) are:

$$F = 2t + (n - 1)(w - 2t - 2r)\tan\alpha + \frac{(n-1)t}{\cos\alpha} + 2nr \qquad \text{-(3.1)}$$

$$S = (n+1)t + (n+1)r \qquad \text{-(3.2)}$$

These equations have been derived for the sulcated spring design to enable the geometric parameters to be related to a measurable quantity. By relating the parameters, an indication of the percentage error can be obtained if the parameters do not equate to the experimental value of free or solid height. If all springs were manufactured or measured accurately, the relationships should give the theoretical value of free or solid height. These equations can also be manipulated to obtain the dimensions of one parameter if others are known, as in the case of the spatial and performance constraint routine.

Equations have been derived to calculate the weight and material cost of a sulcated spring.

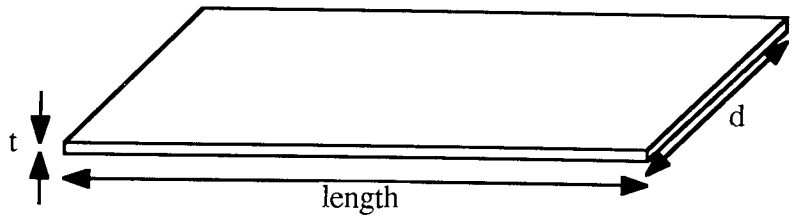

Figure 3.8 Dimensions of spring material.

Sulcated spring mass

Length of 'prepreg' material = $2L_1 + (n-1)L_2 + 2\rho\beta + (n-2)\rho\beta_1$ **-(3.3)**

where $L_1 = w - t - r$ $\quad L_2 = \frac{w - 2t - 2r(1-\sin\alpha)}{\cos\alpha}$

$\beta = \pi - \alpha$ and $\beta_1 = \pi - 2\alpha$ (as shown in Figure 3.12, page 78).

Volume = $(2L_1 + (n-1)L_2 + 2\rho\beta + (n-2)\rho\beta_1)t\,d$ **-(3.4)**

MASS = VOLUME x DENSITY

Mass= $\{2L_1 + (n-1)L_2 + 2\rho\beta + (n-2)\rho\beta_1\}t\,d$ x density **-(3.5)**

Density of Glass fibre / epoxy resin (ρ_g) = 1932.8 kg/m^3

Density of Carbon fibre / epoxy resin (ρ_c) = 1720.0 kg/m^3

Mass of a hybrid spring = $\frac{\text{Volume}}{\text{Total no. layers}}(N_g\rho_g + N_c\rho_c)$ **-(3.6)**

where N_g is the number of layers of glass fibre/ epoxy resin.

N_c is the number of layers of carbon fibre/ epoxy resin

Material Cost

Material cost = Area of one layer x Number of layers x Cost per square metre **-(3.7)**

where Area of one layer = $\{2L_1 + (n-1)L_2 + 2\rho\beta + (n-2)\rho\beta_1\}d$

Material cost of a hybrid spring = Area of one layer $(N_gC_g + N_cC_c)$ **-(3.8)**

where C_g is the cost of glass fibre/ epoxy resin per m^2

C_c is the cost of carbon fibre/ epoxy resin per m^2

3.7 Engineering Mechanics of Sulcated springs

3.7.1 Experimental foundation and force analysis

To analyse the force system acting on a sulcated spring, it is important to examine the experimental loading conditions. Figure 3.9 shows the source of experimental load application and restraints of a sulcated spring under a load test. A load test is usually conducted to obtain the spring stiffness or spring rate. The base platen remains stationary whilst the top platen moves as the load is increased and the corresponding deflection is measured until the solid height is reached as shown in Figure 3.10.

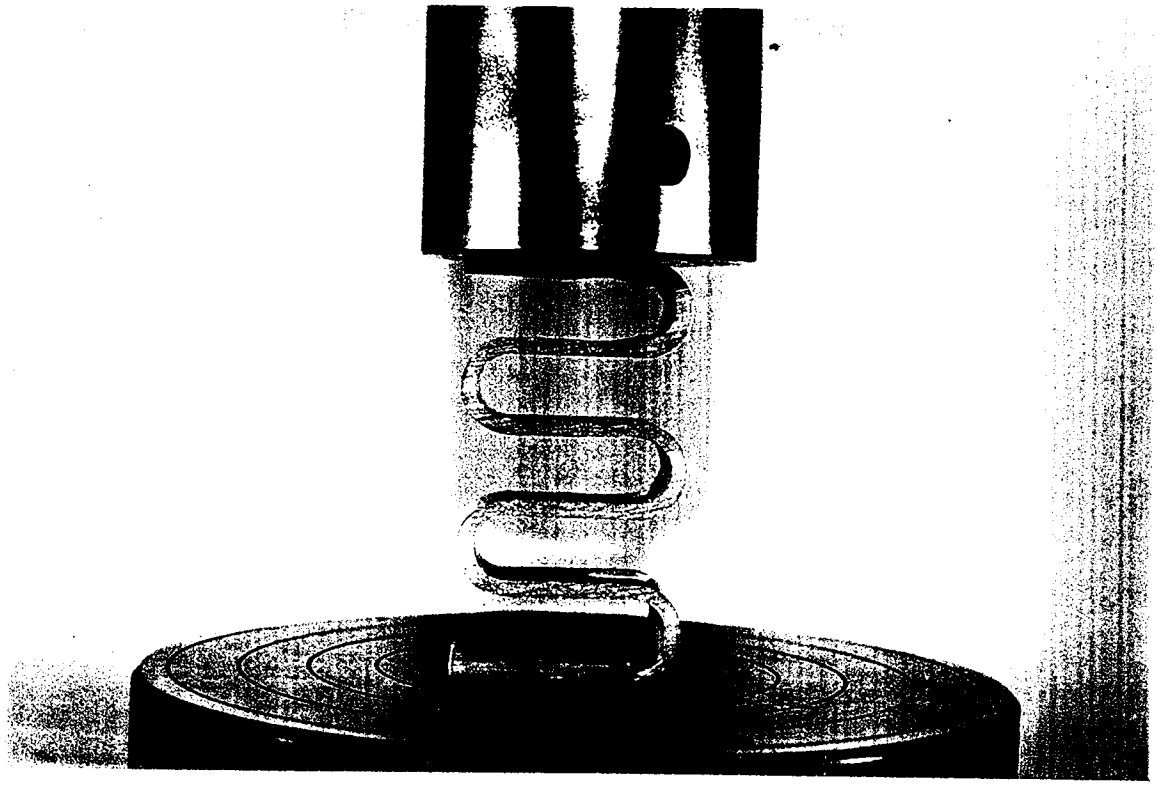

Figure 3.9 Sulcated spring under load test (at free height).

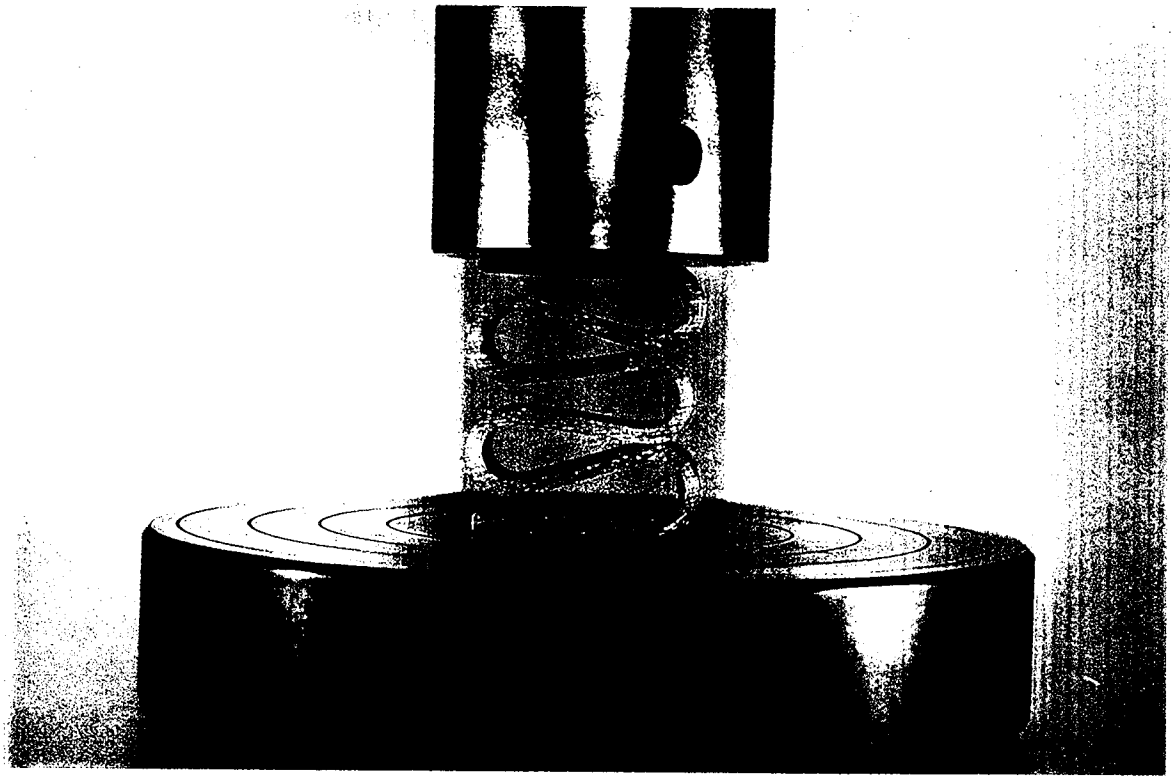

Figure 3.10 Sulcated spring under load test (at solid height).

In analysing the force system of the sulcated spring design, it is particularly important to consider the externally applied loads which cause bending and thus give rise to internal reacting forces. These have to be determined before it is possible to calculate stresses and deflections. When first analysing any force system acting on a component or structure, it is essential to have a free body diagram showing all the known and unknown forces which act on the component. Figure 3.11 shows a free body diagram of a sulcated spring.

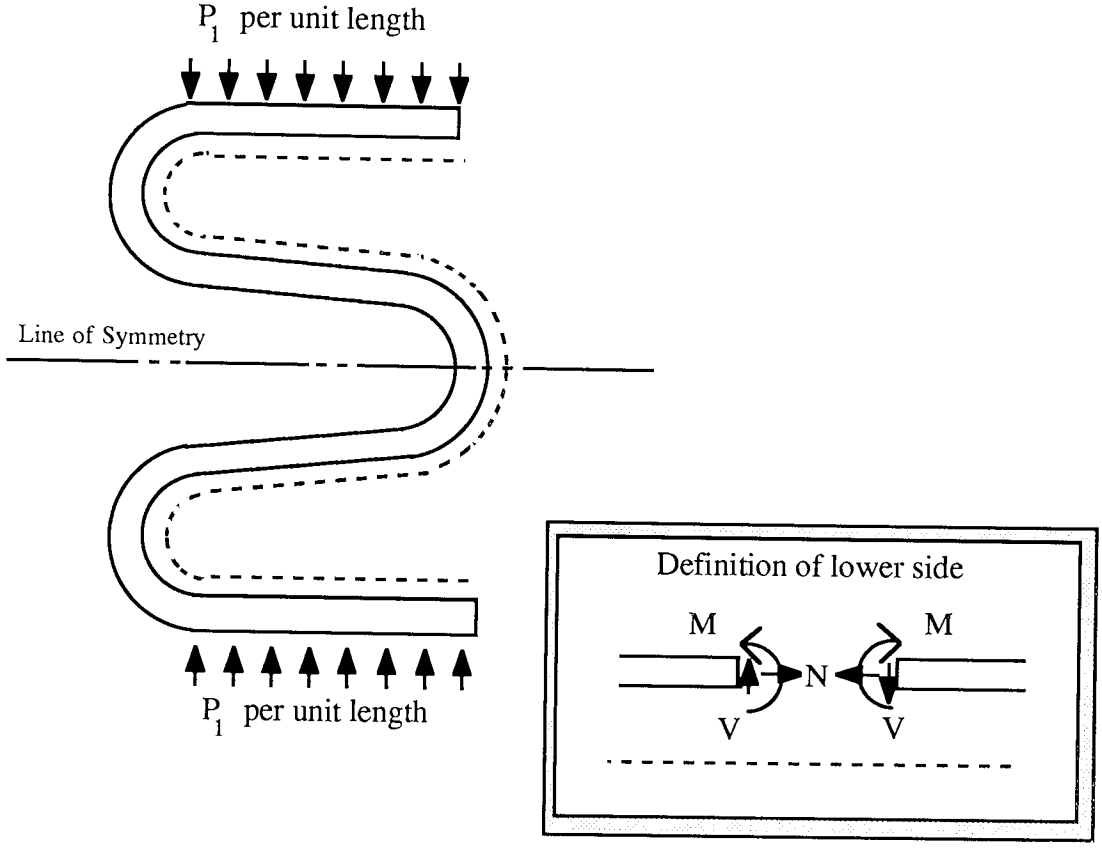

Figure 3.11 Free body diagram of a sulcated spring showing internal and external forces and moments.

The load distribution produced by the platen is assumed to be that of a uniformly distributed load and P_1 is the external reaction per unit length at the base of the sulcated spring. Internal forces and couples are obtained by inserting at the cut sections the necessary forces and moments for equilibrium.

3.7.2 Bending moment, shear and normal force of a sulcated spring

Equations for the internal shear force (V), bending moment (M) and normal force (N) acting at each point along the sulcated spring axis indicate the areas which are subject to the greatest shear, bending or normal stresses. The end straight limb sections remain parallel and in contact with the top and bottom platen surfaces and the model also shows this to be true. Equations of

equilibrium in two dimensions are applied to the remainder of the model to establish the bending moment and shear force of a sulcated spring.

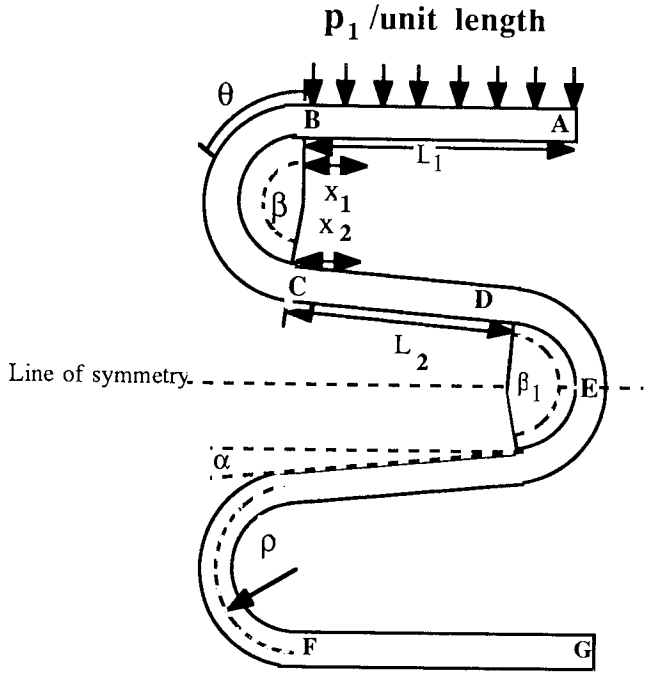

Figure 3.12 Sulcated spring model.

For the curved section BC

$$\Sigma M_{BC} = 0$$

$$M_{BC} + p_1 L_1 \left(\frac{L_1}{2} + \rho\sin\theta\right) = 0 \qquad \text{where } P=p_1L_1$$

$$\mathbf{M_{BC} = -P\left(\frac{L_1}{2} + \rho\sin\theta\right)} \qquad \mathbf{-(3.9)}$$

$\Sigma F_x=0$ $-N\cos\theta - V\sin\theta = 0$

$\Sigma F_y=0$ $-N\sin\theta + V\cos\theta - p_1L_1 = 0$

$$\mathbf{V_{BC} = P\cos\theta} \qquad \mathbf{-(3.10)}$$

$$\mathbf{N_{BC} = P\sin\theta} \qquad \mathbf{-(3.11)}$$

For the straight section CD

$\Sigma M_{CD} = 0$

$$M_{CD} - p_2 L_2 \cos\alpha\left(\frac{L_2}{2} - x_2\right) = 0$$

where p_2 is the force per unit L_2 and $P=p_2 L_2$.

$$\mathbf{M_{CD}=p_2L_2\cos\alpha\left(\frac{L_2}{2} - x_2\right)} \qquad \textbf{-(3.12)}$$

$\Sigma F_x=0 \quad N + P\sin\alpha = 0$

$\Sigma F_y=0 \quad -V - P\cos\alpha = 0$

$$\mathbf{V_{CD} = p_2L_2\cos\alpha = P\cos\alpha} \qquad \textbf{-(3.13)}$$

$$\mathbf{N_{CD} = -P\sin\alpha} \qquad \textbf{-(3.14)}$$

For curved section DE

$\Sigma M_{DE} = 0$

$$M_{DE} + p_2 L_2\left(\frac{L_2}{2} + \rho\sin\theta\right) = 0$$

$$\mathbf{M_{DE} = -P\left(\frac{L_2}{2} + \rho\sin\theta\right)} \qquad \textbf{-(3.15)}$$

$$\mathbf{V_{DE} = P\cos\theta} \qquad \textbf{-(3.16)}$$

$$\mathbf{N_{DE} = P\sin\theta} \qquad \textbf{-(3.17)}$$

3.7.3 Bending stress of a sulcated spring

From the equations for the bending moment and shear force, the bending and shear stress can be calculated. The area of maximum stress concentration is at the curved section. Therefore the bending and shear stresses were calculated

around this region to derive expressions for the maximum stress using beam theory.

The assumptions are:-[20]

1. Transverse sections of the beam which are plane before bending will remain plane during bending.
2. Transverse sections will be perpendicular to circular arcs having a common centre of curvature.
3. Radius of curvature is large compared with the transverse dimensions.
4. Longitudinal elements of the beam are subjected only to simple tension or compression, and there is no lateral stress.
5. Young's modulus for the beam material has the same value in tension and compression.
6. Deflections are small.
7. The cross-section of the beam is symmetrical.
8. The beam material is homogeneous and isotropic.
9. The effects of shear are negligible.

If the laminate thickness is small compared with the radius of curvature, then the stress distribution is linear across the thickness as for straight beams. The bending stress acting on a straight beam with a compressive normal force and bending moment is,

$$\sigma = -\frac{N}{A} + \frac{My}{I} \qquad \textbf{-(3.18)}$$

where $I = \frac{dt^3}{12}$, $A = dt$, the bending moment of the curved section is

$$M = P(\frac{L_1}{2} + \rho\sin\theta) \qquad \textbf{-(3.19)}$$

and the normal force is $N=P\sin\theta$ as in equations 3.11 and 3.17.

At the position of maximum bending stress $\theta=90^{o}$

$$M = P(\frac{L_1}{2} + \rho) \qquad \text{-(3.20)}$$

$$N=P \qquad \text{-(3.21)}$$

However, if the laminate thickness is of the same order as the radius of curvature then a non-linear stress distribution occurs during bending and the neutral axis shifts towards the centre of curvature of the beam by a distance $\bar{y}$, as shown in Figure 3.13.

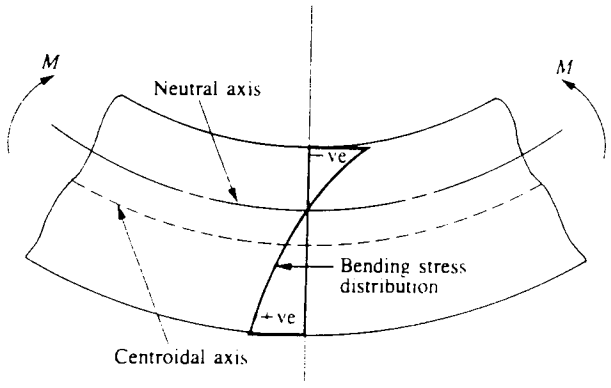

Figure 3.13 Distribution of stress in a thick curved beam.

The neutral axis no longer passes through the centroid of the cross-section, as in the initially straight beam case, and the bending stress distribution over the cross-section is hyperbolic in nature. The bending stress becomes,[21]

$$\sigma = \frac{My}{A\bar{y}(r_n+y)} \qquad \text{-(3.22)}$$

The maximum stress always occurs at the outer fibres on the concave side of the beam, and the neutral axis always lies between the centroidal axis and the centre of curvature. For sulcated spring design the radius of curvature to the neutral axis is

$$r_n = \frac{t}{\ln\left(\frac{r_o}{r}\right)} \quad \text{and} \quad \bar{y} = \rho - r_n \qquad \text{-(3.23)}$$

In a thinner laminate the ratio of r_o to r may be much closer to unity. A better approximation would be,

$$\ln\left(\frac{r_o}{r}\right) \approx \frac{t}{\rho}\left(1 + \frac{t^2}{12\rho^2}\right) \qquad \text{-(3.24)}$$

$$r_n \approx \frac{12\rho^3}{12\rho^2 + t^2} \qquad \text{-(3.25)}$$

$$\text{and } \bar{y} \approx \frac{t^2}{12\rho} \qquad \text{-(3.26)}$$

In the case of the sulcated spring, the formula selected depends on the spring design. In general, a thinner laminate is usually selected because it is easier to fabricate, and there is less chance of fibre misalignment. Therefore the thickness is likely to be less than the radius. Hence the formula for straight beams will apply to the majority of cases. However the formula has been included in this thesis to show how the stress distribution varies if the radius and thickness are of the same order.

3.7.4 Comparison of theoretical and experimental bending stress

The formulae discussed in the previous section were validated with experimental results produced by the University of Sheffield. Strain gauges were attached to a sulcated spring on the outer tensile surface as in Figure 3.14.

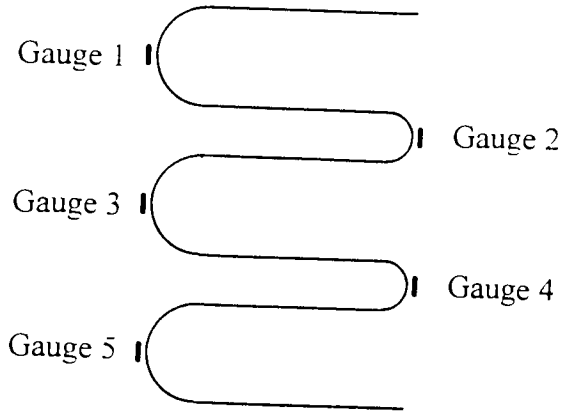

Figure 3.14 Gauges attached to a sulcated spring A6.

The spring was compressed using a Mayes testing machine and the output of load and strain from each strain gauge was recorded using a chart recorder. The results were plotted as shown in Figure 3.15.

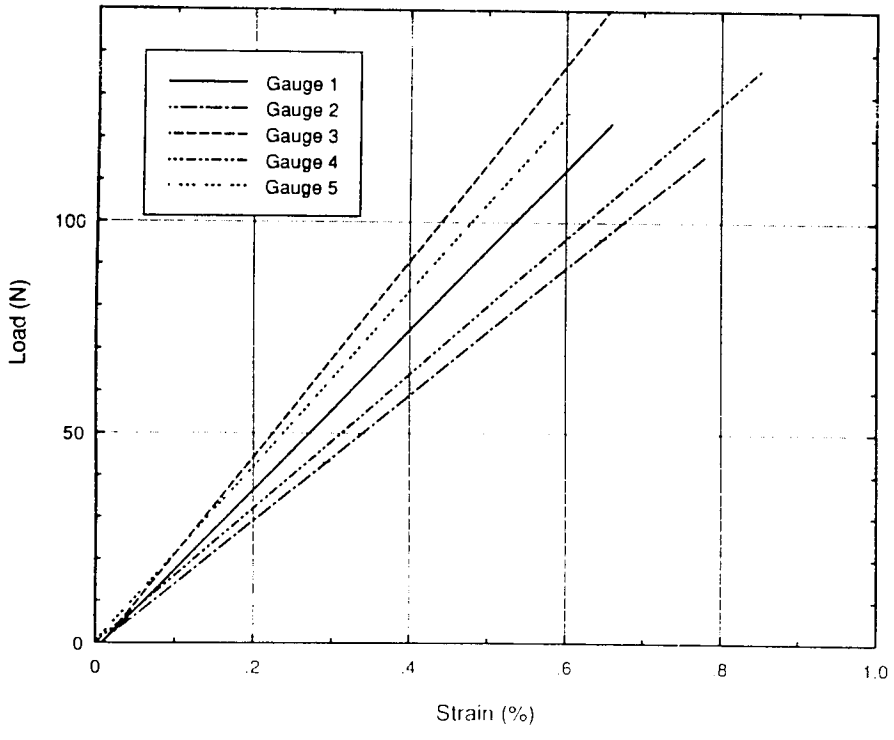

Figure 3.15 Load - strain relationship at each sulcation.

The relationship between compression (P) and maximum tensile stress (σ) using the least square method and a Young's modulus of 40.8 GPa is:

Gauge 1: σ=2.1445P MPa

Gauge 2: σ=2.7167P MPa

Gauge 3: σ=1.7565P MPa

Gauge 4: σ=2.5471P MPa

Gauge 5: σ=1.9592P MPa

The laminate thickness and radius at each sulcation was

Gauge 1: t = 1.38+/-0.06 mm r=7.68 mm

Gauge 2: t = 1.31+/-0.03 mm r=6.01 mm

Gauge 3: t = 1.44+/-0.03 mm r=7.65 mm

Gauge 4: t = 1.36+/-0.02 mm r=5.98 mm

Gauge 5: t = 1.38+/-0.03 mm r=7.68 mm

The experimental determination of strain and following stress calculation shows that the stress distributions at the position of gauges 1,2,3,4 and 5 are not the same. If the spring was perfectly formed and the radius and thickness at gauges 1 and 5 are the same, then the strain would be the same at sulcations 1 and 5, due to symmetry. Similarly gauges 2 and 4 would be the same. Gauge 3 would undergo less strain due to the deflection profile which tends to occur, as shown in Figure 3.10. In Figure 3.10, the left sulcations form closed loops at solid height, with the right sulcations there are open loops where the spring has not made contact. Now if a constant radius and thickness is assumed, as was the case in Figure 3.10, the stress would be greater for a closed loop than for a partially closed loop. This difference between a closed and partially closed loop of the same cross-section and radius could only be due to a difference in the load. Therefore in the case of the sulcated spring, it is the distribution of load throughout the spring which may affect the stress

distribution. It is unclear as to what extent the load distribution affects the stress at the position of the strain gauges.

From the experimental results, measurement of the radius and thickness at the position of placement of the strain gauge reveals that, as well as the differences between the left and right radii, there is a difference in radius and thickness at each sulcation. Therefore there are two points to consider in analysing the experimental results, one is the differences in sulcation radii and thickness, and the other is the effect of the load distribution on the deflection profile.

To obtain theoretical estimates of stress, equation 3.18 with assumptions of a linear stress distribution, and equation 3.22 for a hyperbolic stress distribution across the thickness were applied. The results are shown in Table 3.4.

Gauge	Linear distribution (MPa)	Hyperbolic distribution (MPa)	Experimental (MPa)	Difference of linear distribution from experimental(%)	Difference of hyperbolic distribution from experimental(%)
1	2.472	2.373	2.145	13.2	9.6
2	2.517	2.394	2.717	-7.9	-13.5
3	2.266	2.172	1.757	22.5	19.11
4	2.331	2.214	2.547	-9.3	-15.04
5	2.472	2.373	1.959	20.8	17.5

Table 3.4 Theoretical and experimental results for bending stress under a load of 1 N.

From Table 3.4 it is evident that using the formula which assumes a linear distribution for the tensile surfaces of gauges 2 and 4 provides more accuracy. Assuming a hyperbolic distribution gives a more accurate stress value on the

tensile surface of gauges 1, 3 and 5. It was difficult to form conclusions from these results because of the differences in thickness and radius at each sulcation. The reason for the large discrepancy between the experimental and theoretical predictions could be due to the fact that the resultant force does not pass through the central axis $L_2/2$ of the structure. The theoretical predictions for gauges 2 and 4 are much less than experimental result and for gauges 1, 3 and 5 much greater than the experimental stresses. By using the experimental value of stress to determine the value of $L_2/2$ in the bending stress equation 3.18, the resultant load distribution became off-centre, so instead of being a distance $0.5L_2$ from the larger radii, the distance was between $0.31L_2$ and $0.39L_2$. For the smaller radii the distance was $0.56L_2$ for gauge 2 and $0.57L_2$ for gauge 4. If a value of $0.39L_2$ for gauges 1,3 and 5 is used and $0.61L_2$ for gauges 2 and 4 the discrepancy is substantially reduced, as shown in Table 3.5 for both the linear and hyperbolic distribution.

Gauge	Linear distribution (MPa)	Hyperbolic distribution (MPa)	Experimental (MPa)	Percentage difference of linear distribution from experimental	Percentage difference of hyperbolic distribution from experimental
1	2.148	2.066	2.145	0.14	-3.82
2	2.878	2.733	2.717	5.59	-0.58
3	1.969	1.891	1.757	10.77	7.09
4	2.665	2.527	2.547	4.43	-0.8
5	2.148	2.066	1.959	8.80	5.18

Table 3.5 Table showing theoretical and experimental results for bending stress under a load of 1 N assuming an off-centre load distribution.

3.7.5 Bending stress for a hybrid sulcated spring

The design formula for the bending stress of a symmetrical sandwich hybrid sulcated spring is based on the theory for an initially straight beam, as shown in Figure 3.16.

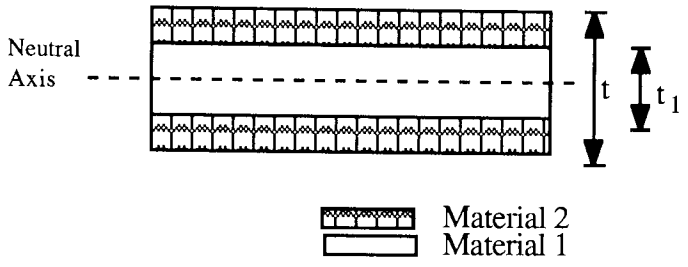

Figure 3.16 Hybrid sandwich beam.

As discussed in the previous section, the thickness must be sufficiently small compared with the radius to apply this formula. The assumptions stated in the last section still apply. The normal stresses σ_x at any distance y from the neutral axis are given by the following equations

$$\sigma_{x_1} = -E_1 \kappa y \qquad \sigma_{x_2} = -E_2 \kappa y \qquad \textbf{-(3.27)}$$

in which σ_{x_1} is the stress in material 1, and σ_{x_2} is the stress in material 2. The elastic modulii in materials 1 and 2 are denoted by E_1 and E_2, and κ is the curvature.

The relationship between bending moment and stresses in beam theory is [22]

$$M = \int \sigma_x y \, dA \qquad \textbf{-(3.28)}$$

$$M = \int_1 \sigma_{x_1} y \, dA + \int_2 \sigma_{x_2} y \, dA \qquad \textbf{-(3.29)}$$

$$M = -\kappa (E_1 I_1 + E_2 I_2) \qquad \textbf{-(3.30)}$$

where the second moments of area are

$$I_1 = \frac{d t_1^3}{12} \text{ and } I_2 = \frac{d}{12}(t^3 - t_1^3)$$

Solving for curvature from equation (3.30)

$$\kappa = \frac{1}{\rho} = -\frac{M}{E_1I_1 + E_2I_2} \qquad \textbf{-(3.31)}$$

where $E_1I_1 + E_2I_2$ is the flexural rigidity of the composite beam.

Substituting (3.31) into (3.27) and taking account of the normal force acting on the curved section gives the bending stresses in materials 1 and 2

$$\sigma_{x_1} = -\frac{N}{A} + \frac{MyE_1}{E_1I_1 + E_2I_2} \qquad \sigma_{x_2} = -\frac{N}{A} + \frac{MyE_2}{E_1I_1 + E_2I_2} \qquad \textbf{-(3.32)}$$

where $y = \frac{t_1}{2}$ for the maximum stress of σ_{x_1}

and $y = \frac{t}{2}$ for the maximum stress of σ_{x_2}

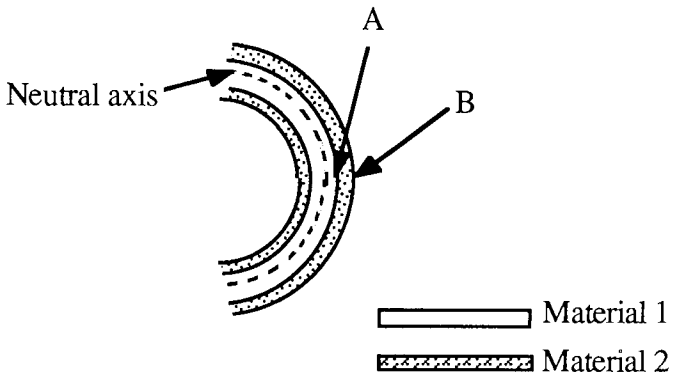

Figure 3.17 Position of maximum bending stress on curved section of a hybrid sulcated spring.

Figure 3.17 shows the curved portion of a hybrid sandwich sulcated spring. The stresses are calculated at the position of maximum bending stress, point A in Figure 3.17, shows where the stresses for σ_{x_1} and σ_{x_2} are calculated. Point B shows where σ_{x_2} is calculated. At the neutral axis the stress is zero, and the

stresses at opposite and equal distances from the neutral axis are equal in magnitude and of opposite sign. The stress distribution is linear except at the interface of the two materials where the stress distribution becomes discontinuous. The experimental stress was not monitored for a hybrid spring, so these formulas have yet to be validated for a sulcated spring.

3.7.6 Theoretical results for the bending stress of a hybrid sulcated spring

The bending stress at the position of maximum bending moment along the curved section of a hybrid sulcated spring is tabulated in Table 3.6. The elastic modulus of the glass fibre/epoxy resin was 40.8 GPa and for carbon fibre/epoxy resin 130.2 GPa was used, the spring dimensions are for spring C3 (see Table 3.7) with a laminate thickness of 24 plies.

		Bending stresses (MPa) for **glass/carbon/glass** scheme.			Bending stresses (MPa) for **carbon/glass/carbon** scheme.		
Ratio	Core thickness (mm)	Outer layers in glass fibre	At interface in glass fibre	At interface in carbon fibre	Outer layers in carbon fibre	At interface in carbon fibre	At interface in glass fibre
1:22:1	2.75	0.18	0.17	0.56	1.10	1.01	0.31
2:20:2	2.50	0.22	0.18	0.60	0.86	0.71	0.21
3:18:3	2.25	0.26	0.19	0.64	0.73	0.54	0.16
4:16:4	2.00	0.31	0.20	0.66	0.65	0.43	0.12
5:14:5	1.75	0.35	0.20	0.67	0.59	0.34	0.10
6:12:6	1.50	0.40	0.19	0.64	0.56	0.27	0.08
7:10:7	1.25	0.44	0.18	0.59	0.54	0.22	0.06
8:8:8	1.00	0.47	0.15	0.50	0.53	0.17	0.04
9:6:9	0.75	0.49	0.11	0.39	0.52	0.12	0.03
10:4:10	0.50	0.51	0.07	0.26	0.51	0.07	0.01
11:2:11	0.25	0.51	0.03	0.13	0.51	0.03	0.00
12:0:12	0	0.51	-	-	0.51	-	-

Table 3.6 Table of bending stress of a hybrid sulcated spring under a 1N load.

By changing the proportion of each material in the sandwich scheme, the maximum stress can be made to occur at the interface of the two materials instead of on the outer surface. In the first example of Table 3.6, for the glass/carbon/glass scheme, by including two layers of glass fibre on each of the outer layers the stress was reduced from 0.51 MPa to 0.18 MPa. It was not until a proportion of 8:8:8 for a core thickness of 1.0 mm was used, as shown in the graph of Figure 3.18, that the overall stress was reduced.

A reduction in stress of the outer layers was noted for the carbon/glass/carbon scheme as the thickness of the glass fibre core material decreased, as shown on the graph of Figure 3.19. It can be concluded that including layers of glass fibre as a core material for a carbon fibre laminate reduces the bending stress on the outer layers. Even though the bending stresses in the carbon fibre layers appear to be higher than the stress in the glass fibre layers, the ultimate tensile strength of carbon fibre is higher, so it is important to consider this. The fatigue life of a hybrid sandwich scheme was shown at the end of Table 3.3, where a carbon/glass/carbon spring was fatigue tested. The results showed an applied stress of 1000 N/mm^2 could be accommodated for infinite life, with only 2% loss in load carrying capacity. Thus showing the higher ultimate tensile strength of the carbon fibre compared to glass fibre allows a greater applied stress to be accommodated. With the help of the model developed it is now possible to configure a hybrid sequence which can minimise the stresses and thus extend the fatigue life. Chapter Seven develops the idea of hybrid sulcated springs further to include the advantages of weight reduction offered by including carbon fibre and investigates the costs involved.

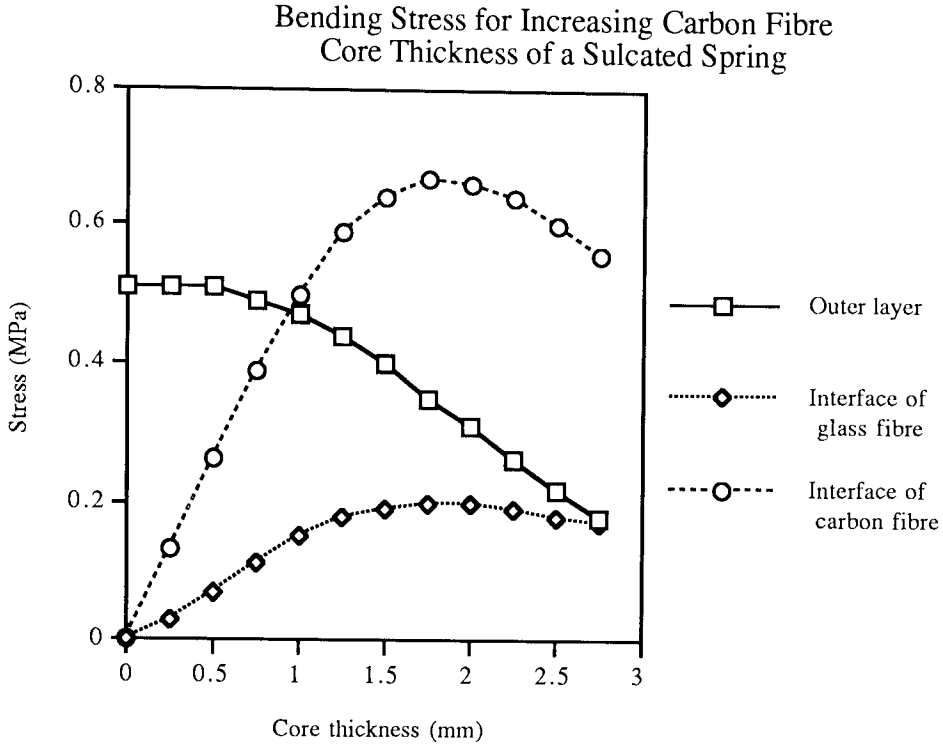

Figure 3.18 Bending stress at position of maximum bending moment for a glass/carbon/glass hybrid sulcated spring under a load of 1 N.

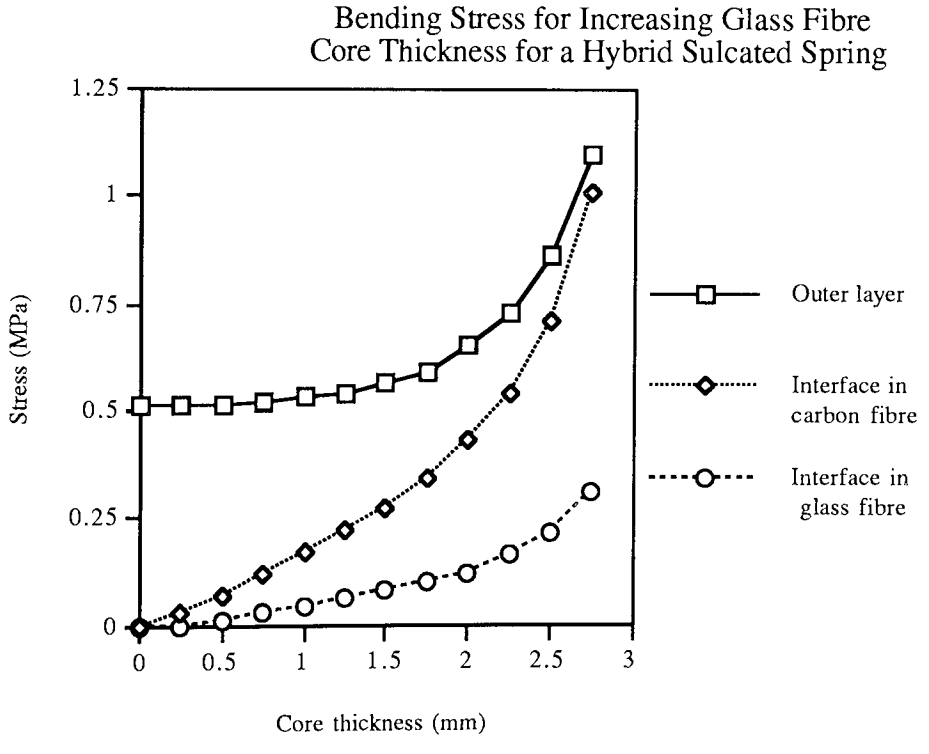

Figure 3.19 Bending stress at position of maximum bending moment for a carbon/glass/carbon hybrid sulcated spring under a load of 1 N.

3.7.7 Shear stress of a sulcated spring

In a beam of rectangular cross section the shearing stress is

$$\tau = \frac{V}{2I}\left(\frac{t^2}{4} - y^2\right) \qquad \text{-(3.33)}$$

This formula is sufficiently accurate for a curved beam it can therefore be applied to the curved section of the spring.[23] The maximum shear stress occurs when y=0 thus

$$\tau_{max} = \frac{3V}{2dt} \qquad \text{-(3.34)}$$

The largest positive shear stress is

$$\tau_{max} = \frac{3P}{2dt} \qquad \text{-(3.35)}$$

at the neutral axis, when $\theta=0^o$ and along the straight limb section when $\alpha=0$.

The largest negative shear stress is

$$\tau_{max} = -\frac{3P}{2dt} \qquad \text{-(3.36)}$$

at the neutral axis, when $\theta=180^o$.

From experimental data on spring A6

t=1.41 mm d=25.64 mm P=165.54 N at solid height

$$\tau_{max} = 6.8726 \text{ MPa}$$

There were no experimental results for shear stress.

3.7.8 Spring stiffness for a sulcated spring

Derivation of the equation for the deflection under load (P) was achieved by using Castigliano's theorem. The theorem states that the displacement of a structural member measured in the direction of the applied load, P, is equal to the partial derivative of the total elastic strain energy of this member with respect to the load P. In the analytical approach to sulcated spring design, only

elastic strain energy caused by bending is taken into account. The assumptions in deriving the equations for the sulcated spring stiffness are:-

1. The material properties are isotropic.
2. The spring is sufficiently stable laterally, so only bending in the plane of curvature requires attention.
3. The theory of pure flexure and Hooke's law applies.
4. The end straight limb sections remain horizontal and completely in contact with the platen surfaces.

Castigliano's principle in terms of rectangular coordinates

$$\delta = \frac{1}{EI}\int M\frac{\partial M}{\partial P}\,dx \qquad \text{-(3.37)}$$

and in terms of polar coordinates

$$\delta = \frac{1}{EI}\int M\frac{\partial M}{\partial P}\,r\,d\theta \qquad \text{-(3.38)}$$

Applying the theorem to find the respective deflections of Figure 3.12 at point B,C and D are:-

Deflection at B (at curved section)

$$\delta_B = \frac{1}{EI}\int_0^{\beta} -P\left(\frac{L_1}{2}+\rho\sin\theta\right)\frac{\partial M_{BC}}{\partial P}\rho\,d\theta \qquad \text{-(3.39)}$$

$$\delta_B = \frac{P\rho^3}{EI}\left(\frac{K^2}{4}\beta - K(\cos\beta - 1) + \frac{1}{2}\beta - \frac{1}{4}\sin 2\beta\right) \qquad \text{-(3.40)}$$

where $P=p_1L_1$, $L_1=w-r-t$, $\rho = r + t/2$, $K=\frac{L_1}{\rho}$, $\beta = \pi - \alpha$, and $I = \frac{t^3 d}{12}$.

Deflection at C (at straight limb section)

$$\delta_C = \frac{1}{EI}\int_0^{L_2} P\left(\frac{L_2}{2} - x_2\right)\cos\alpha \frac{\partial M_{CD}}{\partial P} dx_2 \qquad \text{-(3.41)}$$

$$\delta_C = \frac{P\rho^3 J^3 \cos\alpha}{12EI} \qquad \text{-(3.42)}$$

where $P=p_2L_2$, $L_2 = \frac{w-2t-2r(1-\sin\alpha)}{\cos\alpha}$, and $J=\frac{L_2}{\rho}$.

Deflection at D (at curved section)

$$\delta_D = \frac{1}{EI}\int_{\frac{\beta_1}{2}}^{\beta_1} -P\left(\frac{L_2}{2} + \rho\sin\theta\right)\frac{\partial M_{DE}}{\partial P}\rho d\theta \qquad \text{-(3.43)}$$

$$\delta_D = \frac{P\rho^3}{EI}\left(\frac{J^2}{8}\beta_1 - J\left(\cos\beta_1 - \cos\frac{\beta_1}{2}\right) + \frac{1}{4}\beta_1 - \frac{1}{4}\sin 2\beta_1 + \frac{1}{4}\sin\beta_1\right) \qquad \text{-(3.44)}$$

where $\beta_1 = \pi - 2\alpha$.

Total deflection $\delta = 2(\delta_B+\delta_C+\delta_D)$ -(3.45)

Total deflection for an **n** sulcation spring $\delta = 2\delta_B+(n-1)(\delta_C+\delta_D)$ -(3.46)

Thus the spring rate for an **n** sulcation spring

$$\text{Spring rate} = \frac{P}{\delta} = \frac{EI}{\rho^3(2y_B+(n-1)(y_C+y_D))} \qquad \text{-(3.47)}$$

The load under deflection δ is

$$P = \frac{EI\delta}{\rho^3(2y_B+(n-1)(y_C+y_D))} \qquad \textbf{-(3.48)}$$

and the load supported at solid height defined as the maximum load is

$$P_{max} = \frac{EI\,\delta_{max}}{\rho^3(2y_B+(n-1)(y_C+y_D))} \qquad \textbf{-(3.49)}$$

where

$$y_B = \frac{K^2}{4}\beta - K(\cos\beta - 1) + \frac{1}{2}\beta - \frac{1}{4}\sin 2\beta$$

$$y_C = \frac{J^3\cos\alpha}{12}$$

$$y_D = \frac{J^2}{8}\beta_1 - J(\cos\beta_1 - \cos\frac{\beta_1}{2}) + \frac{1}{4}\beta_1 - \frac{1}{4}\sin 2\beta_1 + \frac{1}{4}\sin\beta_1$$

$$\delta_{max} = \text{Free height - Solid height} \qquad \textbf{-(3.50)}$$

The bending and shear stress at the solid height can be found by using the spring rate to find P_{max}, then substituting P_{max} for P in the equations for shear (3.35) and bending stress (3.18) or (3.22).

3.7.9 Theoretical and experimental results for spring stiffness

The analytical model for sulcated spring stiffness was compared with experimental results for sulcated spring stiffness. The sulcated spring parameters of three springs of five sulcations are given in Table 3.7.

Spring number	C3	C4	C5
Thickness (mm)	3.00	2.99	3.09
Radius (mm)	5.92	5.98	5.98
Depth (mm)	25.48	25.28	25.32
Width (mm)	43.12	43.06	44.38
Angle α (degrees)	0	0	0
Elastic modulus (GPa)	40.8	40.8	40.8
Experimental spring stiffness (N/mm)	55	54	55
Theoretical spring stiffness (N/mm)	55.52	54.46	55.80
Discrepancy of theoretical spring stiffness (%)	0.90	0.84	1.43

Table 3.7 Comparison of theoretical and experimental results for spring stiffness.

From Table 3.7, the analytical model proves to be a very good approximation. The percentage discrepancy of all the theoretical spring rates are less than 1.5%. The accuracy of the results for spring stiffness depends on accurate measuring of the spring dimensions which need to be measured in several places to determine the mean and standard deviation. The mean values were used for the analysis.

3.7.10 Spring stiffness for a hybrid sulcated spring

The model remains essentially the same as that derived for a sulcated spring of one-fibre type, with the exception of a change in the flexural rigidity. There are now two second moments of area I_1 and I_2. These are the second moments of area about the neutral axis of cross-sectional areas 1 and 2, as shown in Figure 3.16 which shows a symmetrical sandwich composite.

For a hybrid symmetrical sandwich sulcated spring, the spring rate becomes

$$\frac{P}{\delta} = \frac{E_1 I_1 + E_2 I_2}{\rho^3 (2y_B + (n-1)(y_C + y_D))} \qquad \textbf{-(3.51)}$$

The load under deflection δ is

$$P = \frac{(E_1 I_1 + E_2 I_2)\,\delta}{\rho^3 (2y_B + (n-1)(y_C + y_D))} \qquad \textbf{-(3.52)}$$

and the load supported at solid height defined as the maximum load is

$$P_{max} = \frac{(E_1 I_1 + E_2 I_2)\,\delta_{max}}{\rho^3 (2y_B + (n-1)(y_C + y_D))} \qquad \textbf{-(3.53)}$$

where y_B,y_C, y_D and δ_{max} remain as shown in equation 3.46

3.7.11 Theoretical results for hybrid sulcated spring stiffness

Theoretical estimates of the spring stiffness have been produced from the analytical model for hybrid spring stiffness, the results are tabulated in Table 3.8.

Ratio	Spring stiffness (N/mm) for **glass/carbon/glass** scheme	Spring stiffness (N/mm) for **carbon/glass/carbon** scheme
0:24:0	177.17	55.52
1:22:1	149.22	83.47
2:20:2	125.92	106.77
3:18:3	106.84	125.85
4:16:4	91.56	141.12
5:14:5	79.66	153.02
6:12:6	70.72	161.96
7:10:7	64.32	168.37
8:8:8	60.02	172.66
9:6:9	57.42	175.26
10:4:10	56.08	176.60
11:2:11	55.59	177.10
12:0:12	55.52	177.17

Table 3.8 Hybrid spring stiffness for different ratios.

Sulcated spring dimensions were for spring C3 as shown in Table 3.7. The elastic modulus of the glass fibre epoxy resin was 40.8 GPa and for carbon fibre /epoxy resin 130.2 GPa was used. A 24 ply laminate was used for spring C3, so the layers for each configuration total 24 layers, and were symmetrical about the midplane. Table 3.8 shows that in the glass/ carbon/ glass scheme as more carbon fibre was incorporated into the core the spring stiffness increased. However by placing fibres in a carbon /glass /carbon scheme the stiffness was further increased for all cases where the proportion of each fibre was the same. For example the ratio 1:22:1 in a carbon/ glass/ carbon scheme has 2 layers of carbon and 20 layers of glass gives a spring stiffness of 83.465 N/mm. If the same number of layers of each are used in a glass /carbon /glass configuration (11:2:11) the spring stiffness is 55.588 N/mm. Thus showing that the order in which the fibres are arranged has a greater bearing on stiffness than the proportion of each fibre used. The outer layers provided a greater contribution to the overall stiffness. By completely changing from glass fibre to carbon fibre the stiffness has been increased over three times.

Table 3.8 aims to show the effect in stiffness that can be gained. A discussion of the cost involved was shown in Chapter Seven. There were no hybrid sulcated springs manufactured from the second experimental programme at the time of writing this thesis, therefore an accurate comparison with experimental results was not possible.

Chapter 4

ANALYTICAL MODEL FOR THE SULCATED SPRING DESIGN BASED ON LAMINATION THEORY

4.1 Introduction

An analytical model for sulcated springs which uses lamination theory is considered in this chapter. By using lamination theory, isotropic and orthotropic material properties can be included. This is particularly advantageous because the material properties of the sulcated spring are orthotropic, that is, the material properties are different in the longitudinal and transverse direction, as opposed to isotropic material properties which are the same in all directions. Therefore the development of this model provides a closer simulation of the sulcated spring. Another advantage of using lamination theory is the ability to consider a sulcated spring constructed with a laminate of different fibre orientations.

4.2 Analysis of an Orthotropic Lamina

4.2.1 Behaviour of an orthotropic material

Unidirectional composites are among the class of materials called orthotropic materials. The difference between an orthotropic material and an anisotropic material can be described by their response to applied loads. If for example, as in Figure 4.1, a cube made of an anisotropic material is subjected to a uniaxial load parallel to one of its edges, the load will produce changes in lengths as well as in the angles, along and between the edges of the cube. If the cube is made from an orthotropic material, the edges are along arbitrary directions. A uniaxial load will produce changes in both lengths and in angles.

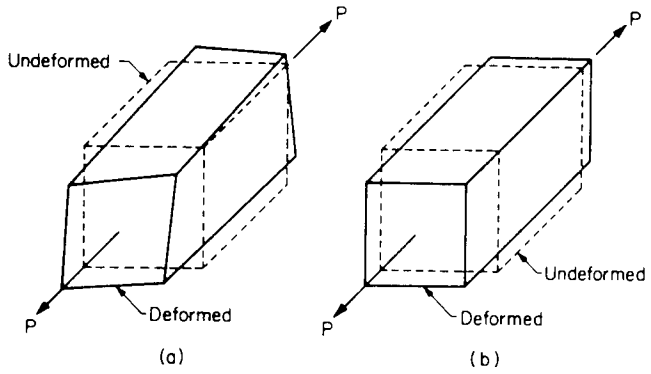

Figure 4.1 Deformation of a cube made of (a) anisotropic material, (b) orthotropic material.

4.2.2 Stress-strain relations for plane stress in an orthotropic material

The generalised Hooke's law relating stresses to strains can be written in contracted notation as [24]

$$\sigma_i = Q_{ij}\,\varepsilon_j \qquad i,j = 1,....6 \qquad \textbf{-(4.1)}$$

where σ_i are the stress components, Q_{ij} are the stiffness matrix, and ε_j are the strain components.

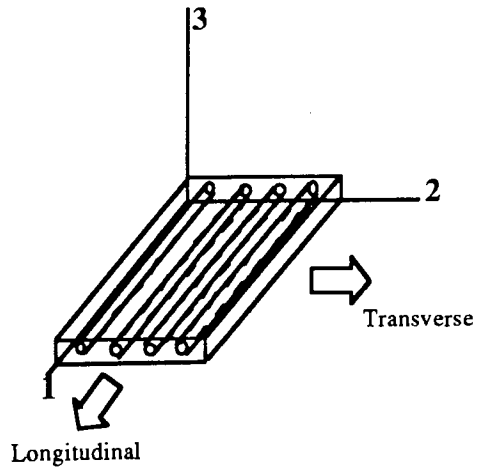

Figure 4.2 A unidirectional composite showing the longitudinal and transverse directions.

For a lamina in the 1-2 plane where 1 is the longitudinal axis, and 2 is the transverse axis, as shown in Figure 4.2, the strain - stress relations reduce to

$$\begin{bmatrix} \sigma_1 \\ \sigma_2 \\ \tau_{12} \end{bmatrix} = \begin{bmatrix} Q_{11} & Q_{12} & 0 \\ Q_{12} & Q_{22} & 0 \\ 0 & 0 & Q_{66} \end{bmatrix} \begin{bmatrix} \varepsilon_1 \\ \varepsilon_2 \\ \gamma_{12} \end{bmatrix} \qquad \textbf{-(4.2)}$$

For orthotropic lamination theory

$$Q_{11} = \frac{E_1}{1 - \nu_{12}\nu_{21}} \qquad Q_{12} = \frac{E_2\nu_{12}}{1 - \nu_{12}\nu_{21}} = \frac{E_1\nu_{21}}{1 - \nu_{12}\nu_{21}}$$

$$Q_{22} = \frac{E_2}{1 - \nu_{12}\nu_{21}} \qquad Q_{66} = G_{12}$$

where E_1 is the elastic modulus in the longitudinal fibre direction 1

E_2 is the elastic modulus in the transverse fibre direction 2

ν_{12} is the major Poisson's ratio

ν_{21} is the minor Poisson's ratio

G_{12} is the shear modulus

The principal material directions often make a different angle with a common set of reference axes as shown in Figure 4.3.

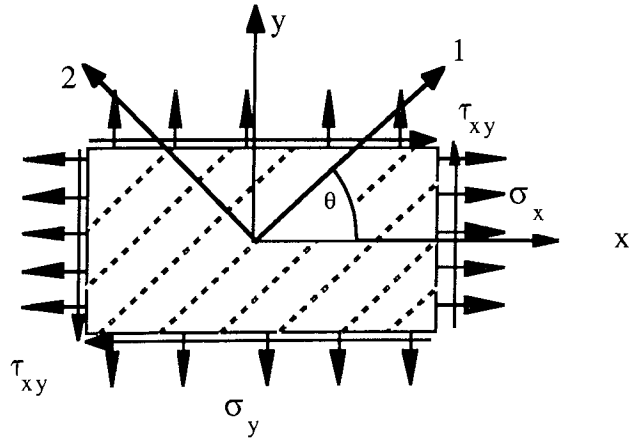

Figure 4.3 Orthotropic lamina with its principal material axes orientated at angle θ with reference coordinate axes.

The principal material axes are oriented at an angle θ. It is therefore necessary to refer the stress - strain relation to a common reference coordinate system.

Stresses and strains can be easily transformed from one set of axes to another using equation 4.3.

$$\begin{bmatrix} \sigma_x \\ \sigma_y \\ \tau_{xy} \end{bmatrix} = [T]^{-1} \begin{bmatrix} \sigma_1 \\ \sigma_2 \\ \tau_{12} \end{bmatrix} \qquad \text{-(4.3)}$$

and

$$\begin{bmatrix} \varepsilon_x \\ \varepsilon_y \\ \frac{1}{2}\gamma_{xy} \end{bmatrix} = [T]^{-1} \begin{bmatrix} \varepsilon_1 \\ \varepsilon_2 \\ \frac{1}{2}\gamma_{12} \end{bmatrix} \qquad \text{-(4.4)}$$

where the transformation matrix [T] is

$$[T] = \begin{bmatrix} \cos^2\theta & \sin^2\theta & 2\sin\theta\cos\theta \\ \sin^2\theta & \cos^2\theta & -2\sin\theta\cos\theta \\ -\sin\theta\cos\theta & \sin\theta\cos\theta & \cos^2\theta - \sin^2\theta \end{bmatrix} \qquad \text{-(4.5)}$$

Thus the stresses in any other coordinate system in the plane of the lamina are the stresses [25]

$$\begin{bmatrix} \sigma_x \\ \sigma_y \\ \tau_{xy} \end{bmatrix} = \begin{bmatrix} \overline{Q}_{11}\overline{Q}_{12}\overline{Q}_{16} \\ \overline{Q}_{12}\overline{Q}_{22}\overline{Q}_{26} \\ \overline{Q}_{16}\overline{Q}_{26}\overline{Q}_{66} \end{bmatrix} \begin{bmatrix} \varepsilon_x \\ \varepsilon_y \\ \gamma_{xy} \end{bmatrix} \qquad \text{-(4.6)}$$

where $[\overline{Q}] = [T]^{-1}[Q][T]^{-T}$ is the transformed reduced stiffness matrix.

4.2.3 Strength of an orthotropic lamina

In all design procedures, it is necessary to compare the actual stress field, as shown in the previous section, with the allowable stress field. For isotropic materials, the principal stress or strain is compared with the allowable stress or strain for the material. The direction of the principal stress or strain has no influence on isotropic materials. In the case of orthotropic materials, the strength changes with direction and the direction of principal stress may not coincide with the direction of maximum strength. Thus the highest stress may not be the stress governing the design.

The allowable stress field for an isotropic material is completely described by knowing the ultimate tensile, compressive and shear strengths. For an orthotropic material, the allowable stress field consists of the five strengths in the principal material directions. These strengths are the longitudinal tensile strength, transverse strength, shear strength, longitudinal compressive strength, and transverse compressive strength. If an orthotropic lamina is subjected to loads which produce complex stress states, the actual stress field must be referred to the material axes, and then compared with the preceding strengths.

4.3 Analysis of Laminated Composites

4.3.1 Constitutive equations

Laminates are fabricated so that they act as single layer materials by placing each lamina on top of the other to form a laminate, as shown in Figure 4.4.

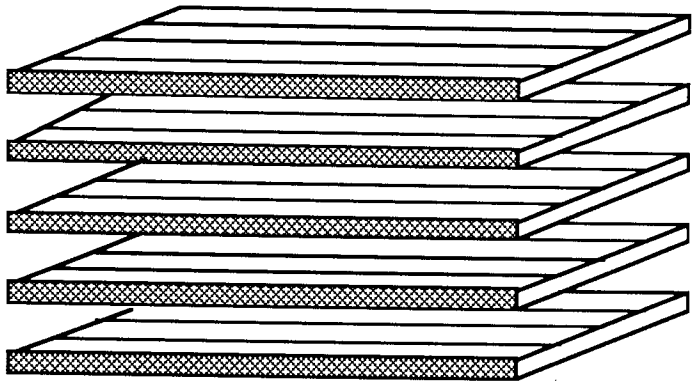

Figure 4.4 A unidirectional laminate.

The bond between two laminae in a laminate is assumed to be infinitesimally thin, and not shear deformable. Thus displacements remain continuous across the bond. Applied force (N) and moment resultants (M) on a laminate are related to the mid-plane strains and curvatures by the following equations. In matrix notation

$$\begin{bmatrix} N_x \\ N_y \\ N_{xy} \end{bmatrix} = [A] \begin{bmatrix} \varepsilon_x^0 \\ \varepsilon_y^0 \\ \gamma_{xy}^0 \end{bmatrix} + [B] \begin{bmatrix} k_x \\ k_y \\ k_{xy} \end{bmatrix} \qquad \text{-(4.7)}$$

$$\begin{bmatrix} M_x \\ M_y \\ M_{xy} \end{bmatrix} = [B] \begin{bmatrix} \varepsilon_x^0 \\ \varepsilon_y^0 \\ \gamma_{xy}^0 \end{bmatrix} + [D] \begin{bmatrix} k_x \\ k_y \\ k_{xy} \end{bmatrix} \qquad \text{-(4.8)}$$

where

$$A_{ij} = \sum_{k=1}^{N} [\bar{Q}]_k (z_k - z_{k-1})$$

$$B_{ij} = \frac{1}{2} \sum_{k=1}^{N} [\bar{Q}]_k (z_k^2 - z_{k-1}^2)$$

$$D_{ij} = \frac{1}{3}\sum_{k=1}^{N}[\bar{Q}]_k (z_k^{\,3} - z_{k-1}^{\,3})$$

where the A_{ij} are called the extensional stiffness, the B_{ij} are called coupling stiffness, and the D_{ij} are called bending stiffness. The presence of the B_{ij} implies coupling between bending and extension of a laminate.[25]

By rearrangement

$$\begin{bmatrix} \varepsilon_x^0 \\ \varepsilon_y^0 \\ \gamma_{xy}^0 \end{bmatrix} = [A'] \begin{bmatrix} N_x \\ N_y \\ N_{xy} \end{bmatrix} + [B'] \begin{bmatrix} M_x \\ M_y \\ M_{xy} \end{bmatrix} \qquad \textbf{-(4.9)}$$

$$\begin{bmatrix} k_x \\ k_y \\ k_{xy} \end{bmatrix} = [C'] \begin{bmatrix} N_x \\ N_y \\ N_{xy} \end{bmatrix} + [D'] \begin{bmatrix} M_x \\ M_y \\ M_{xy} \end{bmatrix} \qquad \textbf{-(4.10)}$$

where

$[A'] = [A^*]-[B^*][D^*]^{-1}[C^*]$ $\qquad$ $[A^*] = [A]^{-1}$

$[B'] = [B^*][D]^{-1}$ $\qquad$ $[B^*] = -[A]^{-1}[B]$

$[C'] = -[D^*]^{-1}[C^*]$ $\qquad$ $[C^*] = [B][A]^{-1}$

$[D'] = [D^*]^{-1}$ $\qquad$ $[D^*] = [D]-[B][A]^{-1}[B]$

4.3.2 Symmetrical and balanced laminates

A symmetrical laminate greatly simplifies the constitutive equations by making the B_{ij} matrix zero and A_{16}, A_{26} zero. A symmetrical laminate is constructed by placing identical (in thickness and material type) lamina an equal distance on either side of the mid-plane. A balanced laminate is one in which for every

lamina of $+\theta$, there is an identical laminae of $-\theta$ orientation. The two laminae at $+\theta$ and $-\theta$ do not have to be at equal distances from the mid-plane. Therefore a balanced symmetrical laminate embodies both definitions, for example a [0 / 30 / -30 / -30 / 30 / 0] laminate. A balanced symmetrical laminate also has the practical advantage of preventing warping of the laminate. The analysis therefore is confined to symmetrical laminates, although from a practical point of view it is recommended that balanced symmetrical stacking sequences are used.

4.3.3 Strain and stress variation in a laminate

Stresses and strains are denoted with double subscripts. The first subscript refers to the direction normal to the plane in which the stress is acting, the second subscript refers to the direction in which the stress is acting. The stresses σ_{xx}, σ_{yy} and τ_{xy} are called in-plane intralaminar stresses, whereas σ_{zz}, τ_{xz} and τ_{yz} are called interlaminar stresses.

The strain displacement relation can be written in terms of the mid-plane strains and the plate curvatures as follows,

$$\begin{bmatrix} \varepsilon_x \\ \varepsilon_y \\ \gamma_{xy} \end{bmatrix} = \begin{bmatrix} \varepsilon_x^0 \\ \varepsilon_y^0 \\ \gamma_{xy}^0 \end{bmatrix} + z \begin{bmatrix} k_x \\ k_y \\ k_{xy} \end{bmatrix} \qquad \textbf{-(4.11)}$$

Equation 4.11 indicates that the strains in a laminate vary linearly across its thickness. Stresses in any lamina (e.g. jth) can be obtained by substituting equation 4.11 into equation 4.6.

$$[\sigma]_j = [\overline{Q}]_j [\varepsilon^0] + z_j [\overline{Q}]_j [k] \qquad \text{-(4.12)}$$

where z_j is the distance from the laminate mid-plane to the jth lamina.

4.3.4 Analysis of laminates after initial failure

The stresses and strains in each lamina of a composite material may be compared with the corresponding allowable values to predict failure. It is possible to predict, whether any of the plies in the laminate will fail, under a given load. The load at which the first ply failure will occur may also be calculated. Since the strength of a ply is a function of its orientation, it is expected that all plies do not fail under the same load. Plies fail successively in increasing order of strength in the direction of loading. After the first ply fails, the laminate response will deviate from that predicted by equation 4.6, and show a discontinuity in its behaviour. As the load is increased further, more ply failures occur, showing more discontinuities in the laminate behaviour, as can be seen in Figure 4.5.

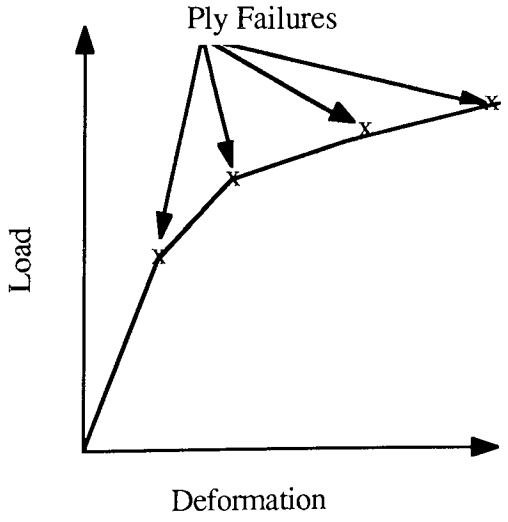

Figure 4.5 Load - deformation behaviour of hypothetical laminate.

4.4 Analytical Model for Sulcated springs based on Lamination theory

4.4.1 Assumptions of lamination theory

The assumptions for this model are:- [26]

(i) The laminate is thin and wide (width >> thickness).

(ii) A perfect interlaminar bond exists between various laminas.

(iii) The strain distribution in the thickness direction is linear.

(iv) All laminae are macroscopically homogeneous and behave in a linearly elastic manner.

(v) Displacements are continuous across lamina boundaries so that no lamina can slip relative to another.

(vi) A plane stress state is assumed for individual laminae.

4.4.2 Analytical model for spring stiffness

The spring rate, stress and strain distribution of a mid-plane symmetrical laminated sulcated spring under a point load has been analysed using the strain energy of an elastic body.[27]

$$\text{Strain Energy} = U = \int_v \frac{1}{2}\sigma_{ij}\varepsilon_{ij}dv = \int_V W\,dv \qquad \text{-(4.13)}$$

where W is the strain energy density function defined as

$$W=\frac{1}{2}\sigma_{ij}\varepsilon_{ij}=\frac{1}{2}\sigma_x\varepsilon_x+\frac{1}{2}\sigma_y\varepsilon_y+\sigma_{xy}\varepsilon_{xy} \qquad \text{-(4.14)}$$

As a plane stress state is assumed for individual laminae, the strain energy for a segment taken from the curved portion, defined in Figure 4.6 between θ_1 and θ_2 is [15]

$$U = \int_{\theta_1}^{\theta_2} \frac{1}{2}\left\{ d\left[\varepsilon^0\right]^T [N] + d\,[k]^T [M] \right\} \rho d\theta \qquad \text{-(4.15)}$$

$$U = \frac{d\rho}{2}\int_{\theta_1}^{\theta_2} \left\{ \begin{bmatrix} N \\ M \end{bmatrix}^T \begin{bmatrix} [A'][B'] \\ [C'][D'] \end{bmatrix}^T \begin{bmatrix} N \\ M \end{bmatrix} \right\} d\theta \qquad \textbf{-(4.16)}$$

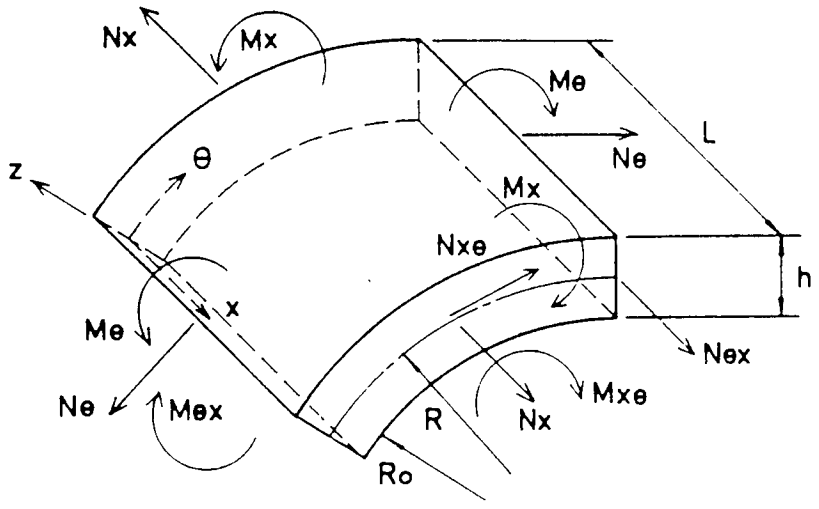

Figure 4.6 Mid-plane stress and moment resultant system.[15]

For a mid-plane symmetrical laminate, [B]=0, $[D']=[D]^{-1}$ and $M_\theta = \frac{M}{d}$ and all other stress and moment resultants equal to zero.

$$U = \frac{d\rho}{2}\int_{\theta_1}^{\theta_2} \left[D' M\right]^T [M] d\theta \qquad \textbf{-(4.17)}$$

$$U = \frac{d\rho}{2}\int_{\theta_1}^{\theta_2} [M]^T \left[D^{-1}\right]^T [M] d\theta \qquad \textbf{-(4.18)}$$

Assuming the θ direction is the principal fibre direction 1, and y is in the transverse direction 2 and applying equation 4.18 to the curved section of the sulcated spring

$$U = \frac{\rho}{2d}\int_{\theta_1}^{\theta_2} D'_{11} M^2 \, d\theta$$

-(4.19)

where $M = P(\frac{L_1}{2} + \rho\sin\theta)$

For a segment along the straight limb section

$$U = \frac{1}{2d}\int_{x_1}^{x_2} D'_{11} M^2 \, dx$$

-(4.20)

where $M = Px$

The vertical displacement (v) of a curved section is

$$v = \frac{\partial U}{\partial P} = \frac{\rho}{d} D'_{11} \int_0^{\beta} M \frac{\partial M}{\partial P} \, d\theta$$

-(4.21)

The vertical displacement (v) of the straight limb section is

$$v = \frac{\partial U}{\partial P} = \frac{D'_{11}}{d} \int_0^{L_2} M \frac{\partial M}{\partial P} \, dx$$

-(4.22)

By following the same procedure as for the sulcated spring model which assumes isotropic material properties (see section 3.7.8).

Thus the spring rate for an **n** sulcation spring

$$\text{Spring rate} = \frac{P}{\delta} = \frac{\det(D)\, d}{\rho^3 (D_{22} D_{66} - D_{26}^2)(2y_B + (n-1)(y_C + y_D))}$$

-(4.23)

The load under deflection δ is

$$P = \frac{\det(D)\, d\, \delta}{\det(D)\, \rho^3 (D_{22} D_{66} - D_{26}^2)\, (2y_B + (n-1)(y_C + y_D))}$$

-(4.24)

and the load supported at solid height defined as the maximum load is

$$P_{max} = \frac{\det(D)\, d\, \delta_{max}}{\rho^3(D_{22}D_{66} - D_{26}^2)(2y_B+(n-1)(y_C+y_D))} \qquad \textbf{-(4.25)}$$

where

$$y_B = \frac{K^2}{4}\beta - K(\cos\beta - 1) + \frac{1}{2}\beta - \frac{1}{4}\sin 2\beta$$

$$y_C = \frac{J^3 \cos\alpha}{12}$$

$$y_D = \frac{J^2}{8}\beta_1 - J(\cos\beta_1 - \cos\frac{\beta_1}{2}) + \frac{1}{4}\beta_1 - \frac{1}{4}\sin 2\beta_1 + \frac{1}{4}\sin\beta_1$$

4.4.3 Analytical model for the stress distribution

If equation 4.8 is applied to the sulcated spring design then

$$M = [D]\{k\}$$

$$k = [D]^{-1} M \qquad \textbf{-(4.26)}$$

where the assumptions are that the sulcated spring design is made from a mid-plane symmetrical laminate, hence [B]=[0]. All other stress and moment resultants are assumed to be equal to zero, with the exception of the bending moment M_x.

$$\begin{bmatrix} k_x \\ k_y \\ k_{xy} \end{bmatrix} = \begin{bmatrix} D'_{11} \\ D'_{12} \\ D'_{16} \end{bmatrix} \{M_x\} \qquad \textbf{-(4.27)}$$

where $D' = [D]^{-1}$

$$D'_{11} = \frac{D_{22}D_{66} - D_{26}^2}{|D|}$$

$$D'_{12} = \frac{D_{16}D_{26} - D_{12}D_{66}}{|D|}$$

$$D'_{16} = \frac{D_{12}D_{22} - D_{16}D_{26}}{|D|}$$

From equation 4.12 the stresses in the curved section of a sulcated spring at a distance z_j from the mid-plane are,

$$\begin{bmatrix} \sigma_x \\ \sigma_y \\ \sigma_{xy} \end{bmatrix}_j = z_j \begin{bmatrix} \overline{Q}_{11} & \overline{Q}_{12} & \overline{Q}_{16} \\ \overline{Q}_{12} & \overline{Q}_{22} & \overline{Q}_{26} \\ \overline{Q}_{16} & \overline{Q}_{26} & \overline{Q}_{66} \end{bmatrix}_j \begin{bmatrix} D'_{11} \\ D'_{12} \\ D'_{16} \end{bmatrix} M_x \qquad \textbf{-(4.28)}$$

For the purposes of the laminate strength analysis, it is desirable that the laminae stresses and strains be obtained along their natural longitudinal and transverse axes. These are obtained by using the transformation equations,

$$\begin{bmatrix} \sigma_1 \\ \sigma_2 \\ \tau_{12} \end{bmatrix} = [T] \begin{bmatrix} \sigma_x \\ \sigma_y \\ \tau_{xy} \end{bmatrix} \qquad \textbf{-(4.29)}$$

4.4.4 Analytical model for the prediction of failure

Initial failure of orthotropic materials can be predicted with the help of a suitable failure criteria. These failure theories are particularly useful for the structural designer in calculating the load carrying capability of laminated structures. The most popular failure criteria in practical use today are, Maximum Strain, Maximum Stress, and the Interactive Criteria of Azzi-Tsai-Hill and Tsai-Wu.[26] Of the three categories, selecting an interactive criteria which takes account of

theory states that failure occurs under some combined (multiplicative and / or additive) set of stresses. The failure theory therefore selected for the analysis of sulcated springs was the comprehensive definition for failure proposed by Tsai and Wu[28] . The basic assumption of this strength criterion is that there exists a failure surface in the stress - space in the following scalar form:

$$f(\sigma_k) = F_i \sigma_i + F_{ij}\sigma_i\sigma_j = 1 \qquad \text{-(4.30)}$$

where i,j,k = 1,2,3,4,5,6; F_i and F_{ij} are the strength tensors of the second and fourth rank. Under plane stress conditions, the Tsai-Wu theory predicts failure in an orthotropic lamina if and when the following equality is satisfied.

$$F_1\sigma_{11} + F_2\sigma_{22} + F_{11}\sigma_{11}^2 + F_{22}\sigma_{22}^2 + F_{66}\tau_{12}^2 + 2F_{12}\sigma_{11}\sigma_{22} = 1 \qquad \text{-(4.31)}$$

where F_i and F_{ij} are the strength coefficients given by

$$F_1 = \frac{1}{S_{Lt}} - \frac{1}{S_{Lc}} \qquad F_2 = \frac{1}{S_{Tt}} - \frac{1}{S_{Tc}}$$

$$F_{11} = \frac{1}{S_{Lt}S_{Lc}} \qquad F_{22} = \frac{1}{S_{Tt}S_{Tc}} \qquad F_{66} = \frac{1}{S_{LTs}^2}$$

and F_{12} is a strength interaction between σ_{11} and σ_{22}. Strength properties are characterized by five independent strength properties,

S_{Lt} = longitudinal tensile strength

S_{Tt} = transverse tensile strength

S_{Lc} = longitudinal compressive strength

S_{Tc} = transverse compressive strength

S_{LTs}= in plane (intralaminar) shear strength

Strength predictions can be made using the first ply failure method which is a simple conservative method whereby failure is defined as occurring when the first ply satisfies the failure criterion. Stresses for a sulcated spring can be obtained from the orthotropic analytical model, and the Tsai - Wu failure criterion applied. As soon as one ply satisfies the failure criterion, failure has occurred, and it can be concluded that the structure has reached its load carrying capacity and is no longer able to support the specified load. For most design purposes, the first ply failure criterion of strength prediction is usually considered to be far too conservative for practical use. It has been applied to the sulcated spring design to, provide an initial estimate of strength, and because of its relative ease of application.

The Tsai - Wu failure criterion has been incorporated into the design computer program, which produces a warning message if the stresses in any lamina exceeds its strength, and hence load carrying capacity, as shown in Figure 4.7. This example shows the stacking sequence of spring C3 which is a 0 degree unidirectional composite sulcated spring of laminate thickness 3 mm. When a load of 500 N is applied, the laminate has not exceeded its load carrying capacity. However when the load is increased to 600 N the laminate of the sulcated spring exceeds its load carrying capacity. This is a useful facility to assist the designer to produce a sulcated spring design which does not exceed its load carrying capacity.

```
**********************************************************************
 TO CALCULATE THE MAXIMUM BENDING STRESS UNDER A SPECIFIED LOAD
**********************************************************************

Enter the load for which bending stress is required > 500

At distance 1.500mm from the midplane
The stresses in the outer layer oriented in the  0 degree direction are
:-

Stressxx =  262.428 N/mm2
Stressyy =   -0.000 N/mm2
Shearxy  =   62.808 N/mm2

Lamina has not yet reached its load carrying capacity


**********************************************************************
 TO CALCULATE THE MAXIMUM BENDING STRESS UNDER A SPECIFIED LOAD
**********************************************************************

Enter the load for which bending stress is required > 600

At distance 1.500mm from the midplane
The stresses in the outer layer oriented in the  0 degree direction are
:-

Stressxx =  314.914 N/mm2
Stressyy =   -0.000 N/mm2
Shearxy  =   75.369 N/mm2

Lamina has reached its load carrying capacity
```

Figure 4.7 Warning message from the design computer program showing laminate strength exceeded.

4.4.5 Comparison of spring stiffness and stress using four methods

The spring rate of a sulcated spring has been derived using Castigliano's theorem in Chapter Three, the flexural rigidity for this formula was based on beam theory, where the flexural rigidity is:

$$D = EI = \frac{Et^3 d}{12}. \qquad \textbf{-(4.32)}$$

In this section, three other methods of calculating the flexural rigidity are considered. These are plate theory, isotropic lamination theory and orthotropic lamination theory as discussed in this chapter. The remainder of the spring rate

formula remains the same for all four methods. Assumptions of applying each method is listed, and the formula for each calculation.

Assumptions and material properties used in each method are as follows:-

Beam Theory [23]

The assumptions of applying beam theory are:-

(i) The beam is of homogeneous material that has the same modulus of elasticity in tension and compression.

(ii) The beam is straight or nearly so, if it is slightly curved, the curvature is in the plane of bending and the radius of curvature is at least 10 times the depth.

(iii) The cross-section is uniform.

(iv) The beam has at least one longitudinal plane of symmetry.

(v) All the loads and reactions are perpendicular to the axis of the beam and lie in the same plane which is a longitudinal plane of symmetry.

(vi) The beam is long in proportion to its depth, the span/depth ratio being 8 or more for metal beams, 15 or more for thin web beams and 24 or more for rectangular timber beams.

(vii) The beam is not disproportionately wide.

(viii) The maximum stress does not exceed the proportional limit.

$$D = EI = \frac{Et^3 d}{12} \qquad \textbf{-(4.33)}$$

Plate theory [23]

The assumptions for using plate theory are:-

(i) The plate is flat, of uniform thickness, and of homogeneous isotropic material.

(ii) The thickness is not more than about one-quarter of the least transverse dimension, and the maximum deflection is not more than about one-half the thickness.

(iii) All the forces - loads and reactions are normal to the plane of the plate.

(iv) The plate is nowhere stressed beyond the elastic limit.

$$D = \frac{Et^3 d}{12(1-\nu^2)} \qquad \text{-(4.34)}$$

Isotropic lamination theory [26]

For lamination theory the assumptions are:-

(i) The laminate is thin and wide (width >> thickness).

(ii) A perfect interlaminar bond exists between various laminas.

(iii) The strain distribution in the thickness direction is linear.

(iv) All laminae are macroscopically homogeneous and behave in a linearly elastic manner.

(v) Displacements are continuous across lamina boundaries so that no lamina can slip relative to another.

$$[Q] = \begin{bmatrix} \frac{E}{1-\nu^2} & \frac{\nu E}{1-\nu^2} & 0 \\ \frac{\nu E}{1-\nu^2} & \frac{E}{1-\nu^2} & 0 \\ 0 & 0 & G \end{bmatrix} \qquad \text{-(4.35)}$$

$$[D] = [Q]\frac{t^3}{12} \qquad \text{-(4.36)}$$

$$D = \frac{\det(D)}{(D_{22}D_{66} - D_{26}^2)} d \qquad \text{-(4.37)}$$

Orthotropic lamination theory

The same assumptions apply as for isotropic lamination theory

$$[Q] = \begin{bmatrix} \frac{E_{11}}{1-\nu_{12}\nu_{21}} & \frac{\nu_{21}E_{11}}{1-\nu_{12}\nu_{21}} & 0 \\ \frac{\nu_{21}E_{11}}{1-\nu_{12}\nu_{21}} & \frac{E_{22}}{1-\nu_{12}\nu_{21}} & 0 \\ 0 & 0 & G \end{bmatrix} \qquad \textbf{-(4.38)}$$

$$[D] = [Q]\frac{t^3}{12} \qquad \textbf{-(4.39)}$$

$$D = \frac{\det(D)}{(D_{22}D_{66} - D_{26}^2)}\,d \qquad \textbf{-(4.40)}$$

The effect of the difference in flexural rigidity (D) is seen in Table 4.1 where the spring rate prediction is compared using each method. From Table 4.1, the effect of the difference in flexural rigidity is noticeable when plate theory is used. The other methods give the same spring rate. The sulcated spring dimensions used in this example are as used in Table 3.6 for spring C3.

Theory	**Material Properties**	**Spring Rate (N/mm)**
Beam	E=40.8 GPa	55.52
Plate	E=40.8 GPa, v=0.227	58.53
Isotropic lamination	E=40.8 GPa, v=0.227, G=4 GPa (0 degree laminate)	55.52
Orthotropic lamination	E_{11}=40.8 GPa, E_{22}=15 GPa, ν_{21}=0.227, and G=4 GPa (0 degree laminate)	55.52

Table 4.1 Spring rate calculation using four methods for estimating the flexural rigidity.

It can be concluded from Table 4.1, that plate theory produces the highest stiffness. In this example, the results from beam and lamination theory are closer to the experimental spring stiffness. It can also be concluded that, for a unidirectional 0 degree laminate, the theoretical prediction of sulcated spring stiffness gives the same result using beam, isotropic lamination and orthotropic lamination theory.

Table 4.2 shows the application of the four methods for the calculation of stress on the outer tensile surface for spring A6, which was compared with experimental results in Table 3.4. The stress calculations in Table 4.2 neglect the effect of the normal force present in the curved section for all four methods.

Gauge	Type of Stress	Beam/Plate (MPa)	Isotropic Lamination (MPa)	Orthotropic Lamination (MPa)
1	σ_{xx}	2.501	2.501	2.501
	σ_{yy}	0	0	0
	τ_{xy}		0.598	0.213
2	σ_{xx}	2.542	2.542	2.542
	σ_{yy}	0	0	0
	τ_{xy}		0.608	0.216
3	σ_{xx}	2.297	2.297	2.297
	σ_{yy}	0	0	0
	τ_{xy}		0.550	0.195
4	σ_{xx}	2.358	2.358	2.358
	σ_{yy}	0	0	0
	τ_{xy}		0.564	0.201
5	σ_{xx}	2.501	2.501	2.501
	σ_{yy}	0	0	0
	τ_{xy}		0.598	0.213

Table 4.2 Comparison of stress predictions for the four methods under a load of 1 N.

The results in Table 4.2 show the stress in the longitudinal direction to be the same for all four methods. Transverse stress values appear to be the same, this

is due to the small load applied. As the load is increased, the transverse stress using beam and plate theory remains at zero, and the difference between the predictions of isotropic and orthotropic lamination theory becomes more noticeable. Isotropic lamination theory produces a higher transverse stress, due to the assumption of homogeneity of the material. In fact, the material properties are less in the transverse direction than isotropic lamination theory assumes. Orthotropic lamination theory models the material properties more concisely and thus produces a better approximation of the transverse stress. The same can be said for the difference in shear stress between isotropic and orthotropic lamination theory.

In terms of stiffness, beam, isotropic and orthotropic lamination theory produce the same result for a 0 degree unidirectional laminate. In terms of stress, the longitudinal stress calculation is the same for all three methods for a 0 degree laminate. The main advantage of the analytical model which is based on lamination theory is the ability of the model to incorporate laminae of different fibre directions, as described in the following section. This facility is not available for the equations which do not use lamination theory, as discussed in Chapter Three, because there is no inclusion of the fibre angle term θ.

4.4.6 Sulcated spring stiffness of different ply orientations

The design computer program has been used to produce theoretical predictions of the spring stiffness based on the theory developed in this chapter. On input of the sulcated spring geometric parameters, orthotropic material properties, and stacking sequence, the theoretical spring stiffness is calculated using equation 4.23. It was not possible to obtain experimental results for different fibre orientations at the time of writing the thesis. However the main reason for developing an orthotropic model has been to obtain an estimate of the likely

change in spring stiffness from the spring stiffness that occurs when a stacking sequence other than all laminae in the 0 degree direction is comtemplated. The 0 degree case has been examined in Chapter Three, which has been validated with experimental results.

Some examples of different types of symmetrical laminates and the sulcated spring stiffness as produced by the design computer program are shown in Table 4.3.

Stacking sequence (degrees)	Ratio of a 24 ply laminate	Spring rate (N/mm)
0		55.52
0 / 90 / 0	10:4:10	55.34
0 / 90 / 0 / 90 / 0	6:4:4:4:6	50.90
0 / 90 / 0 / 90 / 0 / 90 / 0	6:2:2:4:2:2:6	51.97
0 / 45 / 0 / 45 / 0	6:4:4:4:6	50.87
0 / 45 / 90 / 45 / 0	6:4:4:4:6	50.69
0 / 45/ -45 / 90 / -45 / 45 / 0	6:2:2:4:2:2:6	50.69

Table 4.3 Sulcated spring stiffness of different stacking sequences.

The spring dimensions and material properties are as used in the previous section. From Table 4.3, it is evident that a sulcated spring fabricated from a 0 degree laminate produces the highest spring stiffness. Approximately the same stiffness can be obtained from the 0/90/0/90/0 laminate and the 0/45/0/45/0 laminate implying that fibre angles oriented at 45 degrees produce the same spring stiffness when placed in the same position.

Another point to note is that, even though the same number of plies may be in the same direction, if they are placed in different positions the stiffness is affected. Take for example the 0/90/0/90/0 which has eight plies in the 90 degree direction and sixteen plies in the 0 direction. The same number of plies

are in the same direction for the 0/90/0/90/0/90/0 case however the spring stiffness is 51.97 N/mm compared with 50.90 N/mm for the 0/90/0/90/0 case. Thus it is concluded that the spring stiffness is dependent on position of the fibre angle, not necessarily the number of plies in each direction. In the 0/45/90/45/0 case the angle at 45 degree was replaced in the last case with +45/ -45 laminae equivalent in thickness to the total of the 45 degree laminae. This proves that the stiffness is not affected if fibres are oriented in the positive or negative direction. In terms of a balanced symmetrical laminate it is better to have angles of positive and negative angles of equal magnitude on both sides of the mid-plane to prevent warping.

A typical laminate stacking sequence tends to have 0 degree fibres on the outer surfaces to withstand the maximum stresses It is important to consider the point that, a stacking sequence is not selected on stiffness alone, but is often determined from the corresponding stress distribution that is produced. In the following section this is developed further to show the stress distribution predicted by the design computer program for some of the stacking sequences listed in Table 4.3.

4.4.7 Stresses of a sulcated spring of different ply orientations

The stresses σ_{xx}, σ_{yy} and the shear stress τ_{xy} were estimated from the design computer program using equations 4.28 and 4.29. For each change in ply orientation, the stresses were calculated at the interface as well as the outer surfaces of the laminate. The stress variation through the thickness can be compared to the 0 degree laminate to examine the effect that different ply orientations have on the stress distribution. Tables 4.4, 4.5, 4.6 and 4.7 show the values of the stress distribution above the mid-plane, at the outer surface (when the distance is 1.5 mm) and at the interface, the values below the mid-

plane are the same but of opposite sign. The dimensions are for sulcated spring C3 at the position of maximum bending stress under a 100 N load. Table 4.4 shows the longitudinal stress distribution to be linear across the thickness with stresses of 52.49 MPa on the outer surface above the mid-plane and -52.49 MPa below the mid-plane. If 0.6 mm of 90 degree plies are inserted either side of the mid-plane at a distance +/- (0.3 mm to 0.6 mm) from the mid-plane, then a different stress distribution is produced, as shown in the remainder of Table 4.4.

Laminate stacking sequence	Fibre direction for stress calculation	Distance from the mid-plane (mm)	Stressxx (MPa)	Stressyy (MPa)	Shearxy (MPa)
0	0	1.5	52.49	0	4.47
0/90/0/90/0	0	1.5	61.17	-0.61	5.58
	0	0.9	36.70	-0.36	3.35
	90	0.9	10.60	-6.83	8.96
	90	0.3	3.53	-2.28	2.99
	0	0.3	12.23	-0.12	1.12

Table 4.4 Stress distribution at the surface and interface for a 0 and 0/90/0/90/0 degree stacking sequence for a sulcated spring.

Laminate stacking sequence	Fibre direction for stress calculation	Distance from the mid-plane (mm)	Stressxx (MPa)	Stressyy (MPa)	Shearxy (MPa)
0/90/0	0	1.5	52.77	-0.02	4.50
	0	0.3	10.55	0.00	0.90
	90	0.3	3.12	-1.613	3.36

Table 4.5 Stress distribution at the surface and interface for a 0/90/0 degree stacking sequence for a sulcated spring.

Laminate stacking sequence	Fibre direction for stress calculation	Distance from the mid-plane (mm)	Stressxx (MPa)	Stressyy (MPa)	Shearxy (MPa)
0/90/0/90/0/90/0	0	1.5	65.37	-0.90	6.17
	0	1.07	46.63	-0.64	4.40
	90	1.07	13.32	-9.38	11.84
	90	0.64	7.97	-5.61	7.08
	0	0.64	27.89	-0.39	2.63
	0	0.21	9.15	-0.13	0.86
	90	0.21	2.62	-1.84	2.32

Table 4.6 Stress distribution at the surface and interface for a 0/90/0/90/0/90/0 degree stacking sequence for a sulcated spring.

Laminate stacking sequence	Fibre direction for stress calculation	Distance from the mid-plane (mm)	Stressxx (MPa)	Stressyy (MPa)	Shearxy (MPa)
0/45/-45/90/-45/45/0	0	1.5	61.54	-1.09	5.50
	0	0.9	36.93	-0.65	3.30
	45	0.9	13.82	10.10	8.83
	45	0.6	9.21	6.73	5.89
	-45	0.6	6.49	-3.46	5.96
	-45	0.3	3.24	-1.73	2.98
	90	0.3	3.51	-2.43	3.00

Table 4.7 Stress distribution at the surface and interface for a 0/-45/45/90/-45/45/0 degree stacking sequence for a sulcated spring.

From Tables 4.4, 4.5, 4.6 and 4.7 the value of stressxx and the shear stress shearxy are seen to increase on the outer tensile surface as fibres of different orientation are included even though the laminae near the outer surface remain in the 0 degree direction. By including fibres of different orientation, the transverse stress, stressyy increases in all the plies. The stresses in the transverse direction are under compression above the mid-plane and under tension below the mid-plane which is contrary to the behaviour of stressxx with the exception of the 0/45/-45/90/-45/45/0 in Table 4.7. In this case, the 45 degree plies cause a tensile transverse stress above the mid-plane. Layers of fibres in the transverse direction often reduce splitting in the longitudinal direction. Often 0 degree oriented fibres are placed on the laminate surface to extend the fatigue life. Shear stresses in the outer 0 degree laminae were seen to increase as 45 and 90 degree plies were used. The stresses in the longitudinal and transverse direction and shearxy are all zero at the neutral axis. Using the developed software, the stress distribution can be assessed in a similar fashion to assess the best laminate configuration scheme in terms of stress and stiffness to suit the required application.

4.5 Free Edge Effects

For calculating stresses and strains, the laminate analysis discussed in section 4.3, and the analytical model for sulcated springs in section 4.4, are not strictly true for the free boundaries. As was shown in the last section, the stresses σ_{xx} and τ_{xy} are non-zero even on a free boundary parallel to the x-axis. The analye as presented in section 4.3 and 4.4 are adequate in the regions away from the boundary. It was established by Pipes and Pagano [29] that as the free edge was approached σ_{xx} decreases, and τ_{xy} goes to zero, as shown in Figure 4.8. The width of the region in which the stresses differ from those predicted by lamination theory is approximately equal to the thickness of the laminate. Although the graph in Figure 4.8 shows the stresses for a 4 ply +/-45 degree

laminate of a high modulus graphite-epoxy system, the degree of the free edge effect on this particular laminate can be seen.

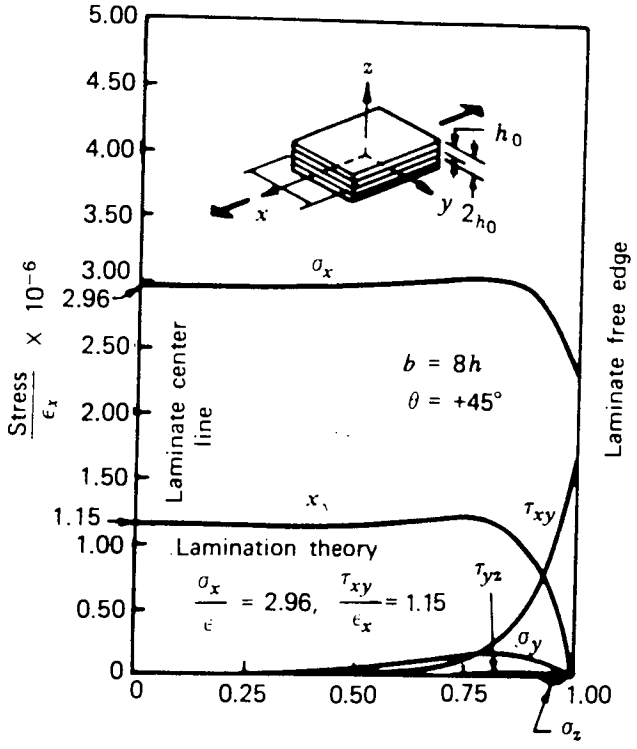

Figure 4.8 Stress variations across width of laminate.[24, 29]

Chapter 5

FINITE ELEMENT MODEL FOR SULCATED SPRINGS

5.1 Introduction

Finite element analysis has been applied to the sulcated spring to obtain design information about the displacements and stresses. Displacements obtained from the finite element model can be expressed in terms of the spring stiffness. The value of spring stiffness using the finite element model has been compared with preditions from the analytical model, and experimental results for spring stiffness. Finally, predictions for the maximum principal stress using the finite element model have been compared with experimental results.

5.2 The Finite Element method

The finite element method is a versatile numerical method for analysing structural parts. It is particularly useful for modelling two-and three-dimensional complex shapes. The structural geometry is subdivided into a large number of discrete elements joined to each other at their node points. As each small element is analysed in turn, a picture of the required distribution develops. The finite element method involves the application of three basic conditions. Equilibrium of forces, compatibility of displacements, and the laws of material behaviour/ stress - strain relationships. These conditions apply whatever the cause of the internal forces and deformations in a structure. Analytical solutions to these equations are seldom possible, so it is often necessary to employ a numerical method.

The implementation of numerical methods has been greatly facilitated by the increasingly widespread use of computers. Finite element software packages are an extremely useful way of applying the finite element method. There are basically three stages of analysis. First a pre-processing stage which involves generating a mesh relative to the geometrical shape, and assigning material properties. By refining the mesh or by using a dense concentration of elements near the areas of greatest stress concentration or areas of particular interest, a more accurate solution may be achieved. This principle applies to the sulcated spring where the areas of greatest stress are at the reflex portion of each sulcation. The processing stage involves the solution of equations, and any other data. Post processing requires the user to select from the options available, for example to list results or display the results graphically.

5.3 Element types

There are numerous element types and combination of elements which can be used in engineering problems. From the PAFEC element library [30], an isoparametric element was selected to represent the sulcated spring structure. This element was selected for the ease with which the sulcated spring geometry could be represented, and the type of results available. Information on the stress variation across the thickness can be produced and orthotropic material properties can also be included. This element is flat and only carries loads in its own plane.

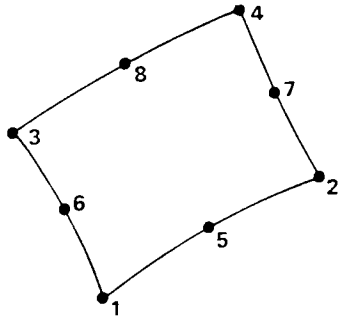

Figure 5.1 Eight-noded isoparametric curvilinear quadrilateral element.

It is assumed that the stresses do not vary through the element thickness (in the transverse direction) for plane stress and plane strain. The element has two degrees of freedom (u_x,u_y) in its own plane at each node. After transformation to a general position in space, there are three degrees of freedom (u_x,u_y,u_z) at each node. The output listing for the isoparametric element gives the principal stresses at each of the eight nodes. The displacement in the x and y direction and the resultant displacement at each node are also calculated.

5.4 Assumptions of the Finite Element model

General assumptions of the model are the assumptions and restrictions of the element selected. At least one constraint must be applied to the model. The beam is assumed to be prismatic, so that the cross-sectional details do not vary along the length of an element. Further it is assumed that flexural and shear centres lie on the line joining the two end nodes. The structure of the sulcated spring is assumed to be under plane stress due to the assumption that the stress across the depth (transverse direction) is zero. This assumption is also analogous with the assumption of plane stress used in lamination theory as discussed in Chapter Four.

5.5 Load and Restraints used in the Finite Element model

A load can either be applied to the geometric structure as a pressure load or point load. It is also necessary to decide what restraints to place on the geometric structure. It is important to select a load distribution and set of restraints which represent the experimental conditions so a direct comparison can be made between experimental and finite element results. The experimental load test condition has been shown in Figure 3.9 and 3.10. A sulcated spring is placed on the base of the free metal surface of the load testing equipment. An upper plate is lowered onto the upstanding sulcated spring until the plate touches the spring. The machine is then calibrated, and measurements for

deflection are taken as the plate is lowered. Figure 5.2 shows the elements and nodes of the finite element model for a sulcated spring and the applied restraints.

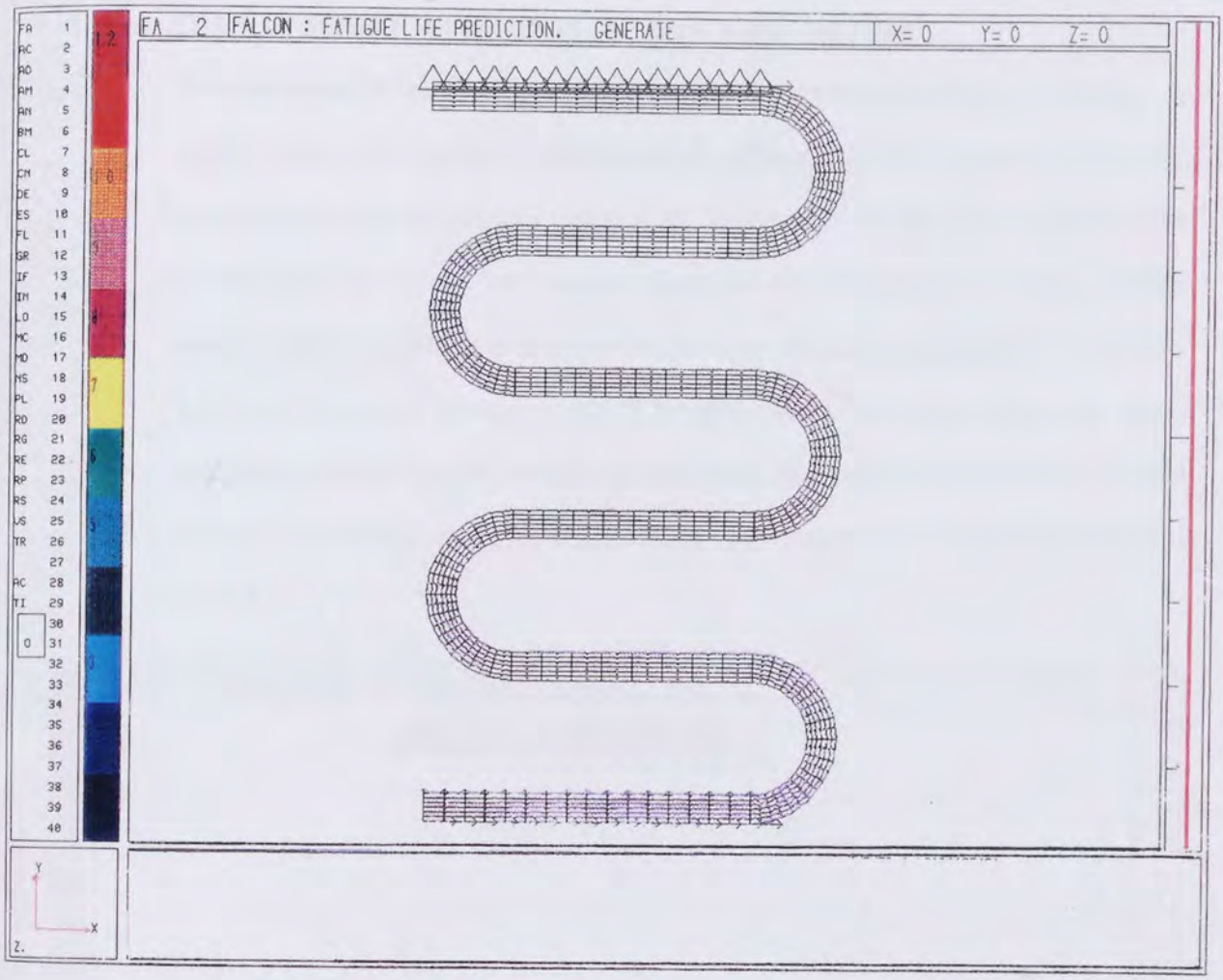

Figure 5.2 Finite element mesh of sulcated spring C3 with restraints displayed.

In the finite element model of the sulcated spring, a pressure distribution has been applied along the top straight limb section to represent the platen load. Restraints have been placed along the end straight limb sections in the x (horizontal) direction to prevent sideways movement and in the y (vertical) direction of the base end straight section to prevent movement beyond the imaginary platen surface of the model. As can be seen in Figure 3.10, the

straight limb at the top end of the spring remains horizontal and in contact with the top platen.

5.6 Displacement Profile of a Sulcated spring

Several attempts were made to recreate the experimental deflection process. A useful feature in PAFEC finite element software is the 'repeated freedoms' command which allows the degrees of freedom to be specified at particular points. This command was applied along the top straight limb section, which would otherwise deflect at an angle rather than remaining horizontal. In Figure 3.10, the sulcated spring at solid height shows that the side with three sulcations makes contact, whilst the side with two sulcations does not. It was important to check that this observation was preserved in the finite element model.

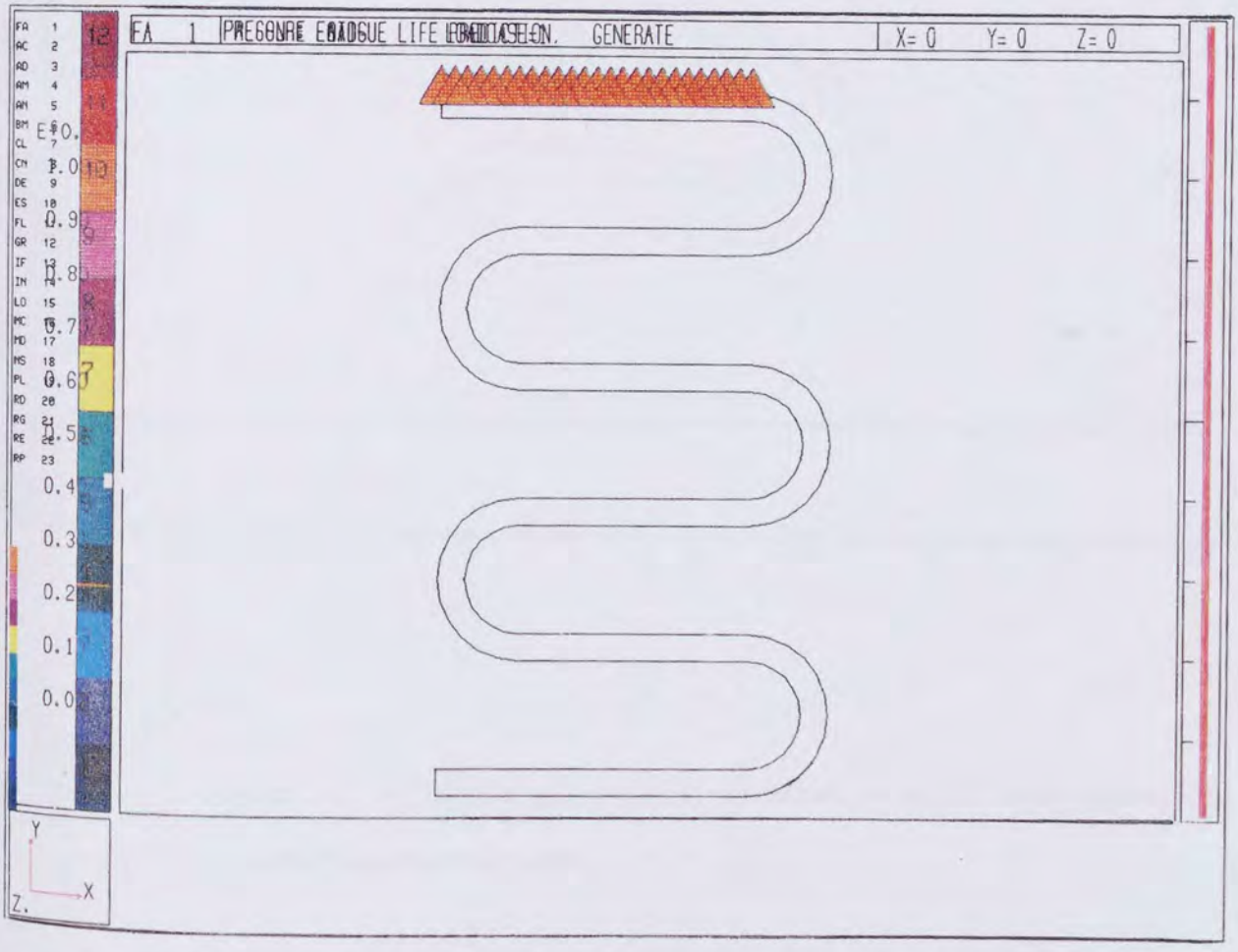

Figure 5.3 Finite element model of sulcated spring C3 at free height.

Figure 5.3 shows the profile finite element model of sulcated spring C3 at the free height with applied restraints as discussed and no applied load. Dimensions of spring C3 has been shown in Table 3.7. Figure 5.4 shows the displacement profile of the same spring under the applied load. Figure 5.5 shows the displacement profile for the solid height of the spring.

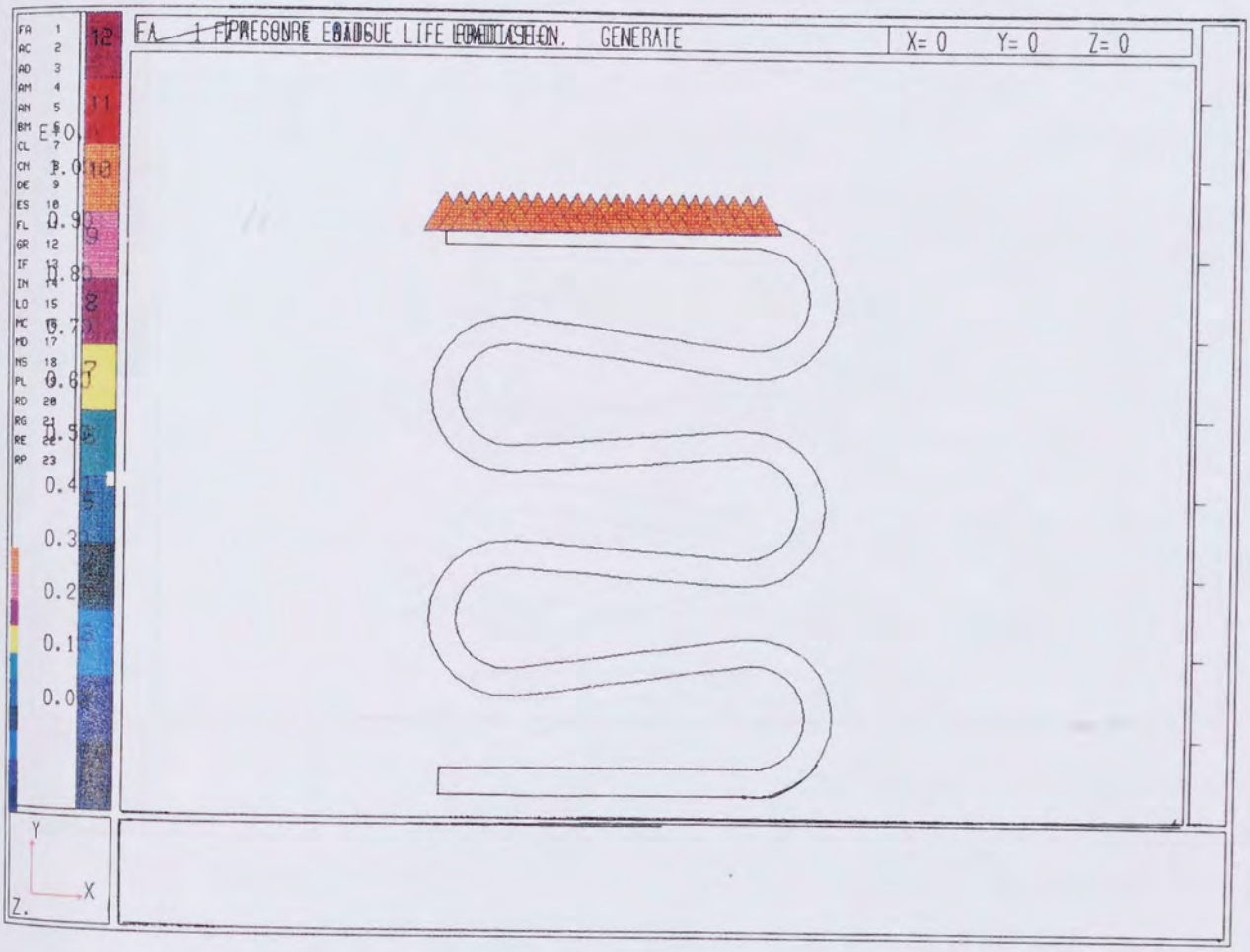

Figure 5.4 Displacement profile of sulcated spring C3 under applied load from the finite element model.

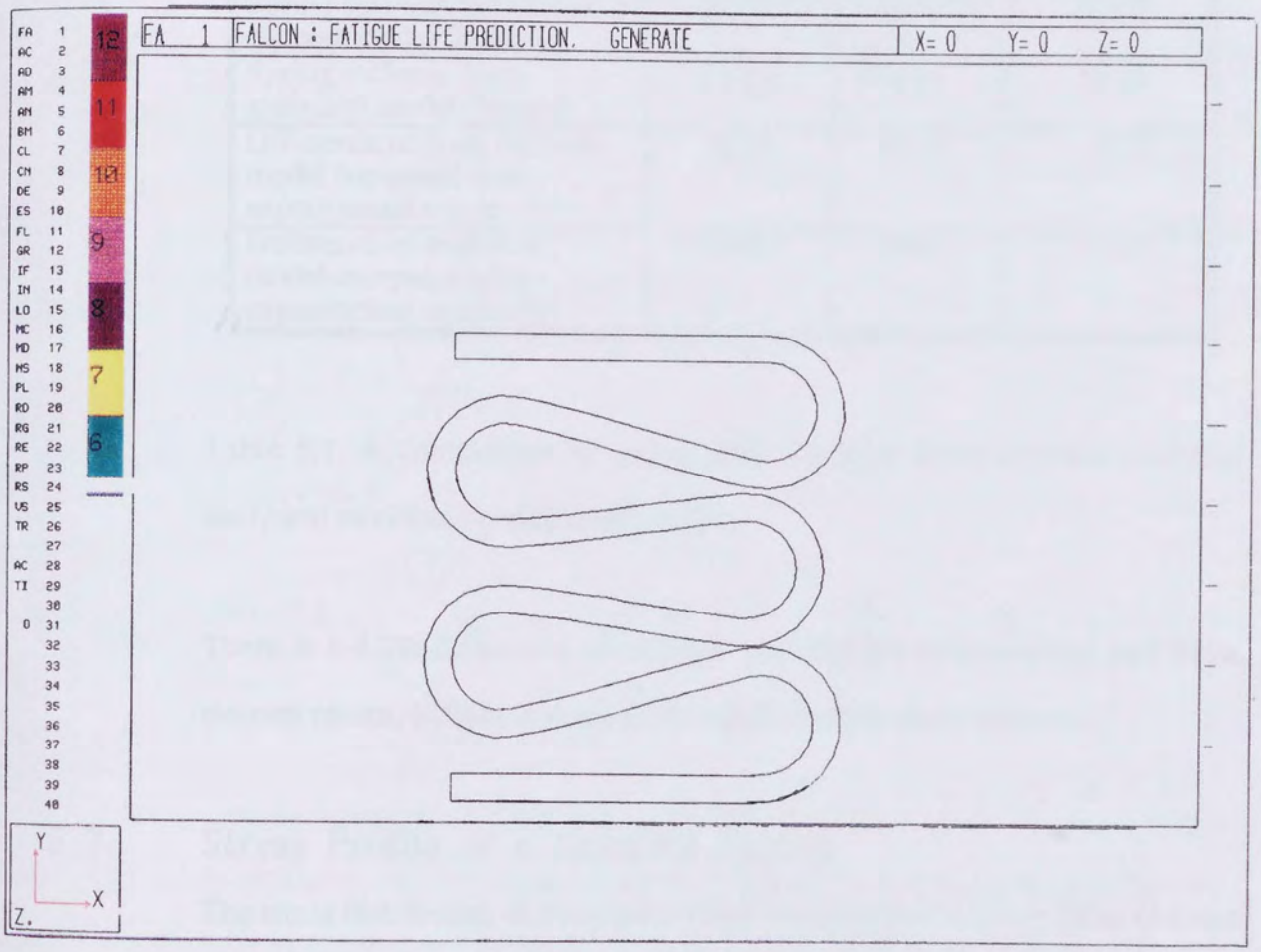

Figure 5.5 Displacement profile for the solid height from the finite element model of sulcated spring C3.

The displacements produced by the finite element model are expressed as spring stiffness in Table 5.1 for three sulcated springs. These values are compared with experimental results and the result from the analytical model.

Spring number	C3	C4	C5
Spring stiffness from experiment (N/mm)	55	54	55
Spring stiffness from finite element model (N/mm)	57.37	56.39	57.46
Spring stiffness from analytical model (N/mm)	55.52	54.46	55.80
Difference of finite element model compared with experimental results (%)	4.13	4.24	4.27
Difference of analytical model compared with experimental results (%)	0.90	0.84	1.43

Table 5.1. A comparison of spring stiffness from finite element analysis, analytical model and experimental results.

There is a 4.2% difference on average between the experimental and finite element results, indicating that the analytical model is more accurate.

5.7 Stress Profile of a Sulcated Spring

The stress distribution of a sulcated spring has been found using finite element analysis. Details about the stress distributions are useful to indicate areas under high stress, so that the areas of likely failure are known. Also it may prove necessary to redesign the spring in view of the results of the stress distribution. Of particular interest in stress analysis is the maximum principal stress and the maximum shear stress distribution. A finite element model of spring A6 has been created and the maximum principal stresses obtained from the model. Spring A6 was chosen so that the numerical results from the finite element model could be compared with experimental values of the longitudinal stress, the analytical results and experimental strain results for this spring were

discussed in section 3.7.4. The experimental measurements were obtained from strain gauges which measured the longitudinal strain on the tensile surface of the curved section of spring A6. Gauge 1 was attached to the top sulcation, with gauges 2,3,4, and 5 following. Table 5.2 shows the stress under a 1 N load using the average thickness at each sulcation using the finite element method predictions for the maximum principal stress compared with experimental measurements.

Gauge no.	Max. Principal Stress from Finite element (N/mm^2)	Experimental stress (N/mm^2)	% difference of Finite element analysis from experimental
1	2.516	2.145	14.6
2	3.114	2.717	12.8
3	2.255	1.757	22.1
4	2.915	2.547	12.6
5	2.417	1.959	18.9

Table 5.2 Maximum principal stress compared with experimental results.

The predictions for bending stress using finite element analysis are on average 16% higher than the experimental results. Whereas the predictions using curved beam theory were on average 15% too high for the side with three sulcations (gauge 1,3, and 5) and around 14% too low on the side with two sulcations (gauges 2 and 4).

One of the advantages of using finite element analysis is that colour-coded contours of the stress distribution can be produced. Figure 5.6 shows the maximum principal stress distribution of spring A6. It can be seen that the maximum stresses occur along the tensile surface of the curved section of the spring. Figure 5.7 shows an enlarged view of the curved section of the second

sulcation from the top, where the stress distribution can be seen in more detail. Figure 5.8 shows a graph of the nodes on the tensile surface at the second sulcation which shows the variation in stress along the tensile surface of this sulcation. Figure 5.9 shows the minimum principal stresses, the minimum stresses were found on the inner surface of the curved section. The minimum principal stress is -3.376 N/mm^2 under a 1 N load. The maximum principal stress under a 1 N load at the same curved section was 3.114 N/mm^2 which indicated the stress in compression was a larger absolute value than in tension, which supports the theory that there is a tendency for the neutral axis to shift towards centre.

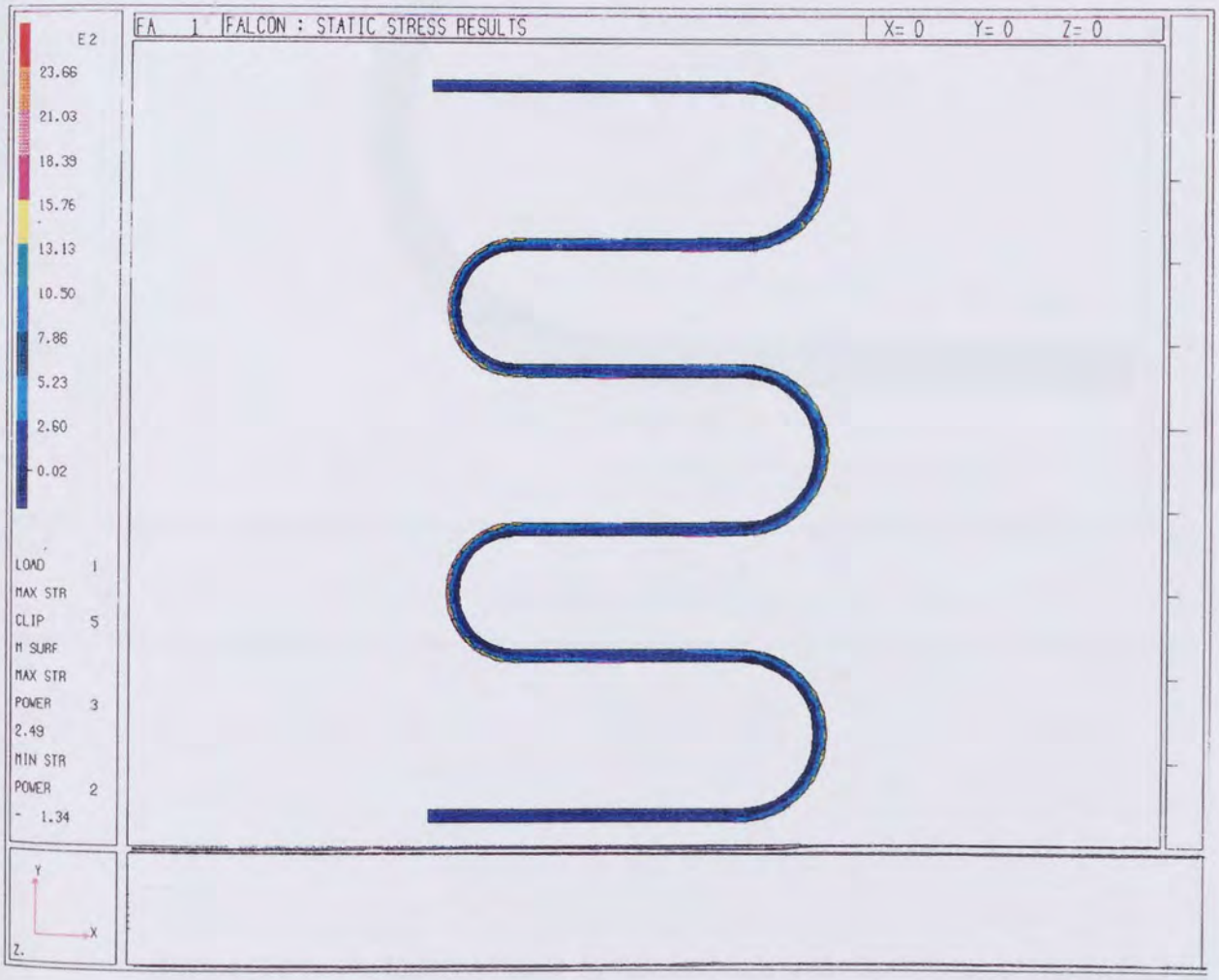

Figure 5.6 Maximum principal stresses of sulcated spring A6.

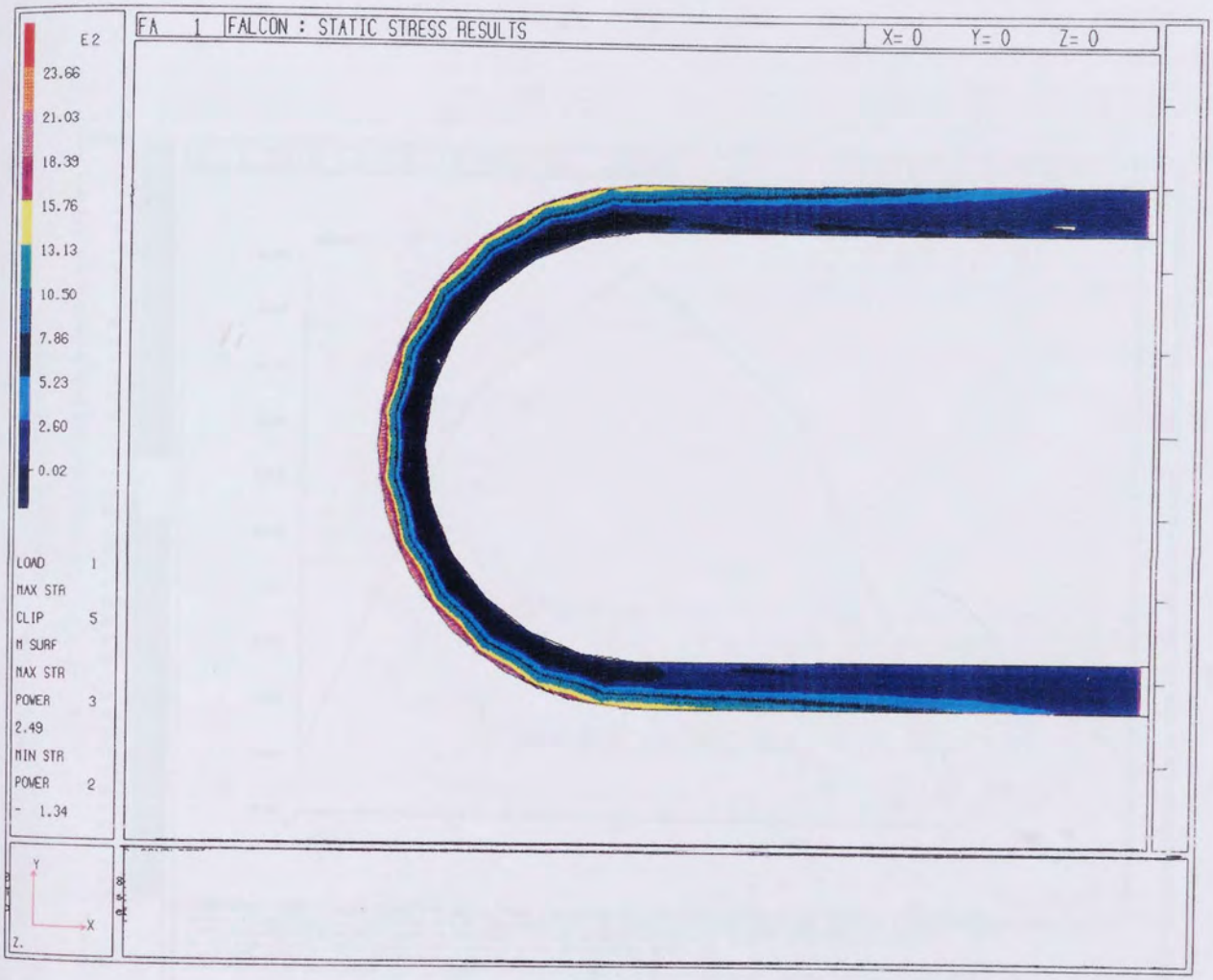

Figure 5.7 Enlarged view of the maximum principal stress of the second sulcation from the top of spring A6.

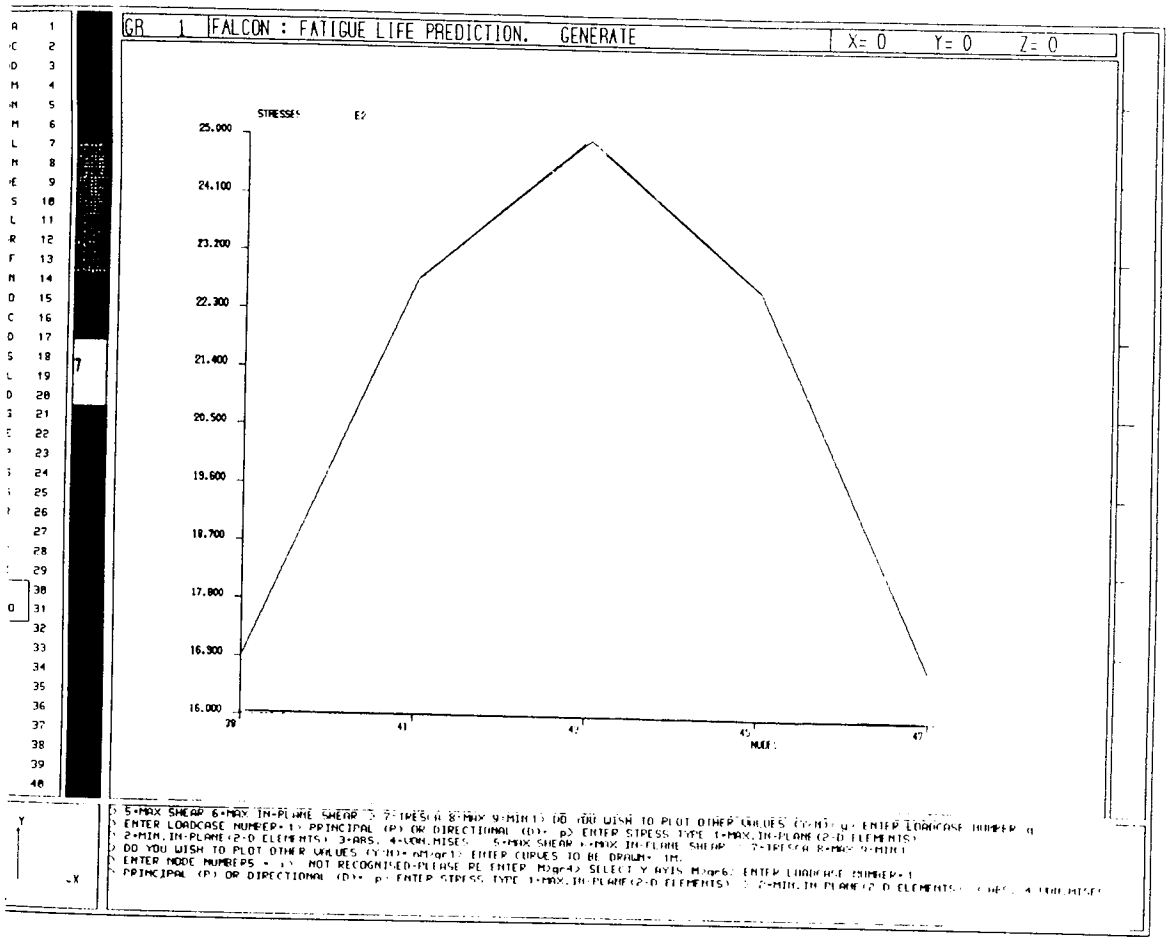

Figure 5.8 Graph of the variation in maximum principal stress along the tensile surface of the second sulcation of spring A6.

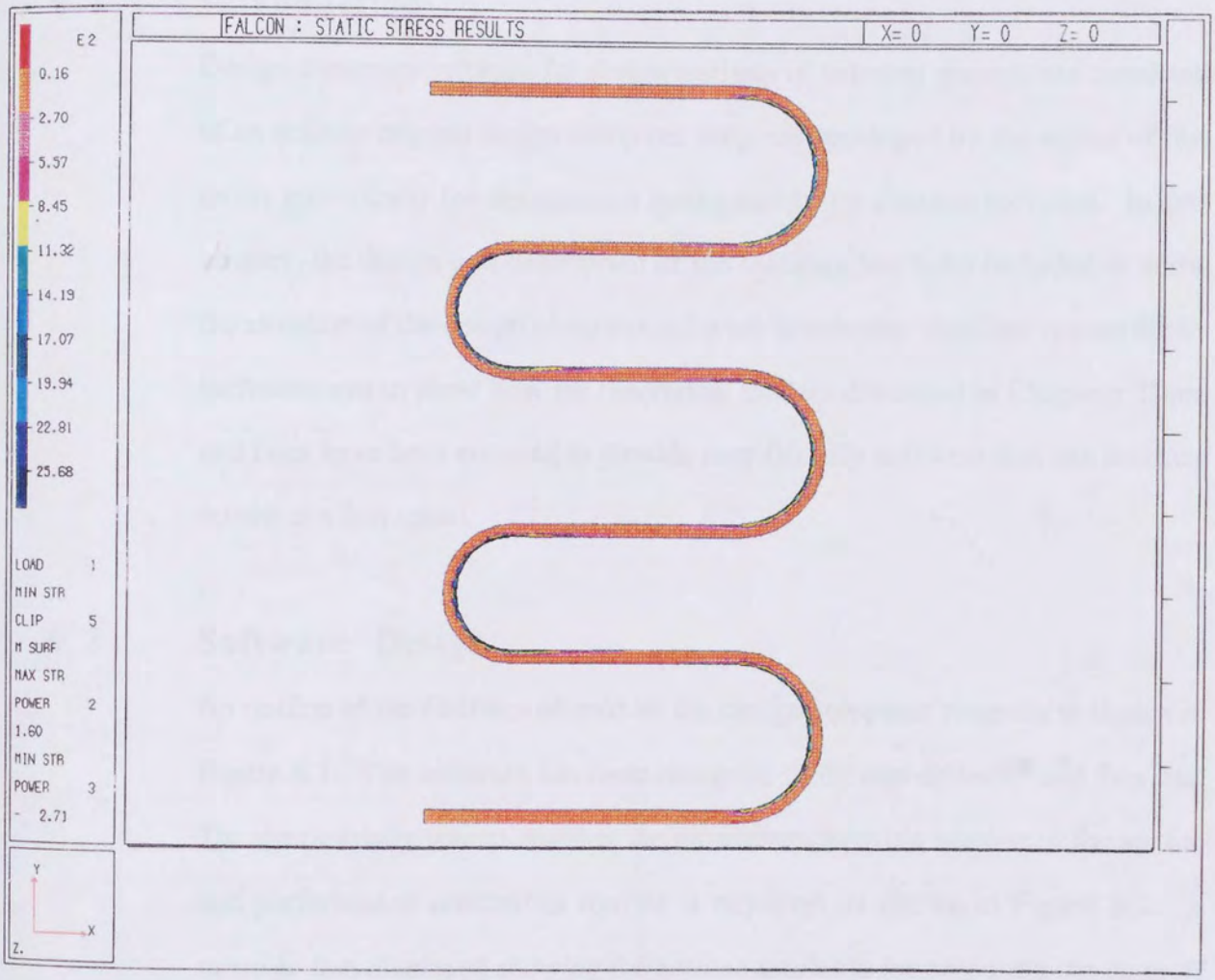

Figure 5.9 Minimum principal stress of sulcated spring A6.

Chapter 6

DESCRIPTION OF THE DESIGN COMPUTER SOFTWARE

6.1 Introduction

Design computer software for design analysis of sulcated springs has consisted of an entirely original design computer program developed by the author of this thesis specifically for the sulcated spring and finite element software. In this chapter, the design and description of the software has been included to show the structure of the design computer software developed. Another reason for its inclusion was to show how the theoretical models discussed in Chapters Three and Four have been encoded to provide user-friendly software that can produce results at a fast speed.

6.2 Software Design

An outline of the facilities offered by the design computer program is shown in Figure 6.1. The software has been designed to be user-friendly and flexible. The user initially selects whether the parameter checking routine or the spatial and performance constraints routine is required, as shown in Figure 6.2. A menu is then displayed showing the options available for preparing the data. If the user has chosen the parametric checking routine then, at this stage, the geometric parameters can be entered interactively. These parameters can be stored in a file on hard or floppy disc, using option two. The parameters can be displayed or changed using option three. Option four is used to retrieve an existing data file. Finally option five is used to continue with the design analysis when the parameters have been retrieved or entered. The screen displaying these options is shown in Figure 6.3.

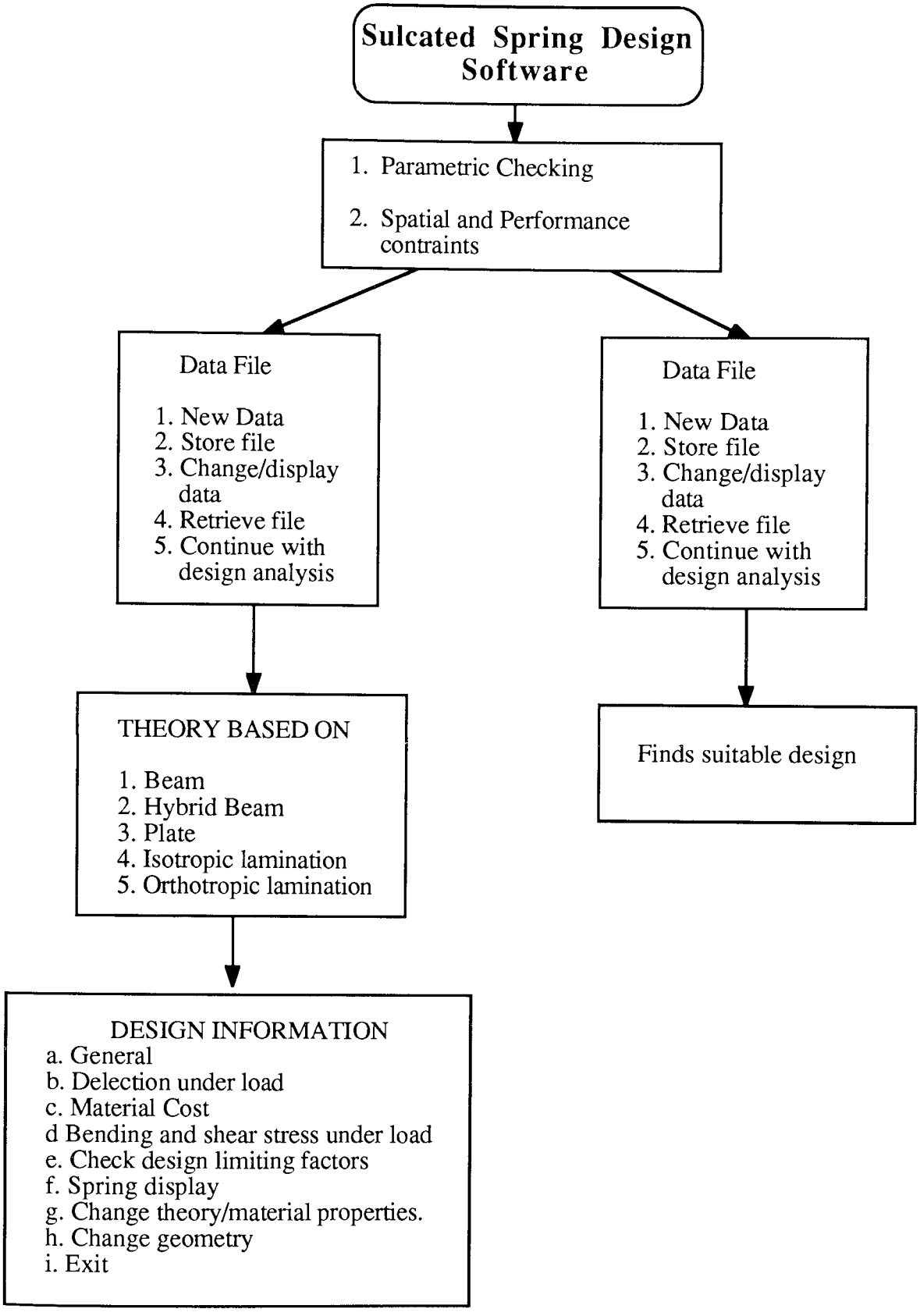

Figure 6.1 Outline of the design computer software.

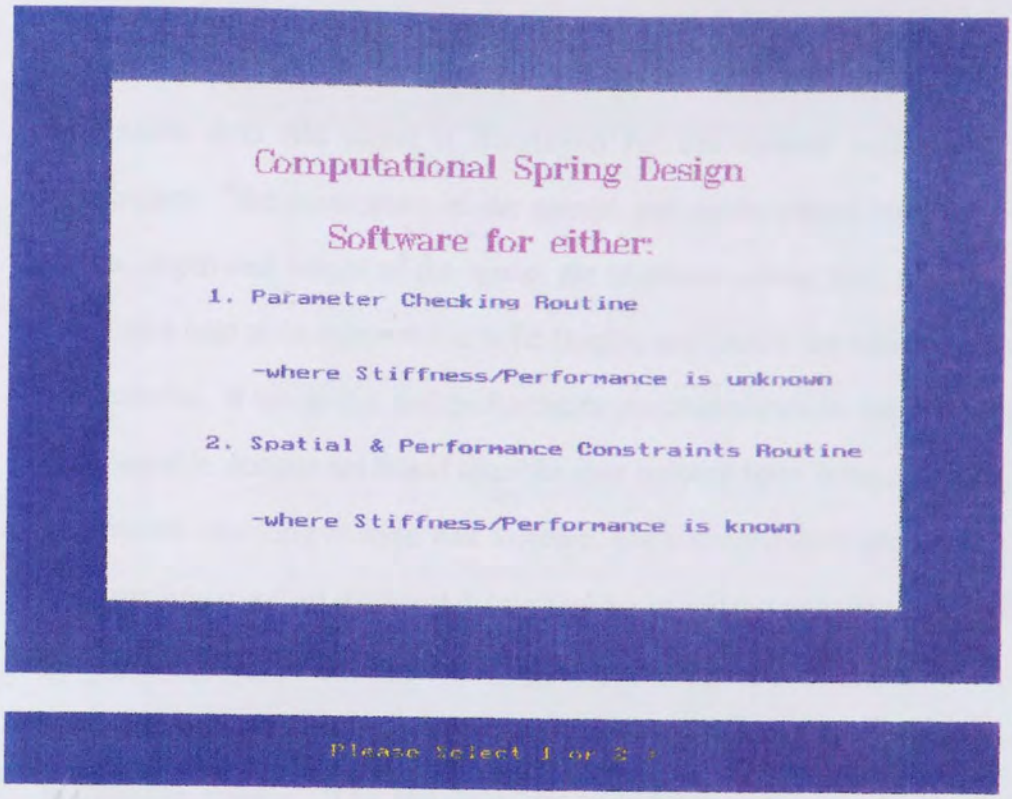

Figure 6.2 Display from screen of sulcated spring design software showing the initial choice of options

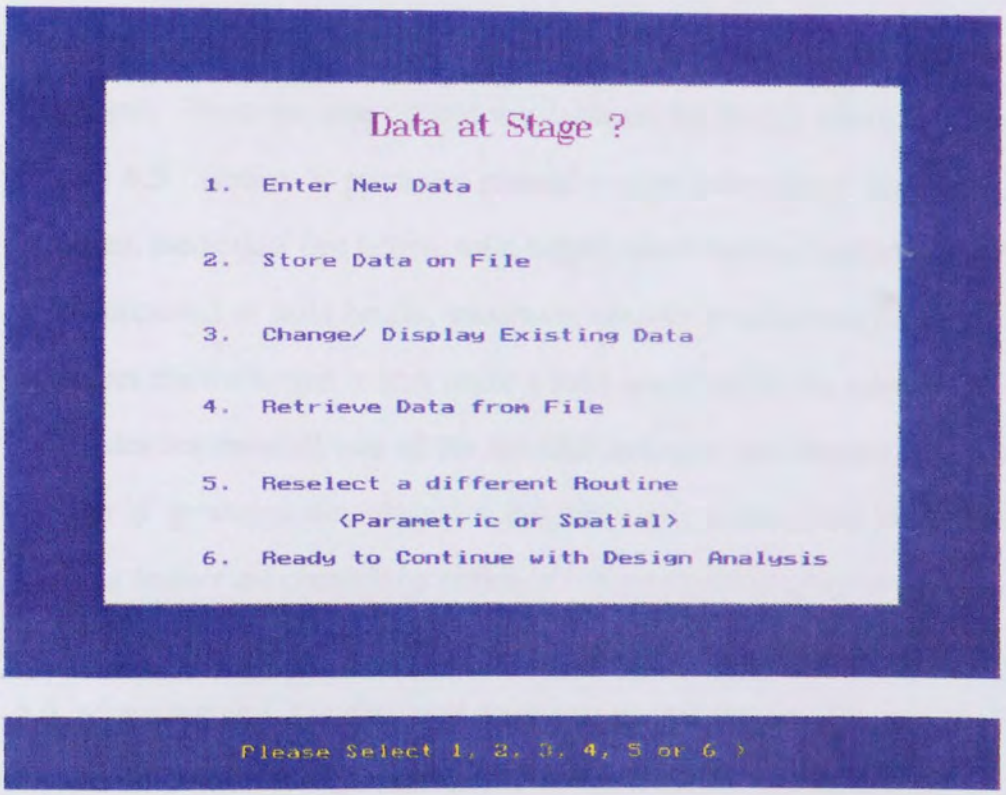

Figure 6.3 Display from screen of sulcated spring design software showing options available for data preparation.

The same data file menu is displayed for the spatial and performance constraints. The parameters in the spatial and performance routine case are width, depth and height of the space, the required spring rate, maximum and minimum load to be supported at solid height, and finally the elastic modulus of the material. If the spatial and performance constraint routine has been selected, then suitable designs are found after the data options have been selected. If the parametric checking routine was selected, the software then produces a menu with options to select different theoretical bases for the calculation of stiffness and stress, as Figure 6.4 illustrates. Options exist for the theory to be based on beam theory for one or two materials, plate theory, isotropic and orthotropic lamination theory. The last two consider fibre orientations other than 0 degrees, and orthotropic lamination theory allows the material properties to be specified in the longitudinal and transverse directions.

After the theoretical basis has been selected, the design information menu is displayed. There are nine options available on the design menu as shown in Figure 6.5. Option 'a' produces general design information such as spring stiffness, theoretical free height, solid height, mass made of glass/carbon fibre, load supported to solid height, maximum stresses at solid height. Option 'b' produces the deflection in mm under a load specified by the user. Option 'c' calculates the material cost of the sulcated spring of the entered dimensions. Option 'd' produces the maximum stresses under a specified load. Design limiting factors are checked by option 'e'. A graphical display of the spring is supplied by option 'f', an example of the type of display is shown in Figure 6.6, where spring C3 is displayed by selecting this option. Option 'g' allows the user to leave the design menu and return to select another theoretical basis or to change the material properties. Option 'h' allows the user to return to the data entry stage to change the geometry. Finally option 'i' allows the user to exit the software completely.

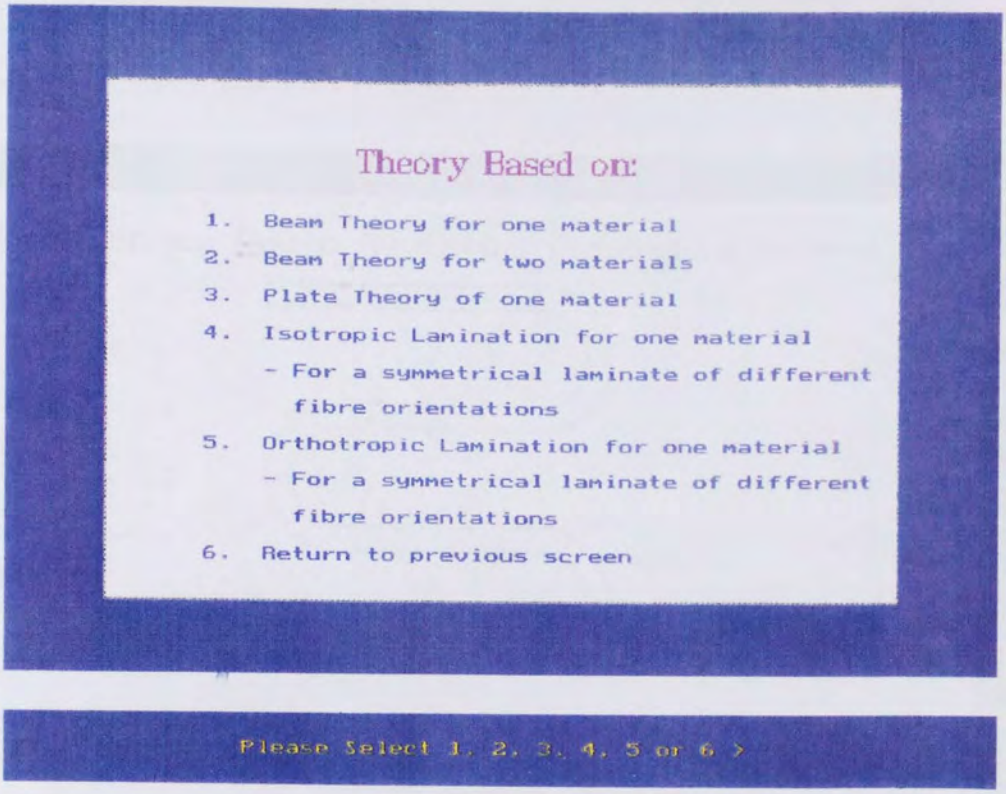

Figure 6.4 Theoretical bases available in the sulcated spring design software.

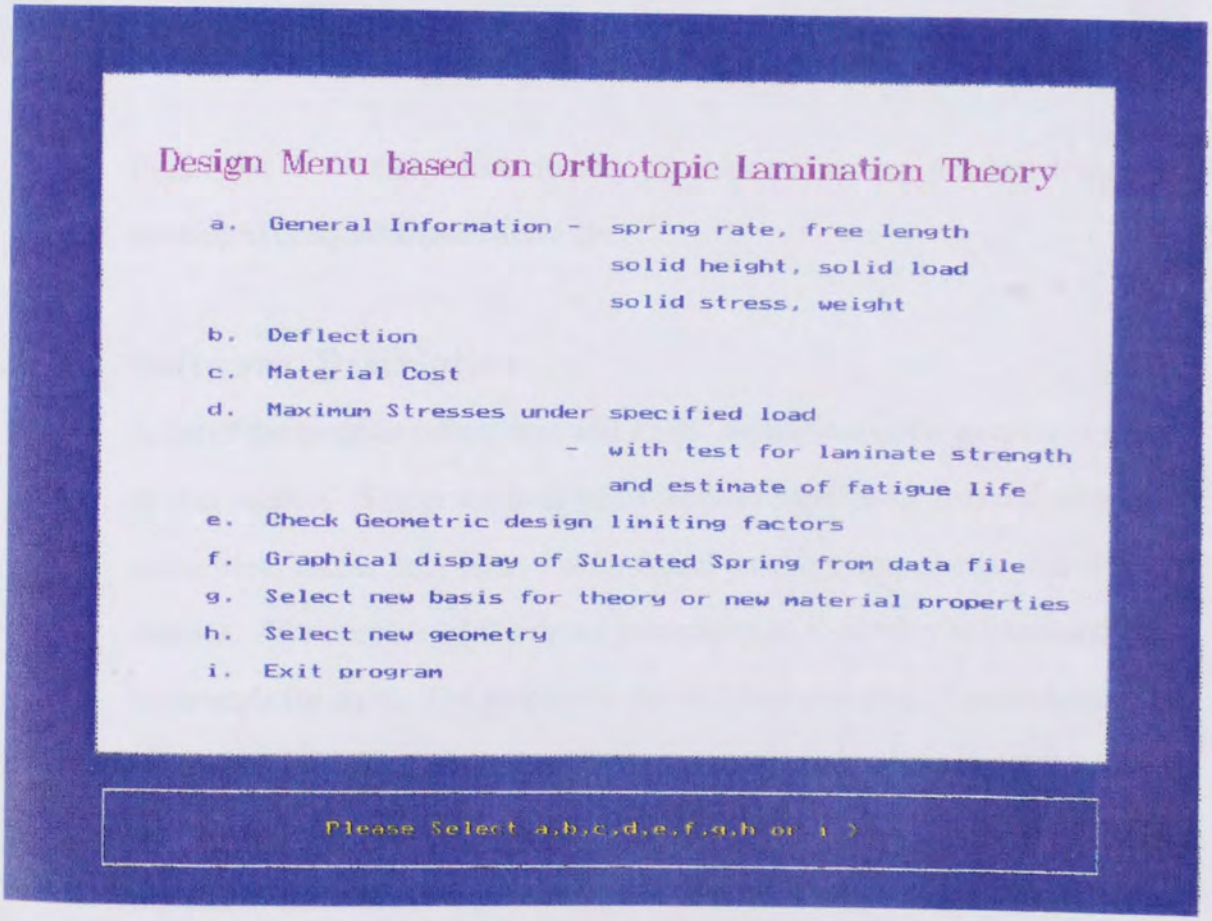

Figure 6.5 Design information menu of sulcated spring design software.

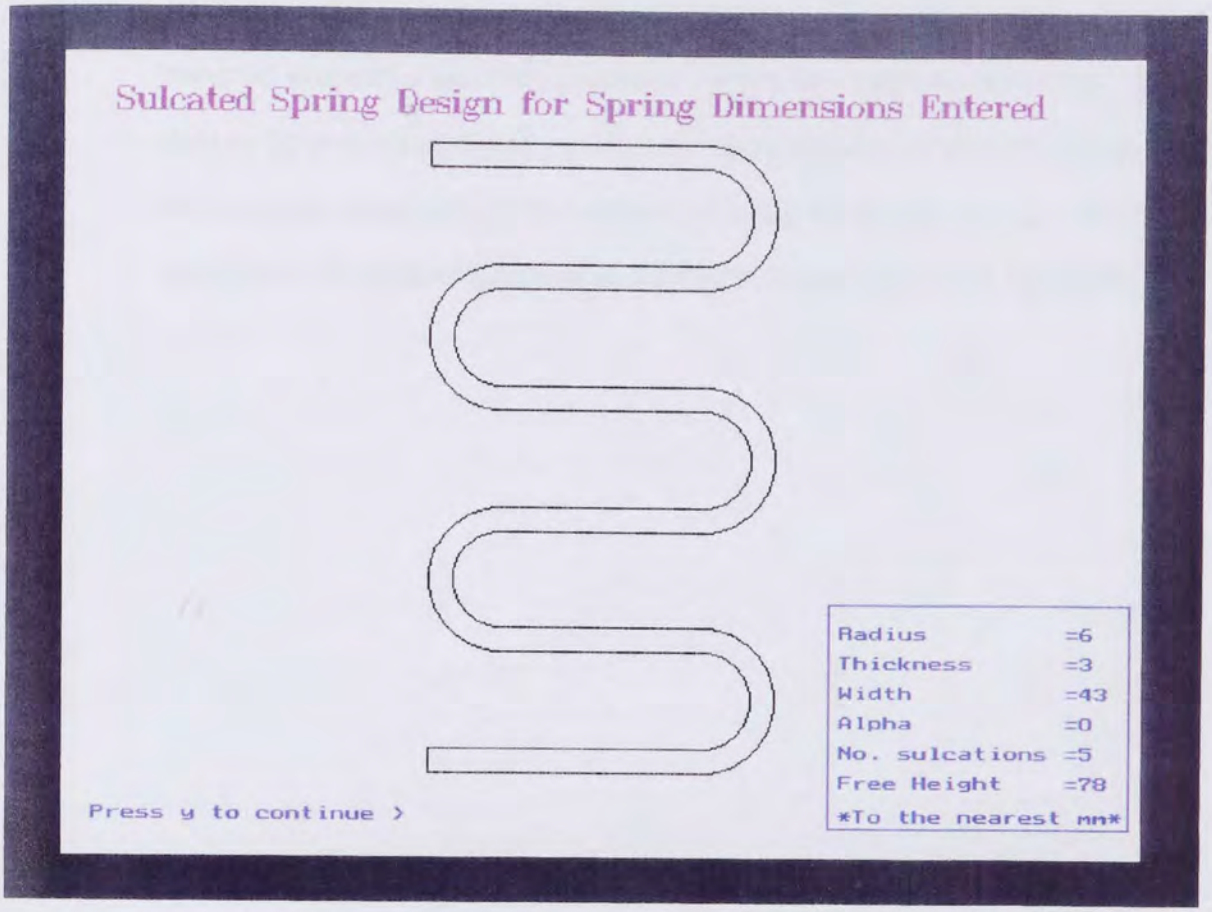

Figure 6.6 Graphical display of sulcated spring produced by the developed design computer software.

6.3 Software Description

A list of the procedures/functions and a brief description of the purpose is given in this section. The procedures and functions have been grouped into four categories, menu, data files, material and stacking sequences, and design options. The purpose of the menu procedures is to display information and commands for input. The purpose of the data files category of procedures is to enter, retrieve, store, change or display parameters in either sulcated spring geometric parameters (radius, laminate thickness, width, depth, angle α and number of sulcations) or spatial and performance constraints (width, depth, and height of the space, the required spring rate, maximum load to be supported at

solid height, and finally the elastic modulus of the material). The material and stacking sequence category contains procedures for the interactive entry of material properties and for lamination theory the stacking sequence. In the design options category, functions and procedures are used to supply the information required of the option selected from the design menu. A description of all these functions and procedures is contained in Appendix 2.

Chapter 7

SULCATED SPRINGS IN APPLICATIONS

7.1 Introduction

This chapter concerns the application of sulcated springs and shows how the design computer program can be applied to real problems. Three applications have been selected where sulcated springs could replace the coil spring. These are namely in: an automotive suspension system, a clutch mechanism and an engine poppet valve. Examples are then given of sulcated spring assemblies with reference to patents which exist for securing a sulcated spring to a suspension component. Although the spring assemblies are for an automotive suspension, the principles of securing a sulcated spring remain the same. Design computer software, as described and developed in this thesis, was then used to generate sulcated spring designs for replacing the coil suspension spring, clutch spring, and engine valve spring. Finally the chapter concludes with an assessment of the commercial feasibility of the sulcated spring in applications.

7.2 Applications

7.2.1 Automobile suspension system

A car frame supports the mass of the engine, power-train components, body and passengers. Wheels are attached to the frame through springs, which support the mass of the vehicle. The springs are placed between the frame and wheel axles, as shown in Figure 7.1.

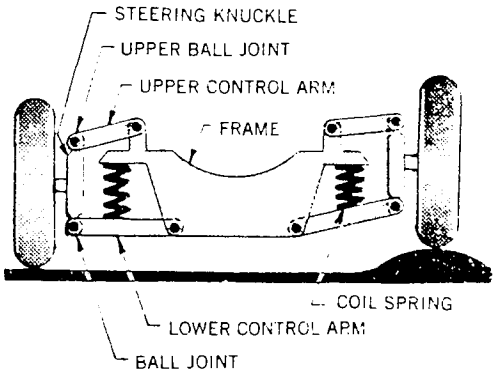

Figure 7.1 Independent front axle.

The mass of the structure applies an initial compression to the springs. As the car wheels encounter irregularities in the road profile, the spring is forced to further compress or expand. Thus the wheels move up and down independently of the frame. This allows the spring to absorb a large proportion of the up and down motion of the car wheels. When the wheel encounters a hole in the road, the wheel falls into the hole causing an expansion of the spring. If a bump in the road is experienced, the spring is compressed. Rubber pads are placed between the ends of the coil spring or suspension device, to prevent vibration transfer. On many cars, a shock absorber is placed inside the coil springs and is usually placed between the axles and the frame to control the spring's deflection and give good ride handling.

7.2.2 Clutch mechanism

A clutch is a mechanism designed to connect or disconnect the transmission of power from one working unit to another. The clutch contains a friction disc which contains an arrangement of springs, and a pressure plate for pressing this tightly against the smooth face of the flywheel, as shown in Figure 7.2.

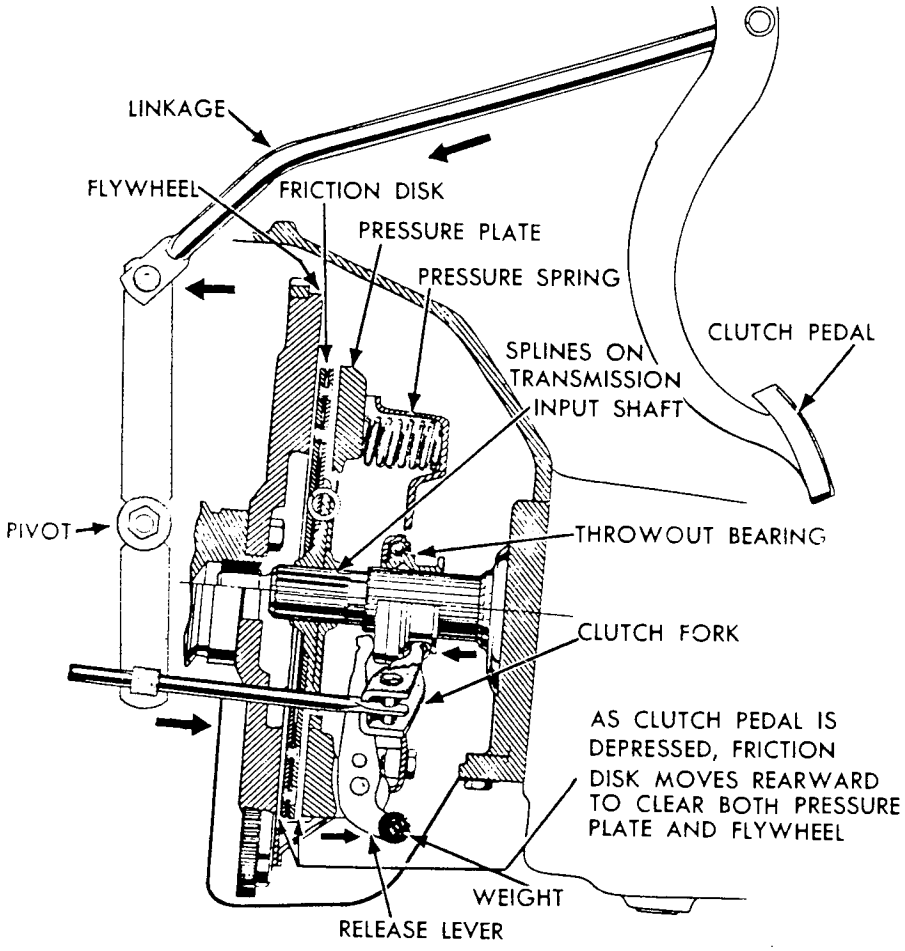

Figure 7.2 Sectional view of a clutch with the linkage to the clutch pedal shown schematically.

When the clutch is engaged, the pressure coil springs push the pressure plate forward, forcing the clutch disc firmly against the flywheel. Consequently, these springs must be strong enough to hold the pressure disc against the flywheel, and transmit the engine power at speeds of 500 rev/min. The pressure plate requires over 7 MPa of pressure to hold the clutch disk against the flywheel. The pressure springs must be of equal length and strength to seat the clutch disc evenly. Any deviations in length results in a lower pressure at some point on the friction surface, and the possibility of slippage. Insufficient pressure in these springs would cause loss of power resulting in a slipping clutch

which could overheat, and thus cause possible failure. Several coil springs are spaced around the pressure plate, and inside cover, as shown in Figure 7.3.

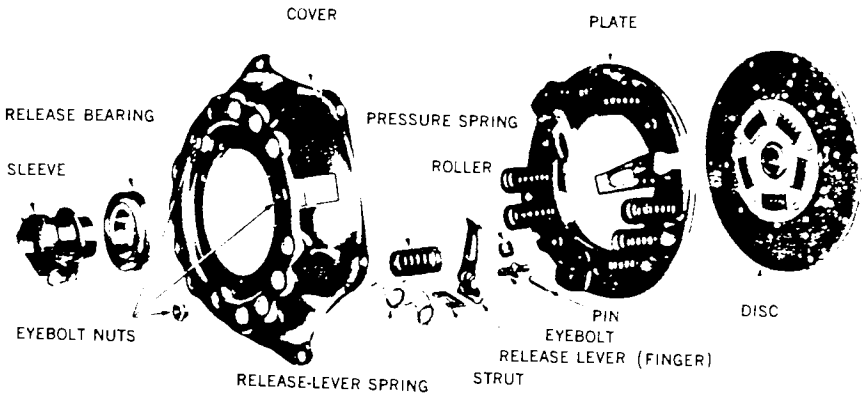

Figure 7.3 Coil Spring - Type Clutch.

7.2.3 Engine valve springs

The valves and valve operating mechanisms control the admission of the air or fuel - air mixture into the cylinder. A spring on the valve stem tends to hold the valve on its seat. The lower end of the spring rests against a flat section of the cylinder head. The upper end rests against a flat washer, or spring retainer lock or keeper. When the spring is under compression, the spring tries to expand keeping the valve seated. Valve springs are wound spirally of high grade spring - steel wire, and are ground flat at each end to ensure an even distribution of pressure. Most engines use one spring per valve, although some may use two or three where one spring is placed inside the other. Multiple springs are used to ensure a more even distribution of pressure.

It is important for the spring to exert sufficient pressure to ensure the valve and lifter follow the cam and close tightly. If the valve does not close tightly, the valve will bounce or flutter causing a high speed engine miss. Unequal valve springs will upset valve face- to- seat alignment producing a poor seal. The operating temperatures in this area vary. Intake valves operate at relatively cool

atmospheric temperatures since it passes only air or a fuel - air mixture. Exhaust valves operate at very high temperatures of 550 to 700 $^{\circ}$ C.

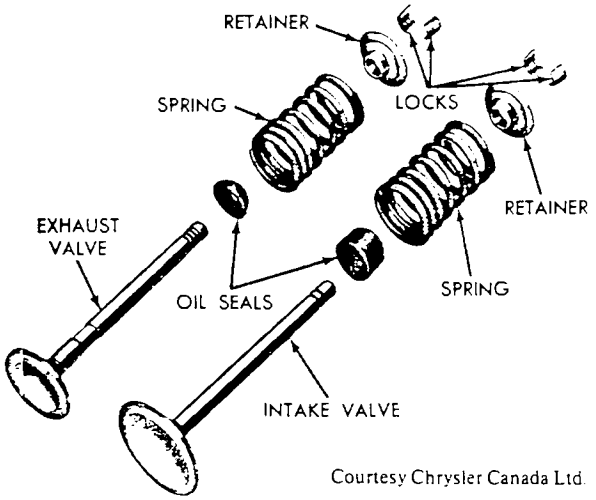

Figure 7.4 Valve assembly.

7.3 Practical Constraints in Applications

Before applying the design computer software, it is important to observe what practical constraints exist which may restrict a theoretically feasible sulcated spring design. There are two practical constraints which need to be addressed. The first constraint concerns the spring assembly within an application. A spring design may need to be altered to enable the spring to be secured in the best way. The second constraint is the spatial and performance criteria, for example restrictions on space, performance or temperature. These factors need to be considered if a practical sulcated spring design is to be found.

7.3.1 Spring assemblies

The sulcated spring can be used as a replacement for the conventional coil spring in numerous applications, as described in section 1.3 on the market potential. Before a sulcated spring can be used in an application, a means of attaching the spring has to be found so that the spring can function in the

proposed application. Sulcated springs are susceptible to damage if the continuity of their constituent fibres is interrupted. This causes a design problem in that fibre disruption caused by drilling, or otherwise providing a hole for a fastener, leads to degradation of the material properties and ultimately to possible spring failure.

Two patents have been filed by GKN Technology Limited which describe different means of securing a sulcated spring in a motor vehicle suspension system. The first of these patents [31] describes an invention which provides for the clamping of the end limb of the spring between the flat surfaces of the support member and anchoring member, as shown in Figure 7.5.

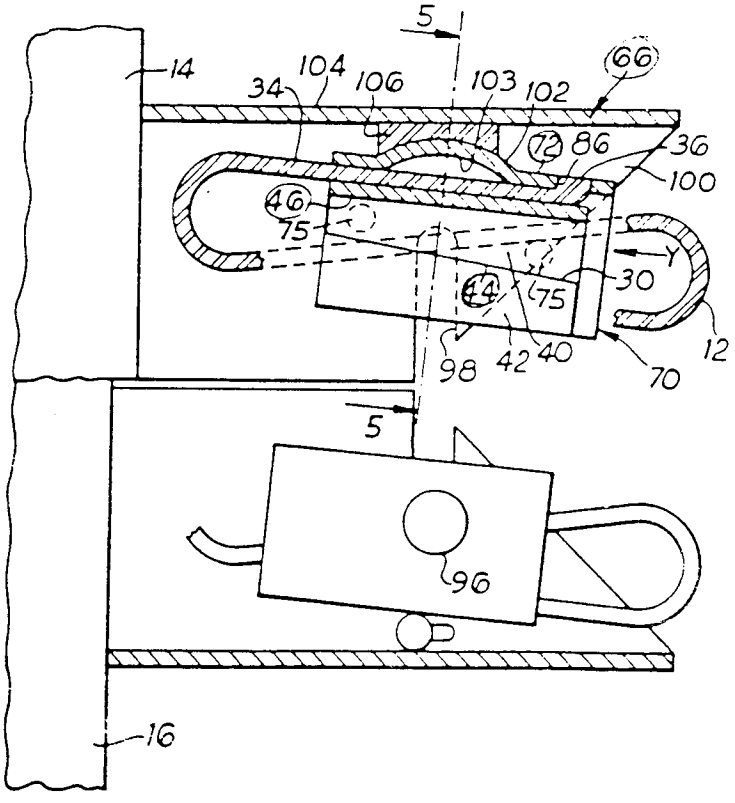

Figure 7.5 Securing a sulcated spring to a suspension component.

Penetration of the straight limb is avoided, and the use of flat surfaces to constrain the sulcated spring has the advantage of avoiding pressure points. A clamping force is thus spread evenly over a substantial portion of the end limb. When the spring limb is satisfactorily clamped between the anchoring surface (46) and support surface (72), the anchoring member can be fixed to the support member by any appropriate means, to prevent any possibility of slackening of the connection. Fixing is carried out by welding between the anchoring member and support member. Welding needs to be carried out at a distance from the spring limb, so that heat damage is prevented.

It has been found that the possibility of failure in the curved portions of a sulcated spring adjacent to an end limb can be reduced if the end limb of the spring is allowed to pivot about an axis normal to the general plane of the spring. This allows the end limb to assume an angle appropriate to the state of compression or extension of the spring, equalising stresses in the adjacent curved portions of the spring.

The life of a sulcated spring is related to the angles through which the curved portions are made to bend when the spring is compressed. If the end limb is clamped at an arbitrary angle to inter-fit with the component, fatigue life may be severely reduced since, when the spring is compressed, one curved portion of the spring will bend through a greater angle than the other curved portions of the spring. This can be detrimental to the life of the spring. The invention described in the second patent [32] attempts to overcome this problem. Figure 7.6 shows this invention.

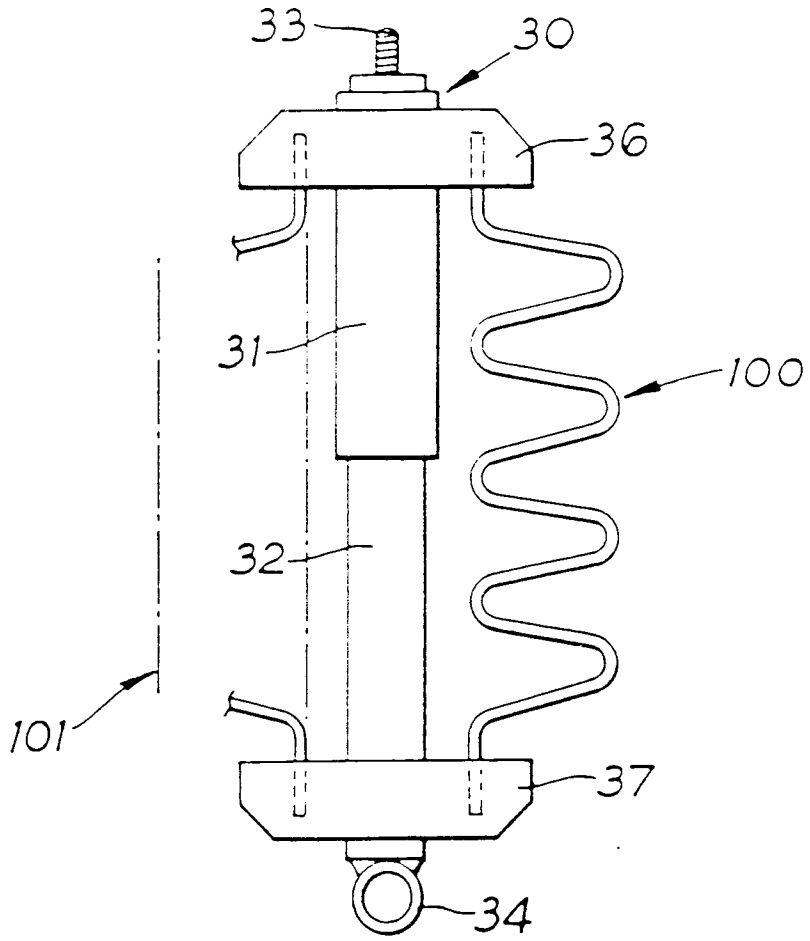

Figure 7.6 Sulcated spring assemblies.

As seen in Figure 7.6, spring assembly in this patent comprises a sulcated spring and a member holding an end portion of the spring. This is effectively the same as pin jointing an end zig-zag limb of the spring at its mid point. By pin jointing spring end limbs in this way, and applying forces to the spring at the pin joints the spring can be made to compress uniformly along its length. Another observation is that alternate limbs of the spring remain parallel to one another. The invention thus has the beneficial effect of providing a potential improvement to the spring life.

7.3.2 Spatial and performance constraints

Restrictions on space and performance need to be known, before a sulcated spring can attempt to replace the coil spring. The applications considered in this chapter have known spatial and performance requirements. Table 7.1 shows the coil spring data for a typical suspension, clutch and engine valve spring which includes the coil spring dimensions, performance requirements, material type, material properties, and mass. Using this data as a basis for spatial and performance requirements of the selected coil springs, the design computer program was used to find sulcated spring designs which satisfied these requirements.

Spring Type:	*CAR SUSPENSION*	*CLUTCH*	*ENGINE VALVE*
Material Type	BS 1429 CrVd Annealed	BS2803 SiCr PreHrd	BS2903 CrVd PreHrd&Temp
End Type:	CLOSED & GROUND	CLOSED & GROUND	CLOSED & GROUND
End Fix:	ENDS FIXED & GUIDED	ENDS FIXED & GUIDED	ENDS FIXED & GUIDED
Wire Diameter (mm)	14.73	4.52	6.04
Outside Diameter (mm)	120.65	19.57	45.54
Total Coils:	11.00	5.25	7.88
Spring Rate (N/mm)	41.36	373.46	36.44
Free Length (mm)	368.30	26.54	80.30
Solid Length (mm)	162.05	23.73	47.56
Solid Load (N)	8 530.75	1 049.42	1193 05
Solid Stress (MPa)	859.13	659.85	662.39
Active Coils:	9.50	3.25	5.88
Spring Index	7.19	3.33	6.54
Inside Diameter(mm)	91.19	10.53	33.46
Helix Angle (deg)	6.25	6.50	5.35
Wire Length (mm)	3 679.74	249.66	980.73
Mass per 100 (kg)	491.14	3.14	22.00
Youngs Modulus (MPa)	206 800	206 800	206 800
Rigidity Modulus (MPa)	79 300	79 300	79 300

Table 7.1 Coil spring data.

7.4 Sulcated Springs for Applications

7.4.1 Suspension sulcated spring designs

The outside diameter for a front car suspension spring is typically 120.65 mm, and the free length is 368.30 mm the dimensions of which are shown in Table 7.1. The width and depth of the sulcated spring needs to be carefully chosen, since the objective is to design as close to the present space occupied by a coil spring to ensure that redesign of the surrounding space is minimised. There is also an additional problem in that most front suspension springs have a shock absorber along the central axis of the coil spring. In the sulcated spring design there is no hole for a shock absorber to be passed through, and drilling is not advisable for reasons as discussed for spring assemblies (section 7.3.1). One proposal is to design two sulcated springs on either side of the shock absorber. An alternative design for more stability is to use four sulcated springs in an arrangement as shown in Figure 7.7.

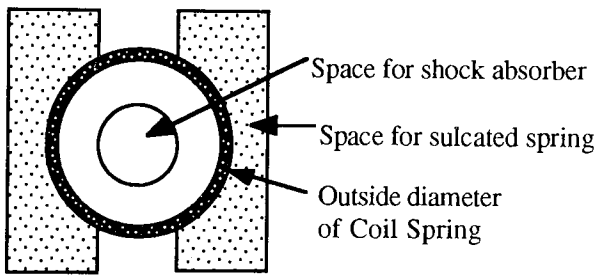

Figure 7.7 Overview of suspension arrangement for 2 sulcated springs.

However, when the computer program was used to find suitable sulcated spring designs within the spatial constraints of the existing coil spring, the designs which were found produced a stress value higher than recommended. One of the constraints within the program was for the width to be greater than twice the thickness plus twice the radius, therefore the wider the spring the more choice of radius and thickness combinations can be obtained from the program. The maximum width can be obtained from the two sulcated spring

configuration on either side of the shock absorber. By increasing the free length to 480 mm, the excess space required outside of the coil diameter was reduced.

For this arrangement, the spatial constraint dimensions and performance requirements for each spring were as follows:-

Width=166 mm

Height=480 mm

Depth=58 mm

Required spring rate = 20.68 (+ 3) N/mm

Elastic modulus=40.8 GPa

Specified Bending stress below 750 MPa

Maximum load for four springs to be supported 4265.38 N each

The elastic modulus of 40.8 GPa is for a glass fibre/epoxy resin system. Using the above constraints with angles of α between 5 to 20 degrees to allow ease of manufacture and fabrication, the design computer program produced five suitable designs for an upper tolerance level of 3 N/mm as shown in Figure 7.8. Although all designs have a solid height bending stress which exceeds the recommended stress, the sulcated spring will never reach the solid height because the user's specified maximum load is less than the maximum load for each design. The most suitable design (first design) was selected on the basis of being the nearest to the required spring stiffness.

SPATIAL AND PERFORMANCE REQUIREMENTS
****

1.	Width	= 166.00 mm
2.	Height	= 480.00 mm
3.	Depth	= 58.00 mm
4.	Required Spring Rate	= 20.68 N/mm
5.	Elastic Modulus	= 40.80 GPa
6.	Upper tolerence on spring rate	= + 3.00 N/mm
7.	Max. bending stress less than	750.00 MPa
8.	Maximum load to be supported	= 4265.38 N

Number of sulcations	= 5
Alpha	= 6 deg
Thickness	= 7.25 mm
Radius	= 40.69 mm
Bending stress at required load	= -703.79 MPa
Mass in glass fibre	= 940.67 g
Mass in carbon fibre	= 837.11 g
Spring Rate	= 22.32 N/mm
Maximum load supported	= 4293.13 N
Maximum deflection	= 192.39 mm

Number of sulcations	= 5
Alpha	= 7 deg
Thickness	= 7.25 mm
Radius	= 40.13 mm
Bending stress at required load	= -703.60 MPa
Mass in glass fibre	= 938.63 g
Mass in carbon fibre	= 835.30 g
Spring Rate	= 22.65 N/mm
Maximum load supported	= 4433.25 N
Maximum deflection	= 195.72 mm

Number of sulcations	= 5
Alpha	= 8 deg
Thickness	= 7.25 mm
Radius	= 39.55 mm
Bending stress at required load	= -703.35 MPa
Mass in glass fibre	= 936.60 g
Mass in carbon fibre	= 833.49 g
Spring Rate	= 23.00 N/mm
Maximum load supported	= 4582.12 N
Maximum deflection	= 199.19 mm

Number of sulcations	= 5
Alpha	= 9 deg
Thickness	= 7.25 mm
Radius	= 38.95 mm
Bending stress at required load	= -703.05 MPa
Mass in glass fibre	= 934.58 g
Mass in carbon fibre	= 831.69 g
Spring Rate	= 23.38 N/mm
Maximum load supported	= 4740.60 N
Maximum deflection	= 202.79 mm

Number of sulcations	= 11
Alpha	= 5 deg
Thickness	= 7.50 mm
Radius	= 12.72 mm
Bending stress at required load	= -744.29 MPa
Mass in glass fibre	= 1674.47 g
Mass in carbon fibre	= 1490.13 g
Spring Rate	= 22.45 N/mm
Maximum load supported	= 5329.07 N
Maximum deflection	= 237.35 mm

There were 5 designs matching your specifications

Figure 7.8 Designs for a two sulcated spring car suspension spring.

Free height=480 mm

Depth=58 mm

Width=166 mm

Number of sulcations=5

Angle α=6 deg

Sulcation radius=40.69 mm

Laminate thickness=7.25 mm

Bending stress at specified maximum load = -703.79 N/mm^2

Mass in glass fibre epoxy resin=0.941 kg

Spring rate 22.32 N/mm

Maximum load supported = 4293.13 N

The total mass of the two springs is 19% of the mass of one coil spring, saving 3.97 kg for each coil spring. Personal communication with a suspension spring manufacturer has revealed that it was acceptable for a spring to support a larger load than was necessary. It was also revealed that the idea of distributing the load in the form of a nested coil spring (where one coil spring is placed inside another) has been used on some cars. This incorporates a similar idea to the proposed sulcated spring design in that the load is distributed between two, three or four sulcated springs.

In a paper by Carter and Murphy [33] a suspension sulcated spring design was proposed which used the outside diameter of a coil suspension spring as the width and depth of a sulcated spring. Although the design was feasible, in terms of replacing the coil spring, it did not cater for a shock absorber passing through the centre of the spring.

7.4.2 Clutch sulcated spring designs

The clutch sulcated spring is the smallest spring of the three applications considered at only 26.54 mm (as can be seen from the free length in Table 7.1). A practical sulcated spring with negligible horizontal deflection has to have at least 3 sulcations. Coupled with the fact that, in the design of composites the radius of sulcation is recommended to be at least 3 mm, in terms of space the proposed sulcated spring was designed to fit within exactly the same space currently occupied by a coil spring.

The spatial constraint dimensions and performance requirements for a clutch spring were:-

Width=13.83 mm

Height=26.54 mm

Depth=13.83 mm

Required spring rate = 373.46 N/mm

Elastic modulus=40.8 GPa

Specified Bending stress below 750 MPa

Maximum load to be supported at least 1049 N

It was desirable from the manufacturing viewpoint to find a sulcated spring design with an angle of α greater than zero, due to the tight curvature at which the laminate is fabricated. However no designs were found to match the constraints. Figure 7.9 shows the results of the design computer program for the spatial and performance criteria of a typical automotive clutch spring. Four designs were produced for the constraint of the angle alpha between 0 and -20 degrees.

SPATIAL AND PERFORMANCE REQUIREMENTS
****

1.	Width	= 13.83 mm
2.	Height	= 26.54 mm
3.	Depth	= 13.83 mm
4.	Required Spring Rate	= 373.46 N/mm
5.	Elastic Modulus	= 40.80 GPa
6.	Accepts spring rates greater than required spring rate	
7.	Max. bending stress less than	750.00 MPa
8.	Maximum load to be supported	= 1049.00 N

Number of sulcations	= 3
Alpha	= -20 deg
Thickness	= 2.50 mm
Radius	= 3.04 mm
Bending stress at required load	= -503.17 MPa
Mass in glass fibre	= 3.40 g
Mass in carbon fibre	= 3.03 g
Spring Rate	= 445.66 N/mm
Maximum load supported	= 1956.53 N
Maximum deflection	= 4.39 mm

Number of sulcations	= 3
Alpha	= -19 deg
Thickness	= 2.50 mm
Radius	= 3.03 mm
Bending stress at required load	= -505.92 MPa
Mass in glass fibre	= 3.40 g
Mass in carbon fibre	= 3.02 g
Spring Rate	= 447.08 N/mm
Maximum load supported	= 1981.09 N
Maximum deflection	= 4.43 mm

Number of sulcations	= 3
Alpha	= -18 deg
Thickness	= 2.50 mm
Radius	= 3.02 mm
Bending stress at required load	= -508.57 MPa
Mass in glass fibre	= 3.40 g
Mass in carbon fibre	= 3.02 g
Spring Rate	= 448.64 N/mm
Maximum load supported	= 2006.91 N
Maximum deflection	= 4.47 mm

Number of sulcations	= 3
Alpha	= -17 deg
Thickness	= 2.50 mm
Radius	= 3.01 mm
Bending stress at required load	= -511.11 MPa
Mass in glass fibre	= 3.39 g
Mass in carbon fibre	= 3.02 g
Spring Rate	= 450.34 N/mm
Maximum load supported	= 2034.05 N
Maximum deflection	= 4.52 mm

There were 4 designs matching your specifications

Figure 7.9 Suitable Automotive Clutch Sulcated Spring Designs.

A typical sulcated spring design to replace a clutch spring would have the following dimensions as shown in the fourth design of Figure 7.9.

Free height=26.54 mm

Depth=13.83 mm

Width=13.83 mm

Number of sulcations = 3

Radius of sulcation =3.01 mm

Laminate thickness=2.50 mm

Angle α=-17 deg

Elastic modulus=40.8 GPa

Bending stress at solid height= -511.11 MPa

Spring stiffness=450.34 N/mm

Mass in glass fibre epoxy resin=3.39 g

Solid load=2034.05 N

One of the advantages of the sulcated spring is that there is a linear relationship between spring rate and depth. So even if the spring rate is higher than required, the depth dimension can be reduced in the same proportion, as in the case of all the designs. Therefore no upper tolerance was specified. The required spring rate was 373.46 N/mm, however the fourth design of Figure 7.9 has a spring stiffness of 450.34 N/mm. The depth can be reduced by 0.829, which is the proportion of 373.46 N/mm to 450.34 N/mm. Multiplying the depth dimension by the same proportion gives a depth dimension of 11.47 mm. So the spring stiffness has been reduced to that required. Another reason for selecting the last spring design was from a manufacturing point of view, it is easier to fabricate for an angle of alpha of -17 degrees than of -20 degrees.

Again, for these spring designs, the maximum load at solid height is higher than specified. In an application this means that the solid height would never be reached. In discussions with a clutch spring designer this was considered acceptable. Although this problem in conventional spring design would be overcome by reducing the free height so the spring would reach within a few millimetres of solid height, in fact, car manufacturers and designers are looking for ways of streamlining the bonnet, so reducing the height of springs would be a useful advantage in the light of the current trend. These proposed sulcated spring designs leave room for a reduction in height because the proposed designs do not reach the solid height under the maximum load currently supported by a coil spring. The bending stress for this clutch spring design is considerably less than the coil spring, so for this sulcated spring design an infinite fatigue life can be expected. Compared with the equivalent steel clutch spring, a mass saving of 89% can be gained by using one of the sulcated spring designs suggested.

7.4.3 Engine valve sulcated spring designs

The replacement engine valve spring has to operate in moist conditions at high environmental temperatures. This poses a problem to the glass fibre epoxy resins as used in sulcated spring manufacture which have operational temperatures of -55°C to +130°C and are sensitive to hot wet environments. Nevertheless replacement sulcated spring designs were attempted because, with new high temperature materials on the market, it may be possible to eventually replace the coil spring in this environment in the future.

An engine valve coil spring has a valve stem passing through its centre. Therefore, in the replacement sulcated spring design, this had to be taken into account, and a similar method to the suspension spring was adopted where a sulcated spring was designed on either side of the valve stem. A valve stem

diameter of 8 mm was assumed. Carter and Murphy [33] have also proposed an engine valve spring design which was a replacement sulcated spring design in terms of space and performance to show that replacement designs were possible, (in their example no account was taken of the valve stem passing through the centre of the spring).

The spatial and performance requirements were as follows:-

Width=32.20 mm

Height=80.30 mm

Depth=12.10 mm

Required spring rate = 18.22 (+ 2.0) N/mm

Elastic modulus=40.8 GPa

Specified Bending stress below 750 MPa

Maximum load for two springs to be supported 59.87 N each.

Sulcated spring designs produced by the design computer program which satisfied these requirements are shown in Figure 7.10. Five designs were produced, the first design has the least mass, the lowest stress, and the radius-to-thickness ratio is quite large in comparison to the other designs which is suitable more easy to fabricate, therefore the first design was considered to be the most suitable.

```
        SPATIAL AND PERFORMANCE REQUIREMENTS
        ************************************

1.      Width                                =  32.20 mm
2.      Height                               =  80.30 mm
3.      Depth                                =  12.10 mm
4.      Required Spring Rate                 =  18.22 N/mm
5.      Elastic Modulus                      =  40.80 GPa
6.      Upper tolerence on spring rate          = + 2.00 N/mm
7.      Max. bending stress less than        750.00 MPa
8.      Maximum load to be supported =        59.87 N

Number of sulcations                 =     3
Alpha                                =    20 deg
Thickness                            =   2.25  mm
Radius                               =  11.19  mm
Bending stress at required load = -89.06 MPa
Mass in glass fibre                  =   8.15 g
Mass in carbon fibre                 =   7.26 g
Spring Rate                          =  18.24  N/mm
Maximum load supported               = 484.13 N
Maximum deflection                   =  26.54  mm

Number of sulcations                 =     5
Alpha                                =    13 deg
Thickness                            =   2.00  mm
Radius                               =   5.16  mm
Bending stress at required load = -125.30 MPa
Mass in glass fibre                  =   9.57 g
Mass in carbon fibre                 =   8.52 g
Spring Rate                          =  18.28  N/mm
Maximum load supported               = 682.95 N
Maximum deflection                   =  37.36  mm

Number of sulcations                 =     5
Alpha                                =    14 deg
Thickness                            =   2.00  mm
Radius                               =   4.99  mm
Bending stress at required load = -125.62 MPa
Mass in glass fibre                  =   9.55 g
Mass in carbon fibre                 =   8.50 g
Spring Rate                          =  18.73  N/mm
Maximum load supported               = 718.58 N
Maximum deflection                   =  38.37  mm

Number of sulcations                 =     5
Alpha                                =    15 deg
Thickness                            =   2.00  mm
Radius                               =   4.81  mm
Bending stress at required load = -126.00 MPa
Mass in glass fibre                  =   9.52 g
Mass in carbon fibre                 =   8.47 g
Spring Rate                          =  19.21  N/mm
Maximum load supported               = 757.45 N
Maximum deflection                   =  39.44  mm

Number of sulcations                 =     5
Alpha                                =    16 deg
Thickness                            =   2.00  mm
Radius                               =   4.62  mm
Bending stress at required load = -126.46 MPa
Mass in glass fibre                  =   9.49 g
Mass in carbon fibre                 =   8.45 g
Spring Rate                          =  19.73  N/mm
Maximum load supported               = 800.02 N
Maximum deflection                   =  40.56  mm


There were 5 designs matching your specifications
```

Figure 7.10 Suitable Automotive Engine Valve Sulcated Spring Designs.

Therefore the best overall design from those listed in Figure 7.10 has the following dimensions.

Free height=80.30 mm

Depth=12.10 mm

Width=32.20 mm

Number of sulcations = 3

Radius of sulcation =11.19 mm

Laminate thickness=2.25 mm

Angle α=20 deg

Elastic modulus=40.8 GPa

Bending stress at solid height=-89.06 MPa

Spring stiffness=18.22 N/mm

Weight=8.15 g

Solid load=484.13 N

The cumulative mass of the proposed engine valve sulcated spring design is only 7.4 % of the original engine valve coil spring mass constituting a 92.6 % saving in mass. If, for example, a 4-cylinder engine, where 8 valve springs are used for the inlet and exhaust valves, there would be a saving of 1.63 kg. There is also the potential for reducing the free height. It is evident from Figure 7.10 that the maximum load supported is far above the load to be supported. Some car manufacturers are using beehive springs (cone shaped coil spring where the top of the spring is smaller than the outside diameter at the bottom). So the top outside diameter of the spring effectively closes inside the coils below, in order to reduce the free height of the valve spring and, in turn, reduce the height of the engine.

Figure 7.11 shows a graphical display produced by the design computer program of the proposed engine valve sulcated spring design.

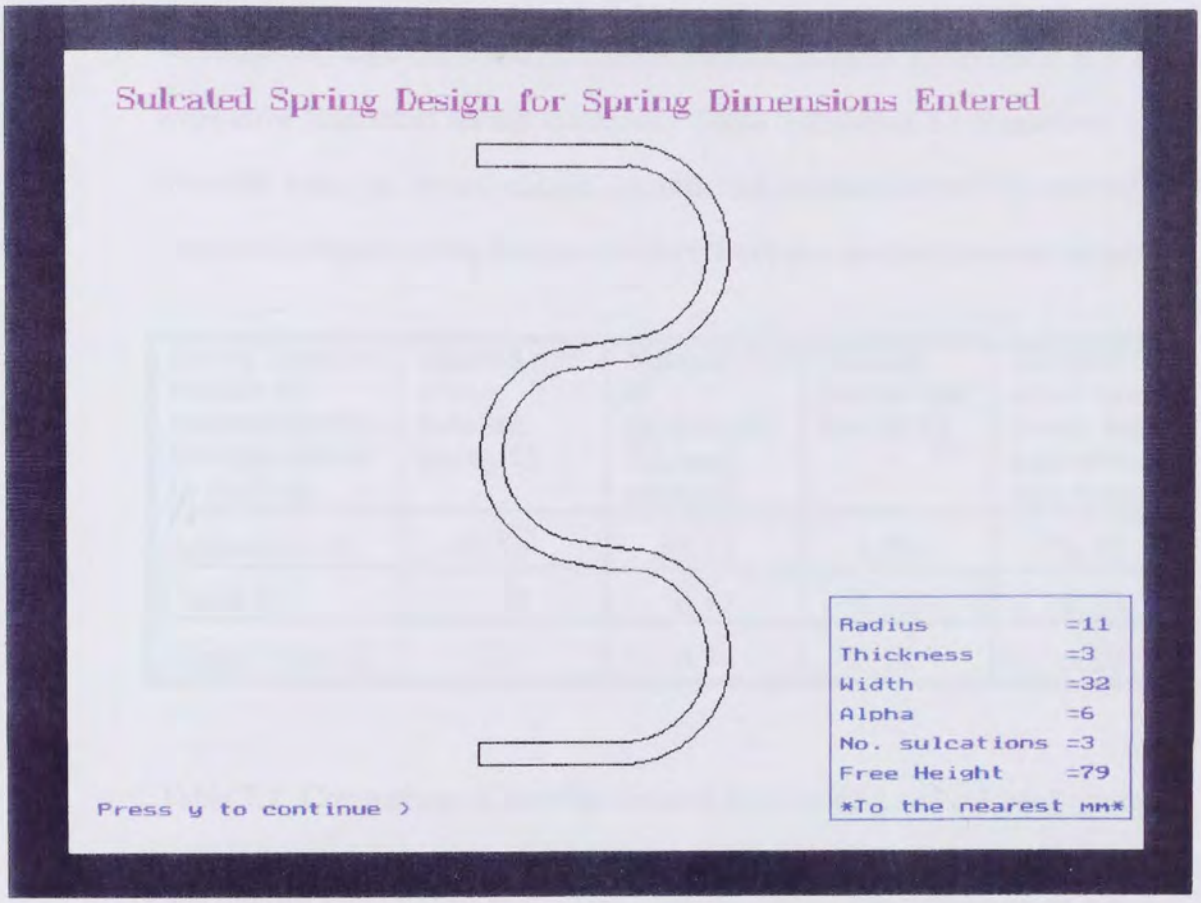

Figure 7.11 Engine valve sulcated spring, produced by the design computer program.

7.5 Commercial Feasibility

To obtain a clearer picture of the commercial feasibility of the sulcated spring, the costs and benefits have to be assessed. Costs for the purposes of this analysis have included material costs and manufacturing costs. Labour and time are other cost considerations. For coil spring manufacture, the basic tooling cost for a car suspension spring has been quoted at £1,375. For an engine valve or clutch coil spring, the spring tooling costs are approximately £700. A mould for an engine valve sulcated spring would cost £1,300. It is

evident from these costs that the tooling costs are double for producing a sulcated spring.

In terms of material costs, fibre-reinforced plastics in general are more expensive than most spring materials. Table 7.2 shows a comparison of the material costs of a suspension, clutch and engine valve coil spring and proposed sulcated spring designs obtained from the design computer program.

Spring Type and number of sulcated springs for replacement in brackets.	Material cost of one Sulcated spring(£)	Material cost of replacement Sulcated spring(£)	Material cost of Coil spring (£)	Number of times more costly than equivalent coil spring
Suspension (2)	42.56	85.12	1.50	56.75
Clutch (1)	0.15	0.15	0.10	1.50
Engine Valve (2)	0.37	0.74	0.14	5.29

Table 7.2 Comparison of material costs of a coil spring and sulcated spring.

Coil spring material costs are based on 50% of the spring manufacturer's selling price. The clutch spring replacement is the most cost effective, with a sulcated spring costing 50% more than the coil. For the engine valve spring, the cost differential is greater: just over five times the cost of an engine valve coil spring. The four sulcated spring suspension design is approximately 57 times the cost of a coil spring. More variation in cost was noted for each design than the mass variation, which was always in the order of 81-94% mass saving.

From this cost analysis, it is clear that the sulcated spring designs proposed need to be re-examined in terms of reducing the costs. It is possible to reduce the spatial constraints, thereby decreasing the size and cost of the sulcated

spring while maintaining the same performance. The extent to which the spatial constraints can be reduced can only be done with a spring designer's detailed specification which states what is to be achieved in terms of load and deflection from the manufacturers and designers of the respective applications.

In terms of labour, fabrication of a sulcated spring the size of an engine valve spring takes one hour and the curing takes one hour. Coil spring manufacture takes about 6 hours from the heating of the material to completion of the finished product. Thus showing that sulcated spring manufacture is quicker and less labour intensive, most of the work being at the fabrication stage for hand lay up. Sulcated springs also have the advantage that several springs can be made in one mould and then cut into smaller springs. With the use of automation of sulcated spring manufacture, the time taken in the fabrication process will be reduced.

Another area where the commercial considerations need to be addressed is in the design of springs made from carbon fibre, or a hybrid combination of glass and carbon fibre, as described in section 3.3.2. The material cost of a sulcated spring of one and two fibres is compared in Table 7.3 and 7.4. A glass fibre sulcated spring is 68% of the cost of a carbon fibre spring of the same size. It is important to bear in mind that the stiffness and stresses in a carbon fibre sulcated spring are different to a glass fibre spring of the same size, so redesign of the carbon fibre spring is necessary to achieve the same stiffness. For hybrid combinations of glass and carbon fibre, the cost decreases as fewer layers of carbon fibre are used. The mass of a carbon fibre spring is approximately 90% of the mass of a glass fibre spring of the same size. In terms of mass per unit cost, the mass of a hybrid spring is dependent on the number of layers of each material and not the position of the material, as is the case for the spring stiffness.

Ratio	Core thickness (mm)	Cost (£)	Mass (kg)	Spring rate per unit cost (N/mm)	Mass per unit cost (kg)
0:24:0	3.00	2.56	0.0345	69.205	0.0135
1:22:1	2.75	2.49	0.0348	59.927	0.0140
2:20:2	2.5	2.43	0.0352	51.817	0.0145
3:18:3	2.25	2.36	0.0356	45.270	0.015
4:16:4	2.0	2.29	0.0359	39.983	0.0157
5:14:5	1.75	2.22	0.0363	35.885	0.0164
6:12:6	1.5	2.16	0.0367	32.742	0.0170
7:10:7	1.25	2.09	0.0370	30.774	0.0177
8:8:8	1.0	2.02	0.0374	29.714	0.0185
9:6:9	0.75	1.96	0.0377	29.295	0.0192
10:4:10	0.5	1.89	0.0381	29.672	0.0201
11:2:11	0.25	1.82	0.0384	30.540	0.0212
12:0:12	0	1.75	0.0388	31.724	0.0222

Table 7.3 Comparative cost and mass of glass/carbon/glass fibre scheme for sulcated spring design C3.

Ratio	Core thickness (mm)	Cost (£)	Mass(kg)	Spring rate per unit cost (N/mm)	Mass per unit cost (kg)
0:24:0	3.00	1.75	0.0388	31.724	0.0220
1:22:1	2.75	1.82	0.0384	45.860	0.0212
2:20:2	2.5	1.89	0.0381	56.490	0.0201
3:18:3	2.25	1.96	0.0377	64.207	0.0192
4:16:4	2.0	2.02	0.0374	69.862	0.0185
5:14:5	1.75	2.09	0.0370	73.214	0.0177
6:12:6	1.5	2.16	0.0370	74.981	0.0170
7:10:7	1.25	2.22	0.0363	75.840	0.0164
8:8:8	1.0	2.29	0.0359	75.397	0.0157
9:6:9	0.75	2.36	0.0356	74.264	0.0151
10:4:10	0.5	2.43	0.0352	72.676	0.0145
11:2:11	0.25	2.49	0.0349	71.122	0.0140
12:0:12	0	2.56	0.0345	69.205	0.0135

Table 7.4 Comparative cost and mass of carbon/glass/carbon fibre scheme for sulcated spring design C3.

When the spring stiffness per unit cost is examined, as in column 5 of Tables 7.3 and 7.4, the carbon fibre spring gives more N/mm per unit cost than the glass fibre spring and in the carbon/glass/carbon scheme produces more N/mm per unit cost than the glass/carbon/glass scheme, therefore more stiffness can be obtained per unit cost. The least cost effective in terms of stiffness is the 9:6:9 case in the glass/carbon/glass scheme, the most cost effective in terms of stiffness was the 7:10:7 ratio for the carbon/glass/carbon scheme in Table 7.4. This scheme was even more cost effective than using all carbon fibre.

The commercial considerations of a hybrid scheme are very advantageous, by including a small proportion of carbon fibre/epoxy resin to a glass fibre/epoxy resin spring, a larger stress value can be accommodated, and the fatigue life extended, as was shown in Table 3.3. Another commercial advantage of using a hybrid scheme is the cost is increased within the range of 0-46% depending on the amount of carbon fibre/epoxy resin used. For example by using 20% carbon fibre /epoxy resin and 80% glass fibre epoxy resin, the material cost only increased by 8%, thus showing a promising option for improving performance whilst only marginally increasing the cost.

Chapter 8

DISCUSSION

8.1 Achievement of Objectives

The objectives of this research work were as follows:-

(i) To publicise the findings of the research and promote the development of sulcated springs.

(ii) To review literature on sulcated springs and other types of composite springs, so that the problems encountered in composite spring design are appreciated, and to generate ideas which may assist in the development of the theoretical model.

(iii) To develop mathematical models for sulcated spring design.

(iv) To validate the model by comparing the results with those from finite element analysis and experimental work.

(v) To produce design computer software developed for theoretical modelling of the sulcated spring.

(vi) Using the software to show how a sulcated spring can be housed in an application, and to demonstrate how the design computer program can be used to find replacement sulcated spring designs for selected applications.

If these are considered in turn, the results are as follows. Research has been carried out, the results of which have been published in this thesis. One of the reasons for the first objective was due to the lack of published material on sulcated springs. There has only been one paper published before the author's first paper, and three patents, one on the sulcated spring design and two on sulcated spring assemblies. Even published material on other types of

composite springs is sparse, in particular information regarding the theoretical design analysis of composite springs is infrequent.

The second objective of reviewing literature on springs of different types was achieved by showing the research that had been carried out on other types of composite spring. Also by showing the diverse composite spring types that had been developed. By reviewing the composite spring literature, problems which occurred when attempting composite spring design were noted, and how the design was affected by a change in material behaviour. Mathematical models for sulcated spring design were shown in Chapters Three, Four, and Five, which represents an original contribution in view of the lack of published material showing the development of a mathematical model in composite and sulcated spring design. Results from the model have been validated with those from finite element analysis and experimental work, so that an estimate can be made of the error, and accuracy of the model.

Documentation of software is important so that the software can be understood or modified more easily by a user. This thesis can also be used as a reference to the design software users who wish to obtain a more detailed explanation of the software, its functions, and the theoretical basis of the model. This objective has been achieved by the documentation included in Chapter Six. The final objective was achieved in Chapter Seven by showing how a sulcated spring can be housed in an application by referring to existing patents. Using the design computer program which was developed as the main part of the research work, sulcated spring designs have been produced which were capable of being housed in the equivalent space of a coil spring, providing the same spring stiffness, and supporting the maximum load of the application. The research carried out in Chapter Seven shows that although the sulcated spring has been considered in isolation without a means of attachment in previous

Chapters, the spring needs to function in an application in order to be of service. Sulcated spring designs for specific applications can be produced using the design computer program, and can function within applications using the spring assemblies described in Chapter Seven, and other forms.

8.2 Is There a Market ?

The main aim or purpose of this study described in section 1.2.1 was to assess the design of the sulcated spring as a viable replacement for the conventional helical compression steel spring. The first question that needs to be asked before assessing the design is: is there a need or a market for a sulcated spring ? If there are perceived advantages to replacing the coil spring, then manufacturers will be more convinced of the beneficial change expected. This is why a section was included in Chapter One which described the market for sulcated springs, although this placed a slight commercial angle on the thesis. The author thought it necessary to include this section due to the likely diverse readership of this thesis. It has therefore been the aim to satisfy both the commercial and academic reader. After market reports were studied, it was decided that there was a market for the sulcated spring.

The next question that needs to be addressed is, what are the inherent advantages of the sulcated spring compared with the coil spring ? In section 1.3.2 the advantages of less mass, low noise transmission, corrosion resistance, no catastrophic failure, compact storage, manufacture in one operation, and the ability to manipulate the material properties to optimise the design were outlined. Although these advantages are known, it is still necessary to obtain further design information so that the design limitations can be quantified and a true comparison made with the metallic coil spring.

8.3 Experience of other Researchers involved in the Field of Composite Springs

The next step in assessing the design was to see what research had been done before, and what principles can be applied to the sulcated spring. In order to construct a clear picture of the likely pitfalls from other researchers' experience. For example, in the case of the carbon fibre coil spring the authors used the coil spring concept manufactured from carbon fibre. As a result, the same manufacturing method for conventional spring manufacture could not be used for carbon fibre, and the design formulae had to be changed. So a direct replacement design is not always as straightforward as it may seem. Composite leaf springs on the other hand involved a change of manufacturing method and design from a multi-leaf steel spring to a single leaf composite spring, with successful consequences, and currently leads the way in composite spring design. The composite cylindrical spring in the literature review did not state the application, and the composite elliptic spring specified the application, but did not demonstrate the spring's potential, which perhaps explains why these springs have not reached the commercial stage of development.

If the experience gained from the researchers mentioned in the literature review is used, it would appear that the sulcated spring could follow the composite leaf spring. Firstly because it fully utilises the material properties and secondly the sulcated spring replaces the coil spring in general, and there are hundreds of applications of the coil spring. Therefore there must be many applications to choose from. For the purposes of this thesis, only three of the mass market applications were considered.

8.4 Spring Design Software

To assist the assessment of the sulcated spring design, computer software was written to obtain theoretical predictions of the probable mechanical behaviour of the spring. There was no readily available software for sulcated springs as in the case of metallic springs, therefore software had to be developed. This software had to contain the sort of design information which was available to metallic spring designers. Hence the same format for metallic spring design software was adopted, which comprised a parametric checking routine and a spatial and performance constraint routine. The parametric checking routine requires the user to enter the dimensions of the sulcated spring parameters of the, sulcation radius, laminate thickness, width, and depth, with the number of sulcations and angle α, as was defined in section 3.2. Design information such as spring stiffness, which is the slope of the load-deflection curve, as defined in Appendix One, and information on the stress distribution can be obtained from the routine. A knowledge of the stress distribution is important to know the possible points of failure. If this is known then it may be possible to redesign a spring to minimise the stresses in particular regions. Equations relating the spring geometry to free height (the length of the spring under no load), and solid height (the height to which the spring can move no further vertically) are also provided by this routine. Cost and weight and information on fatigue and laminate strength are also produced by this routine.

In the spatial and performance constraint routine, the spring stiffness, elastic modulus of the material, maximum load to be supported by the spring design, and the space which the spring should occupy are entered by the user. Suitable sulcated spring designs to fulfil these criteria are then found by the routine. Both the parametric checking and the spatial constraint routine need to have a series of design formulae from which the calculations are obtained.

Results from the experimental research programme and design rules have also been incorporated into the computer program to advise spring designers of the practical limitations of a particular design. These practical limitations were that the number of sulcations must be an odd number greater than or equal to three. The maximum number of sulcations is not known, but for a large number of sulcations of a small width, a buckling effect is likely to occur, although this has not been tested. The sulcation radius should be greater than the thickness, and the sulcation radius should be no less than 3mm, preferably larger for ease of fabrication. The angle of α should be greater than zero which allows for better spring manufacture. The maximum bending stress is recommended to be less then 750 MPa for glass fibre and less then 1200 MPa for carbon fibre.

Results of fatigue tests on sulcated springs have been included in the design computer software. From fatigue tests conducted elsewhere it was found that for a design life of 10^6 cycles a maximum applied stress of up to 590 N/mm^2 was possible, with up to a 5% loss in load carrying capacity. The fatigue results were summarised in Table 3.3, and have been included in the design computer software to prevent spring designers from designing beyond the recommended design stresses, and to promote awareness of the possibility of 'set down' or loss in load-carrying capacity.

8.5 Theoretical Model based on Beam Theory

For the metallic coil spring, design formulae can be obtained from literature. However with the sulcated spring design no such literature exists, so these design formulae have to be derived from first principles. Time and effort can be saved and costs reduced by developing a theoretical model which can be used before manufacture to obtain results on the likely performance of the spring. The mechanics of the sulcated spring must be studied (described in section 3.7) so that a theoretical model can be developed which accurately

models the spring under experimental conditions. Photographs of the spring under a load test were shown at the free height and solid height. These photographs were very important to the development of the theoretical models derived in Chapters Three and Four and, the finite element model discussed in Chapter Five. By taking the photographs the exact deflection process could be recorded visually, so that the process could be compared with the model. Another reason why these photographs are significant was that the two straight end sections which were in contact with the platen do not deflect away from the platen surface, so this observation has been included in the model. Without these photographs this behaviour would not have been included.

Equations for bending moment, shear and normal force were derived in section 3.7.2. These equations were necessary to calculate the bending and shear stresses described in sections 3.7.3 and 3.7.7. Two forms of the equation are permissible, one assumes the stress distribution across the laminate thickness to be linear, the other assumes it to be hyperbolic. Strain gauges were cemented to the outer tensile surface at the position of maximum bending stress, and a comparison made between the theoretical and experimental values of bending stress. The sulcated spring design used in the experiment had larger radii on one side and smaller radii on the other side, the spring was manufactured by using a thinner laminate in an existing mould. The mould of a sulcated spring usually has different sized radii on the left and right sides. There was a significant difference between the theoretical predictions and experimental results. In analysing the experimental results there were two points to consider, one was the difference in sulcation radii and thickness and the other was the effect of the load distribution on the deflection profile. Although the equations for bending stress take account of the differences in the radius and thickness, the contribution of the deflection profile on the stress distribution is more difficult to quantify. However it was noted that, by assuming an off centre

resultant force for this particular spring design, the percentage difference of the theoretical and experimental results was substantially reduced.

Hybrid sulcated springs have been successfully manufactured and have a future in sulcated spring design. For this reason equations have been derived for this type of design. The hybrid spring theoretically examined consisted of a sandwich scheme of a core material and material of a different type on the outer layers. Equations for the bending stress of the curved section of a sulcated spring have been derived which assumed a linear through thickness distribution. In a hybrid sulcated spring the maximum bending stress may not be on the outer tensile surface, but may be at the interface of the two materials, as the theoretical results in Table 3.6 have shown. Sandwich schemes of a glass/carbon/glass fibre epoxy resin and a carbon/glass/carbon fibre epoxy resin were examined to see the effect on bending stress. In terms of fatigue hybrid sulcated springs have been shown to accommodate a stress of 1000 MPa for infinite life, as shown in Table 3.3. With use of the hybrid model to calculate the bending stresses at the curved portion of the sulcated spring a configuration scheme can be selected which can minimise the stresses in this region. It is also important to consider the differences in the ultimate tensile strengths of each material, together with the stress values.

Unfortunately, although hybrid springs were manufactured, the measurement of the spring parameters was not as accurate as the springs measured for springs of one material, due to the different manufacturing and experimental test programmes conducted. Therefore it was not possible to reliably assess the accuracy of the theoretical equations in the hybrid sulcated spring design. It would have been impossible to have measured the stresses at the interface, so only the outer tensile surface could have been experimentally tested and verified theoretically.

Equations for the maximum shear stress have also been derived, the equation used for calculating the shear stress is not dependent on the material property so the equation was no different for the shear stress of a hybrid sulcated spring. The maximum shear stress occurred along the neutral axis when θ=0 degrees and along the neutral axis of the straight limb section for a sulcated spring with angle α=0. There were no experimental results for shear stress.

As well as the stress distribution, designers need to know the spring stiffness. To calculate the spring stiffness requires a knowledge of the spring displacements. Castigliano's theorem was chosen to calculate the displacement and hence expressions for the spring stiffness and deflection under a specified load were derived. The theorem seemed the most appropriate in view of the assumptions for modelling the sulcated spring. The theoretical results for spring stiffness compared favourably with the experimental results, as was shown in Table 3.4, with difference of less than 1.5%. The accuracy of the theoretical results was found to be dependent on accurate measurement of the spring dimensions.

Again in parallel to previously discussed work on the stress distribution, expressions for the stiffness of hybrid sulcated springs were also derived. The results of these expressions for a sandwich scheme were tabulated in Table 3.8. A sandwich scheme of carbon fibre / epoxy resin on the outer layers and a core material of glass fibre / epoxy resin, revealed that as the core material decreased the spring stiffness increased when the overall laminate thickness remained constant. This was due to the thickness of the high elastic modulus of the carbon fibre material increasing in the outer layers, thus contributing more notably to the overall stiffness. When the materials were reversed so that glass fibre was on the outer layers, the spring stiffness was seen to decrease. Another important point was that the position of the material had a greater

influence than the percentage of each material, thus confirming that a higher or lower stiffness may be obtained by judicious arrangement of the type of fibre, the thickness of each section of fibres and the distance of the section from the midplane. For the purposes of this thesis, only symmetrical hybrid schemes were considered. However, it is possible to have different materials on alternate layers, which thus proves the adaptability of fibre reinforced plastics.

8.6 Theoretical model based on Plate and Lamination Theory

Equations derived in Chapter Three for the stress and stiffness of a sulcated spring were further developed in Chapter Four where lamination theory was used to include orthotropic material properties. The equations derived in Chapter Three had no inclusion of a fibre angle term, so it was not possible to analyse the effect of different fibre orientations. In order to understand the different approach adopted in Chapter Four it was imperative to explain the difference between isotropic and orthotropic material properties and the theoretical basis and assumptions of lamination theory. Expressions for the sulcated spring stiffness and stress strain distribution were derived based on lamination theory and a strain energy approach.

With the theoretical expressions for the position of maximum bending stress at the curved section it was possible to assess the likelihood of failure. To assess the laminate strength, the Tsai-Wu failure criterion was selected to determine whether the laminate strength had been exceeded under a specified load, thus establishing if the load carrying capacity had been exceeded. Having established the model for sulcated spring stiffness, stress and strain, subroutines were incorporated into the design computer program so that lamination theory using isotropic and orthotropic material properties could be used. Warning messages were also included if a sulcated spring design

exceeded its laminate strength at solid height, or if the load applied would cause laminate failure in one or more of the plies.

So far the theoretical model has considered isotropic material properties based on beam theory (as in Chapter Three) or isotropic and orthotropic lamination theory (as in Chapter Four). Due to the slender nature of the laminate and large depth compared to thickness, it was also possible to use plate theory. The different forms of theory affect the calculation of the flexural rigidity in the equations for spring stiffness for the different approaches considered. In section 4.4.5 a comparison of the methods of beam and plate theory assuming isotropic material properties, and lamination theory assuming isotropic and orthotropic material properties was shown. The results showed the spring stiffness to be the same for beam, isotropic lamination and orthotropic lamination theory assuming that the elastic modulus for isotropic material properties and the elastic modulus in the longitudinal direction were the same. Plate theory, on the other hand, produced a higher spring stiffness of approximately 5%. Comparing the findings with experimental results showed the lower spring stiffness values to be the closer to the experimentally measured results. The different forms of theory were also found to affect the stress distribution for a 0 degree laminate, as was shown in Table 4.2. For all four methods, the longitudinal stress was the same. Transverse stress values differed for isotropic and orthotropic lamination theory due to the specification of the elastic modulus in the transverse direction for orthotropic lamination theory. Although at smaller loads the difference was not noticeable. A difference in shear stress between isotropic and orthotropic lamination theory was observed, which again is attributed to the inclusion of orthotropic material properties. Orthotropic lamination theory provides the more accurate model.

One of the main reasons for developing a theoretical model was to examine the effects of the contribution of the material properties in the transverse direction, and the effect of different fibre orientations. The contribution of material properties in the transverse direction for a 0 degree unidirectional laminate appeared to have a minimal effect on the prediction of sulcated spring stiffness from the model as was shown in Table 4.1. The effect of different ply orientations was shown in Tables 4.4, 4.5, 4.6 and 4.7, where the spring stiffness was seen to reduce as fibres were laid at angles other than the 0 degree direction. Practical stacking sequences were selected which would not be conducive to warping, so balanced symmetric stacking sequences were selected with the exception of the laminates with plies as 45 degrees. The same stiffness could be obtained by placing layers at 45 and -45 degrees of equivalent thickness to the laminate with layers at 45 degrees. The advantage of using +45 and -45 degrees is that the laminate becomes balanced, and so prevents warping. At each interface, when a change of fibre direction was experienced, an abrupt transition in stress was noted. The stress in the longitudinal direction increased in the outer 0 degree surface as the stacking sequence of intermediate layers was changed. Fibres orientated at angles other than 0 degrees can assist in reducing cracking in the longitudinal direction and can thus extend the fatigue life.

8.7 Theoretical model based on the Finite Element method

In Chapter Five, a numerical approach was adopted by creating a finite element model to find the sulcated spring stiffness, displacements and stresses. The deflection process of the finite element model was closely monitored to match the photographed experimental displacement, particularly at closed height. This involved carefully selecting an appropriate load distribution and restraints. When comparing the spring stiffness of the finite element model with the analytical and experimental spring stiffness, the finite element results were

approximately 4.2% higher than the experimental results for the three spring designs examined. The analytical model proved to be a better approximation than the finite element model.

Another spring design was used to compare the stresses from the finite element results, so that the values could be compared with experimental results for stress, although the spring had different sizes of sulcation radii on the left and right sides. Differences of 12-19% higher than the experimental results for stress were found. Colour coded stress contours of the sulcated spring were also plotted to show the maximum principal and minimum principal stress distribution. The minimum principal stress on the inner surface of the curved section of the finite element model was slightly larger than the outer surface stress, thereby supporting the curved beam theory approach that the neutral axis has a tendency to move toward the longitudinal compressive stresses.

8.8 Software Design

Chapter Six contains a description of the design computer program which is based on the theoretical models developed in Chapters Three and Four. An outline of the design computer software was provided to show the options available on the menu selection screen and screen copies of the options provided by the software was shown in Figures 6.2, 6.3, 6.4, 6.5 and 6.6. The software has options to store, change, display, retrieve and enter data for either the parametric checking or finding a suitable design by providing spatial and performance constraints. There is a large degree of flexibility in the program which allows the theoretical basis of the calculation to be selected from beam, hybrid beam, plate, isotropic lamination, or orthotropic lamination theory. Assumptions, theoretical basis and results for each theoretical basis have been discussed in Chapters Three and Four. After the required theory has been selected, a choice of the type of design information is provided, as shown

in Figure 6.1. The design computer program offers a 'tailor made' software package which allows information for sulcated springs to be easily retrievable even for the non-specialist user of the software.

8.9 Can Sulcated Springs Operate in Established Spring Applications ?

The potential applications of sulcated springs were discussed in Chapter Seven. Three automotive applications were chosen for which the sulcated spring could be a viable replacement for the coil spring. These applications were selected on the basis of having a large market and heavy demand. The way in which the spring operates within the application was briefly described.

Using sulcated springs as a replacement design brings with it restrictions on the method of assembly or attachment to secure the spring in place, together with restrictions on space into which the spring is housed. Both these issues were addressed by reference to patents which have been filed showing several methods of clamping, and variations of the sulcated spring design. The main point arising was that fibre-reinforced plastics require alternative methods of attachment to avoid fibre disruption, which is not so important in metals. This requires alternative methods of securing the spring than would otherwise be used in securing a metallic component.

With regard to the space which the spring is to be housed in, the free length of the coil spring was used as the initial height of the space available. The maximum rectangular area possible within the area of the outside diameter of a coil spring was used as the initial width and depth dimensions of the sulcated spring. Coil spring dimensions, performance, material type, material properties and the mass of, a car suspension, clutch and engine valve spring were presented in Table 7.1. The spatial and performance requirements were used to

observe if the spatial and performance constraints routine of the design computer program as described in section 3.4.3 could be used to find sulcated spring designs. Sulcated spring designs have to satisfy at least coil spring requirements and provide additional advantages to be fully feasible.

Suspension coil springs have another limitation in that a shock absorber is placed inside the coils. For sulcated spring design placing a shock absorber inside the spring would lead to fibre disruption which should be avoided. If the continuity of the fibres is disrupted, a degradation of the material properties occurs. So an alternative to this was to design around the shock absorber, however, no suitable designs could be found within the outside coil diameter space dimension. The selected design only exceeded the outside diameter dimension by 23 mm, the free length was increased to reduce the area occupied by the width and depth dimension, whilst still satisfying the performance criterion of a suspension coil spring. For the replacement engine valve spring the valve stem passes through the centre of the coil spring, therefore the replacement sulcated spring design consisted of two springs on either side of the valve stem. The sulcated spring designs produced by the design computer program for the engine valve spring was still within the space presently occupied by an engine valve coil spring and yielded the same performance. Replacement of the clutch spring was more straightforward in that this could be replaced by one sulcated spring.

The sulcated spring designs were between 6-19% of the mass of a coil spring. Even when two sulcated springs replaced one coil spring, this saving in mass was maintained. From the list of sulcated spring designs produced for each application, the maximum load supported by the coil spring was often exceeded. The software had difficulty finding spring designs with exactly the same solid height, so designs with a greater solid height were found so that the

solid height was never reached under the maximum load of the coil spring. Thus there was the potential to reduce the free height or other dimensions so that a closer approximation to the required solid height could be found. Whilst there was nothing wrong with the present sulcated spring design, there is still wasted energy and space in the proposed designs by not using the spring to its full potential. This is of importance, particularly when car manufacturers are looking for ways of trimming components for savings in mass and better performance, in addition to the reduction in material cost gained when the size is reduced.

Sulcated springs can be manufactured to a variety of specifications. The patents show that a sulcated spring can be assembled in a suspension system. Sulcated spring designs with the same performance requirements as a coil spring have been found. From this, the conclusion is that sulcated springs can operate in applications, providing the environmental influence has been taken into consideration.

8.10 Coil Spring or Sulcated Spring ?

The decision to use a coil spring or sulcated spring depends on the application requirements. If the application requirements are for corrosion resistance at whatever cost, then the sulcated spring would be the solution. In most applications, cost is an important consideration, and from section 7.5, which examined the commercial feasibility, it was evident that, if a replacement of the same size was used, the cost of the sulcated spring would always be greater. Hybrid sulcated springs, where a combination of glass and carbon fibre layers are used, are more expensive than a glass fibre/ epoxy resin sulcated spring. Tables 7.3 and 7.4 showed that a marginal increase in cost may be worth the increased benefit in terms of reducing stresses or providing more stiffness per

unit cost. A re-design of the spring, whereby less material may be used, would prove to be another method of reducing costs

The benefits to be gained using a sulcated spring were, considerable reductions in mass of the order of 81-94% for a similar size spring replacement. If the size of the sulcated spring can be less than the coil spring, then the potential for a reduction in mass is even greater. The sulcated spring experiences no corrosion, so the fatigue life is not affected by corrosion, as is the case in coil springs. A sulcated spring is fail safe in terms of complete breakage. Failure of a sulcated spring is defined as a greater than 5% loss in load carrying capacity, the spring gradually softens and loses its original stiffness. This allows the spring to be replaced conveniently without abrupt disruption to the operation. Coil springs however fail catastrophically, often with no warning. Other benefits are that noise transmitted through the sulcated spring diminishes, thus producing a silent spring. Coil springs on the other hand creak and can accentuate noise. Sulcated springs can be interlaced in storage, avoiding wasting storage space. Manufacturing is done in a clean working environment, and the number of operations is reduced in comparison to the coil spring.

One of the most important factors is the end user's or customer's needs. From the benefits of the sulcated spring discussed, the advantages to the consumer are apparent. However although these benefits exist, will the consumer be prepared to pay the additional cost for these benefits ? It is a question which is perhaps best answered by market research for the concerned applications. If the cost differential is negligible or, in the unlikely event that the cost of a sulcated spring is less than the coil spring, is the conversion from coil to sulcated spring worthwhile ? If this is the case then in the present author's opinion it would be beneficial most notably in terms of mass.

Chapter 9

CONCLUSIONS AND RECOMMENDATIONS FOR FUTURE WORK

9.1 Conclusions

1. The design of the sulcated spring has been assessed, the conclusions of which are contained in this chapter. It has been shown that there is a market for the sulcated spring because the advantages constitute an improvement on the traditional coil spring. Advantages of the sulcated spring are less mass, low noise transmission, corrosion resistance, no catastrophic failure, compact storage, manufacture in one operation, and the ability to manipulate the material properties.

   From the experience of researchers in the field of fibre reinforced composite springs, several lessons can be appreciated. Firstly direct replacement of a steel spring with a composite spring using the same design may not provide the most efficient solution, due to the differences in material characteristics. Secondly, various manufacturing methods need to be investigated to find the most suitable. Finally the replacement design often had to be changed in view of the material characteristics, and methods of securing the spring to avoid fibre disruption had to be found.

2. Software developed for the purpose of determining the probable mechanical behaviour of the sulcated spring included known practical limitations in sulcated spring design to prevent impractical designs being created. From the experimental programme conducted, the practical limitations were established. These were, the number of sulcations should be greater than three, and be an

odd number for a sulcated spring with horizontal straight end sections, as studied in this thesis. For even sulcations, an excessive lateral displacement was observed. A laminate thickness of 0.125 mm is the minimum laminate thickness, equivalent to one ply. Sulcation radii were recommended to be greater than the thickness to allow ease of fabrication, and to reduce stress. In fatigue tests conducted, a maximum applied stress of up to 590 N/mm^2 was possible with up to 5% loss in load-carrying capacity for a design life of 10^6 cycles for glass fibre /epoxy resin sulcated springs. Having established the practical limitations, these limitations were included in the design software to prevent impractical designs, and warn against the possibility of 'set down' or loss in load carrying capacity.

3. To form a theoretical basis for the sulcated spring software, equations were derived for the sulcated spring stiffness and stress. The effect of the contribution of the load distribution to the deflection profile had not been taken into account in the equations for bending stress. However, the equations revealed that assuming an off-centre resultant load distribution produced a greater accuracy for the spring design examined. Equations derived for the spring stiffness were accurate to within 1.5% of the experimental results, and provided a good approximation. However the precise measurement of the spring dimensions had a direct bearing on the closeness of the theoretical and experimental results for stiffness. Equations were also derived for spring stiffness and stress of a hybrid sulcated spring. No reliable experimental results were available, so the theoretical results have yet to be compared. However conclusions can be made from the theoretical results. The spring stiffness was found to increase as more layers of carbon fibre were placed in the laminate. Placing carbon fibre layers on the outer sections of the sandwich scheme provided a greater contribution to the sulcated spring stiffness, than being used as the core material.

4. Different forms of the theoretical basis of the model affected the flexural rigidity. A comparison of four methods showed the spring stiffness to be the same for beam, isotropic, and orthotropic lamination theory. Plate theory produced an approximate increase in spring stiffness of 5%. In comparison with experimental results, the methods of beam, isotropic and orthotropic lamination theory proved to be closer to the experimental values. When the stress values of the four methods were computed, the longitudinal stress was the same for a 0 degree laminate. There were differences in the transverse stress which became more distinct as the load increased. For isotropic and orthotropic lamination theory, this was due to the contribution of the elastic modulus, which for the isotropic case was the same in the longitudinal and transverse direction, thus producing a conservative estimate for all predictions involving the transverse direction. A similar observation occurred in the computation of the shear stress. The effect of the material properties in the transverse direction was found to have a negligible effect on the stiffness for a 0 degree laminate. When stacking sequences other than all laminae in the 0 degree direction were considered, the spring stiffness was reduced. In terms of stress, an abrupt change in the theoretical stress value was noted along the interface when a change in fibre orientation was experienced. An increase in stress at the position of maximum bending stress was observed in tension and compression in the 0 degree outer layers when different stacking sequences were used in the intermediate layers.

A finite element model of the sulcated spring showed a 4% higher spring stiffness than experimental results. Thus showing the analytical model to be more accurate in terms of stiffness than the finite element model. The finite element predictions for the maximum principal stress of a sulcated spring design was 12-19% higher than experimental results. This is in line with the finite element predictions for spring stiffness which were higher than the

experimental results, although not as high as the stress predictions. Finite element results for the minimum principal stress supported the theory of the neutral axis shifting away from the centroidal axis towards the compressive surface.

5. Replacement sulcated spring designs have been found for the car suspension, clutch, and engine valve springs to work within the same space or close to the space currently occupied by the coil spring, whilst yielding the same stiffness and supporting the required maximum load. When replacement sulcated spring designs for the suspension spring and engine valve spring were attempted, at least two sulcated springs were required. This allowed for the shock absorber to pass through the suspension spring, and valve stem to pass through the engine valve spring. However, for the clutch spring, one sulcated spring was a sufficient replacement. For all the applications considered, the sulcated spring designs which were found often supported a greater maximum load than was required, in particular the clutch and engine valve spring. This suggests that there is the potential for designing the spring within a smaller space while still satisfying the present coil spring requirements, and reducing the mass even further, thus satisfying the current trend of car manufacturers looking for ways of reducing component size and mass. Mass savings for the proposed sulcated spring designs were in the order of 81-94%, even when several sulcated springs were used the mass saving was still maintained. Redesign of the proposed sulcated spring designs as proposed by the design computer program is inevitable, one of the main reasons would be to reduce costs.

A cost analysis of the proposed designs revealed the material costs to be 1.5-56.8 times the material cost of a metallic coil spring for the respective application. The material cost calculations of a hybrid sulcated spring of glass and carbon fibre /epoxy resin showed a marginal increase in cost in the range 0-

46%, which could provide an alternative to using all carbon fibre, and also improves the performance. Again redesign of the sulcated spring may prove necessary to provide the required stiffness and stress.

For the replacement designs where the maximum load supported at solid height is much greater than required, it is possible to reduce the sulcated spring size whilst maintaining the required stiffness and supporting the maximum load, however an exact specification of the applications requirement is necessary to know how far the size can be reduced. Although the exercise of finding replacement sulcated spring designs has been useful in demonstrating the capability of the design computer program developed, a design specification would have produced a more cost-effective solution than a direct replacement in terms of size and performance.

6. The design computer software for sulcated spring design developed by the author of this thesis during the course of the research has provided a user-friendly direct method of obtaining design information. By selecting the options from the menu, the dimensions of a sulcated spring design can be entered and calculations for sulcated spring stiffness, stress, mass, cost, solid height, stress at solid height, and maximum load supported can be obtained. This is all possible using the theoretical basis of beam, plate, isotropic and orthotropic lamination theory. For a hybrid sulcated spring, beam theory for two materials can be used. As well as providing design information on the input of the spring dimensions, suitable sulcated spring designs can be found by entering spatial dimensions which the required sulcated spring should occupy. A substantial contribution to the development of the sulcated spring has been provided by the design computer program and the mathematical models described in this thesis.

9.2 Recommendations for Future Work

This section addresses the recommendations for future work for the theoretical modelling of the sulcated spring, as in the title of the thesis. Although future work could be interpreted as being for the sulcated spring in general. The theoretical model needs to be validated further, by manufacturing and testing different sandwich schemes and alternate layer schemes for hybrid sulcated springs, so that experimental results for spring stiffness and stress are available for comparison. Sulcated springs with various stacking sequences need to be manufactured and tested to compare with the theoretical predictions of the model. The theoretical model also needs to be tested with different material properties, such as carbon fibre. Therefore experimental results need to be obtained for different materials and the model tested under these conditions. Another recommendation would be to test the accuracy of the theoretical model for a range of designs. It would be interesting to see how the model coped with a small design or large design and if the equations were less accurate for a particular type of design.

The results of fatigue could be included more extensively in the design computer software to include fatigue results for carbon fibre, hybrid sulcated springs and sulcated springs of different fibre orientations. The theoretical model could be extended to include a sulcated spring with a laminate for a hybrid spring with different fibre orientations. For example 0 degree carbon fibre on the outer surface with layers of 0 degree, 90 or 45 degree glass fibre for the layers in between. The present design software as described in this thesis produces a warning message if the laminate strength has been exceeded. This could be further developed to assume that if the laminate strength has been exceeded then the ply has failed, and thus the stiffness will be reduced as a consequence. An algorithm could be written to show the loss of stiffness occurring when a ply or several plies fail.

Research using finite element analysis for sulcated springs could be developed further by using orthotropic material properties, and comparing the predictions with experimental work. Finite element analysis in 3 dimensions would be interesting, to observe the stress variation across the depth. With some leading finite element software packages it is also possible to assess the edge effects, as discussed in section 4.4.8. Different types of spring assemblies can also be assessed by finite element analysis. There are many software packages which include optimisation options to optimise the structures for minimum mass, stress and volume. Predictions for fatigue life can also be obtained from some finite element software, however the fatigue life assessment uses metallic fatigue algorithms, which may not be very reliable.

So far, the theoretical model has been based on horizontal end portions, which has proven stability. Sulcated springs can also be designed with angled end sections, which may be easier to manufacture, however the stability has yet to be investigated. It may be possible to develop the theoretical and finite element model to consider angled end sections, and assess the effect of a change in design.

It may be interesting to see if the spatial and performance constraints routine could also provide an equivalent sulcated spring design which would occupy the minimum amount of space, instead of only supplying a design to suit the users spatial requirements. Thermal and environmental effects play an important role in deciding which applications a sulcated spring can operate in. Thermal effects could also be included in the theoretical model to observe changes in stiffness or stress as the temperature is varied.

Theoretical modelling in this thesis has been confined to linear rate sulcated springs. Variable rate sulcated springs can be manufactured to produce a non-linear load deflection characteristic. Further investigation could be conducted to develop a theoretical model to simulate a variable rate spring, and to produce variable rate sulcated spring designs to fit within a confined space, and yielding a prescribed performance. The present model considers only uniform thickness and radius, depth, width and angle α, throughout the spring. It is possible to develop the model further to accept different radii and thickness at each sulcation, for extreme precision, or for sulcated spring designs as mentioned in this thesis which have different sizes of radii on the left and right sides.

Finally the last recommendation is for consultation and collaboration with application designers and users to examine their requirements. This will give sulcated spring designers a specification with which to work, rather than approaching the problem from a direct replacement point of view. This will enable the software and theoretical model discussed in this thesis, and any further developments, to be used effectively.

References

1 Wootton, A. J., et al. (1985) "Structural Automotive components in fibre reinforced plastics", *3rd International conference on composite structures in fibre reinforced plastics*, 3, 19-42.

2 The Secretary of State for Industry, "Springs for High Specific Energy Storage", Scowen, G. D., (14.06.84), 1-14, WO 85/ 00207.

3 Final Technical Report for the Commission of the European Communities under the BRITE/EURAM programme; (1991) "The Sulcated Spring. The development of an advanced resin fibre composite 'Z' shaped replacement for the traditional steel coil spring"; Contract no. RI1B-277, Proposal no. P-2025-87.

4 Business and Market Research plc. (1989) "The Market for Engineering Springs in West Germany, France, Italy and Spain", A report prepared for The Spring Research and Manufacturers Association.

5 Therén, K. and Lundin, A. (1990) "Advanced Composite Materials for Road Vehicles", *Materials and Design* , 11(2),71-75.

6 Yu, W. J. and Kim, H. C. (1988) "Double tapered FRP beam", *Composite Structures*, 9(4),279-300.

7 Goette, T. Jakobi, R. and Puck, A. (1985) "On the development of fibre/ plastics composite leaf spring for commercial vehicle application", *Kunstoffe German Plastics*, 75(6),20-24.

8 Lo, K. H. McCusker, J. J. and Gottenberg, W. G. (1987) "Composite leaf spring for tank trailer suspensions" *Journal of Reinforced Plastics and Composites*, 6(1),100-112.

9 Gottenberg, W. G. and Lo, K. H. (1986) "Glass fibre reinforced epoxy leaf spring design", *Int. J. Vehicle Design, Special Publication SP6*,245-255.

10 de Goncourt, L. and Sayers, K. H. (1987) "A composite automobile suspension", *Int. J. of Vehicle Design*, 8(3),335-344.

11 Starkey, M. S. and Wood, P. (1985) "Glass epoxy composite as a leaf spring material", *Composites* ,17-24.

12 Chang, B. T. A. and Lo, K. H. (1988) "Failure Analysis of FRP Springs", 43rd Annual Conference, Composites Institute, The Society of the Plastics Industry, Session 10-D,1-6.

13 Hendry, J. C. and Probert, C. (1986) "Carbon Fibre Coil springs", *Material & Design*, 7(6), 330-337.

14 Mallick, P. K. (1987) "Static Mechanical Performance of Composite Elliptic Springs", *Transactions of the ASME*, 109, 22-26.

15 So, C. K., *et al.* (1991) "Static Mechanical Behaviour of Composite Cylindrical Springs", *Composites Science and Technology*, 40,251-263.

16 Scowen, G. and Hughes, D., (1985), "The sulcated spring", paper presented at *International Seminar, Autotech 85 Congress, The Institution of Mechanical Engineers, Automobile Division, Birmingham, UK, November 1985.*

17 Thompson, J. M. *et al.*, (1992) "Computer Aided Design of FRP Sulcated Springs", *3rd International Conference on CAD in Composite Materials Technology*, 1992,445-462.

18 Lekhinitskii, S.G., (1968) "Anisotropic Plates", Gordon and Breach Science Publishers.

19 Carter, F. *et al.* (1991), "Development of the Sulcated Spring", Synthesis Report for the Commission of the European Communities, BRITE/EURAM.programme, Contract no. RI1B-277, Proposal no. P-2025-87.

20 Benham, P. P. and Crawford, R.J. (1987), "Mechanics of Engineering Materials", John Wiley & Sons, Inc.

21 Nash, W. A., (1977), "Strength of Materials", McGraw-Hill Book Co.

22 Gere, J. M. and Timoshenko, S. P., (1984), "Mechanics of Materials", PWS Publishers, Wadsworth International.

23 Roark, R. J. and Young, W. C., (1975), "Formulas for Stress and Strain", McGraw-Hill, Inc.

24 Agarwal, B. D. and Broutman, L. J., (1990), "Analysis and Performance of fiber Composites", John Wiley & Sons.

25 Jones, R. M., (1975), "Mechanics of Composite Materials, McGraw-Hill Book Co., Scipta Book Co.

26 Mallick, P. K., (1988), "Fiber-Reinforced Composites: materials, manufacturing and design", Marcel Dekker, Inc.

27 Vinson, J. R. and Sierakowski, R. L., (1989), "The Behaviour of Structures Composed of Composite Materials", Martinus Nijhoff Publishers, Dordrecht.

28 Tsai, S. W. and Wu, E. M. (1971) "General theory of strength for anisotropic materials", *Journal of Composite Materials*, 5,58-77.

29 Pipes, R. B. and Pagano, N. J. (1970) "Interlaminar Stresses in Composite Laminates Under Uniform Axial Extension", *Journal of Composite Materials*,4(4),538.

30 'PAFEC', Data Preparation Manual, Pafec Ltd., Nottingham, UK.

31 GKN Technology Limited; "Securing a sulcated spring to a suspension component"; 8th Oct 1986, 4 pages, GB 2196093 A.

32 GKN Technology Limited' "Spring assemblies "; 9th Nov 1987, 4 pages, GB2197424 A.

33 Carter, F. and Murphy, S. (1991). "Theoretical Modelling of a Composite Compression Spring", *Sixth International Conference on the Mechanical Behaviour of Materials*, The Science Council Japan, Paper PS3-17, 193, 194.

APPENDICES

APPENDIX 1

SPRING TECHNOLOGY

1.1 Functions of a Spring

A mechanical spring is an elastic body whose primary function is to deflect or distort under load, and absorb energy. The original shape of the mechanical spring is recovered after being distorted under load. A spring is made for the purposes of converting mechanical work into potential energy and re-converting it into mechanical work, by virtue of its elastic deformation. Springs are therefore suitable for temporarily storing energy, reducing shocks, cushioning or controlling moving masses, and measuring forces due to the natural dependence between force and deformation. A spring has four primary functions; firstly to absorb energy and migrate shock, secondly to apply a definite force or torque, thirdly to support moving masses or isolate vibration, and finally to indicate or control load or torque.

1.2 Primary Spring Design Objectives

The primary objective of a spring designer is to design a spring that will perform the task required, in the most economical way with all factors considered. This usually means that the spring must fit the space available and have a satisfactory life in service, which includes fatigue breakage, excessive relaxation or set-down. In other cases, a designer may require maximum reliability, even at increased cost, where failure may endanger life or property. In such cases more expensive materials and additional processing costs may be justified. For certain applications, a designer may wish to obtain a spring of minimum mass, volume or length.

1.3 Selection of Materials for Springs

A spring material can be defined as any substance which has the capacity for storing energy by elastic deformation. However there are other features which need to be taken into consideration when choosing a material for springs. Metals have so far been considered to possess the most attractive properties and so are used in the majority of applications.

The most important features to consider when choosing a material for a particular application are:-

1. Material meets the required stress conditions either static or dynamic.
2. Material is capable of functioning satisfactorily at the required operating temperature.
3. Material is compatible with its surrounds for example corrosion problems.
4. Consideration of special requirements such as conductivity, constant modulus, weight restrictions and magnetic limitations.

1.4 Purpose and Principles of Spring Calculation

Springs can be divided into three main groups depending on the method of loading bending springs, torsion springs and tension and compression springs. Calculations are based mainly on the uses of three groups of equations namely,

1. Dependence of deformation on load or of elastic force on deformation.
2. Dependence of stressing of the material on load or on deformation.
3. Dependence of elastic energy on deformation and on load or stress.

As a result of deformation of the spring due to a load P, the point of application of the load travels a distance f, which is the travel displacement or deflection. The diagrammatic representation of P as a function of f is known as the load-deflection line, as in Figure A(1.1). This line is frequently straight, however

there are load-deflection lines which are curved, either concave or convex towards the x-axis as in Figure A(1.2). The unit deflection is represented by C.

$$\lim \frac{\Delta f}{\Delta P} = \frac{df}{dP} = \tan\alpha = C$$

The reciprocal value $\frac{1}{C}$, is the unit force. When the load-deflection line is practically straight, the elastic behaviour of the spring is defined by the specific deflection or by the spring rate.

The problem of stress set up in the material by a force P or a deflection f can generally be solved by developing sufficiently precise formulae for the maximum stress as a function of P and f. By taking into account the tensile properties of the material chosen, this maximum stress alone decides the correct dimensioning of a spring from the point of view of strength. The work done is of particular importance in the dimensioning of springs, whose purpose is to bring moving masses to a standstill. The energy A is denoted by the shaded area of the graph. The energy equation is given by A=1/2Pf.

Many springs are fully loaded and unloaded again, more frequently. For example, irregularities of a road surface will cause load variations on a vehicle suspension spring. Such frequent and periodically repeated variations in load and the corresponding stress fluctuations, causes the material to behave differently from the way it behaves under relatively infrequent, but large load variations. If the number and amplitude of the stress variations exceed certain values, the spring will break without any preceding permanent deformation, even when the stress peaks are far below the proof stress. A spring which is subjected to frequent load variations cannot be calculated using the strength

properties only as in static tests. Consideration of fatigue strength obtained from fatigue tests is necessary.

The life of a spring (the number of load cycles to failure) depends on the mean stress and stress amplitude. At a given mean stress, life increases as the stress amplitude decreases. If the amplitude is such that the spring withstands 10 million load cycles without breaking, it can be concluded that the spring will last indefinitely. This amplitude limit is therefore called the endurance limit. The endurance limit for zero mean stress is known as the endurance limit under alternating stress. The amplitude and stress range for zero initial stress is important, in this case amplitude and mean stress are then the same.

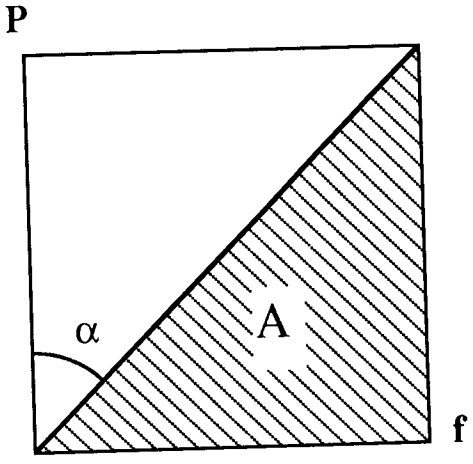

Figure A(1.1) Straight load-deflection line.

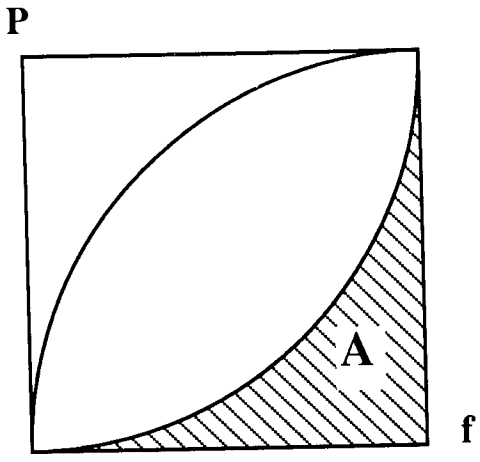

Figure A(1.2) Curved load-deflection line.

APPENDIX 2

SOFTWARE DESCRIPTION

This Appendix contains a description of each procedure and function developed for use in the design computer program. The descriptions are divided into procedures and functions for the menu, datafile, material and stacking sequence, and design options.

MENU

WaitToGo	A procedure which allows the user to continue with the program by pressing any key, or 'esc' to exit the program. The option is given at the end of the option screens.
IGraph	Initialises graphics options, and exits the program if for some reason the graphics option cannot be initialised.
Title	Displays the colour graphics rectangles with the initial title that appears on the screen 'Aston University and Eltek Research Ltd., Sulcated Spring Design Software'.
Name	This states the name of the person responsible for the software development (F.Carter).
CheckorSpace	Displays the options in colour graphics for either, parametric checking or Spatial and Performance Constraints Routine.
Datafile	Displays six options in colour graphics where the user can select the form of the data or the stage the data is at.
SelectTheory	Displays a choice of five different theoretical bases in colour graphics.

DesignMenuBeam	Displays nine options in colour graphics concerning design information options.
TopofMenuBeam1	Displays the title of the design information menu, for a design menu based on beam theory, and the prompt to select an option.
TopofMenuBeam2	Displays the title of the design information menu, for a design menu based on hybrid beam theory, and the prompt to select an option.
TopofMenuPlate	Displays the title of the design information menu, for a design menu based on plate theory, and the prompt to select an option.
TopofMenuIso	Displays the title of the design information menu, for a design menu based on Isotropic lamination theory, and the prompt to select an option.
TopofMenuOrtho	Displays the title of the design information menu, for a design menu based on orthotropic lamination theory, and the prompt to select an option.
TopSpace	Displays a colour screen confirming the option to find a sulcated spring design according to the users specification.
TopParameter	Displays a colour screen confirming the option to obtain theoretical estimates for spring stiffness, deflection, stresses, cost or mass by entering the dimensions and material properties. Procedure WaitToGo is also called in this procedure, so that the user can exit the program at this stage, or continue.

DATAFILES

EnterConstantData	Allows data entry of geometric parameters for the parametric checking routine.
WriteOutput	Writes geometric parameters to a file.
ChangeConstant	Displays the current geometric parameters and allows the user to change the value of any parameter.
FileInput	Retrieves an existing file containing the geometric parameters from floppy or hard disc.
EnterSpace	Allows data entry of spatial and performance constraints.
WriteSpace	Writes spatial and performance constraints to a file.
ChangeSpace	Displays the current spatial and performance constraints and allows the user to change the value of any parameter.
FileSpace	Retrieves an existing file containing the spatial and performance requirements from disc.

MATERIAL AND STACKING SEQUENCE

EnterBeamMat	Allows interactive data entry of the Elastic modulus of the material upon selection of the beam theory option.
EnterHybridBeamMat	Allows data entry of the Elastic modulus of two materials and the laminate thickness of the core material.
EnterPlateMat	Allows data entry of the Elastic modulus and Poisson's ratio ready for calculations based on plate theory.
EnterIsoMat	Allows data entry of the Elastic modulus, Poisson's ratio, shear modulus, number of sections, the angle of fibres within each section, and the distance of each section from the neutral axis.

EnterOrthoMat	Allows data entry of the Elastic modulus in the longitudinal and transverse direction, shear modulus and number of sections, the angle of fibres within each section, and the distance of each section from the neutral axis.

DESIGN OPTIONS

BeamSpringRate	A function that calculates the spring stiffness based on beam theory.
Deflection	A procedure which calculates the deflection from the spring stiffness, under a load specified by the user.
CostOneMat	Calculates the two material costs of a sulcated spring of the dimensions specified in the data file made from carbon fibre and glass fibre epoxy resin.
CurvedBeamStress	Calculates the bending stress based on curved beam theory.
ShearStress	Calculates the shear stress under a load specified by the user, applies to theory based on beams and plates.
GeometricLimit	Tests the geometric parameters to see if any parameters are beyond or under the recommended design limitations.
SpringGraph	Produces a pictorial display of the sulcated spring corresponding to the entered geometric parameters.
IntToStr	Converts any integer type to a string which can be output using graphics commands. This is useful for displaying the numeric values in graphics mode.
HybridBeamSpringRate	A function to calculate the spring stiffness of a hybrid sulcated spring using beam theory.

CostTwoMat	Computes the cost of a sulcated spring manufactured from two materials.
HybridBeamStress	Calculates the maximum bending stresses of a hybrid sulcated spring.
PlateSpringRate	A function to calculate the spring stiffness of a sulcated spring based on plate theory.
IsoLamSpringRate	A function to calculate the spring stiffness of a sulcated spring based on isotropic lamination theory.
StressIso	A procedure to calculate the stresses at the position of maximum bending stress based on isotropic lamination theory.
OrtLamSpringRate	A function to calculate the spring stiffness of a sulcated spring based on orthotropic lamination theory.
StressOrtho	A procedure to calculate the stresses at the position of maximum bending stress based on orthotropic lamination theory.
CADSolution	A procedure to find sulcated spring designs which matches spatial and performance requirements entered by the user.
AreaOneLayer	Calculates the area of one layer of prepreg material.
FreeHeight	Calculates the theoretical free height of a sulcated spring from the geometric parameters.
SolidHeight	Calculates the theoretical solid height of a sulcated spring from the geometric parameters.
SpringRateCalc	Calculates the spring stiffness without the contribution of the flexural rigidity.
MaximumCurvedBeamStress	Calculates the value of maximum bending stress for curved beam theory under the solid load.

MaximumShear	Calculates the value of shear stress under the solid load.
WeightOneMat	Calculates the mass of a sulcated spring manufactured from one material.
FatigueCheck	Uses the maximum stresses to check if the fatigue life has been exceeded.
GeneralBeam1	A procedure which contains all the procedures necessary to produce general information in the design menu for the beam and plate theory selection.
WeightTwoMat	Calculates the mass of a hybrid sulcated spring.
HybridMaxBeamStress	Calculates the bending stresses at solid height for a hybrid spring.
GeneralBeam2	A procedure which contains all the procedures necessary to produce general information in the design menu for a hybrid spring.
LaminationStress	Calculates the stresses for orthotropic and isotropic lamination theory.
MaxLamStress	Sorts through the stresses across the thickness to find the maximum value.
GeneralLam1	A procedure which contains all the procedures necessary to produce general information in the design menu for isotropic lamination theory selection.
LaminationPrintStress	Displays the stresses for isotropic and orthotropic lamination theory.
GeneralLam2	A procedure which contains all the procedures necessary to produce general information in the design menu for orthotropic lamination theory selection.
QandQbarIso	Calculates the values of the Q matrix in isotropic lamination theory.

DMatrix	Calculates the values of the D matrix in lamination theory.
QandQbar	Calculates the values of the Q matrix in orthotropic lamination theory.
Strength	Assesses the strength based on the Tsai Wu failure criterion.
Fatigue	Contains general design rules to check that stresses do not exceed the recommended value of percentage of material strength.

APPENDIX 3

PAPERS PUBLISHED BASED ON THE WORK IN THIS THESIS

THEORETICAL MODELLING OF A COMPOSITE COMPRESSION SPRING
F. Carter and S. Murphy
Paper presented at the Sixth International Conference on the Mechanical Behaviour of Materials, Kyoto, Japan.
July 29th-August 2, 1991

UTILISING MATERIAL PROPERTIES IN A SULCATED SPRING
F. Carter, S Murphy, T.H.E. Richards
Paper presented at the Sixth International Conference on Fibre Reinforced Composites, Newcastle, UK.
March 29th-31st, 1994

A THEORETICAL MODEL FOR SULCATED SPRINGS
F. Carter, S Murphy, T.H.E. Richards
Paper presented at the Second Biennial European Conference on Engineering Systems Design and Analysis, London, UK.
July 4th-7th, 1994

Aston University

Content has been removed for copyright reasons